BIOCHEMICAL AND FUNCTIONAL IMPACT OF PATHOGEN INACTIVATION ON PLASMA AND PLATELETS FOR TRANSFUSION

BRITT VAN AELST

Rode Kruis
Vlaanderen

UNIVERSITEIT
GENT

BIOCHEMICAL AND FUNCTIONAL IMPACT OF PATHOGEN INACTIVATION ON PLASMA AND PLATELETS FOR TRANSFUSION

BRITT VAN AELST

Promotor:
Prof. Dr. V. Compernolle

Proefschrift voorgelegd tot het behalen van de graad van
Doctor in de Geneeskunde en gezondheidswetenschappen

2016

Promotor:

    Prof. Dr. Veerle Compernolle

        Department of Clinical Chemistry, Microbiology and Immunology, Ghent University, Belgium

Members of the PhD guidance committee:

    Prof. Dr. Katrien Devreese

        Department of Clinical Chemistry, Microbiology and Immunology, Ghent University, Belgium

    Prof. Dr. Lucien Noens

        Department of Internal Medicine, Ghent University, Belgium

    Dr Hendrik B. Feys

        Transfusion Research Center, Red Cross-Flanders in Ghent, Belgium

Members of the jury:

    Prof. Dr. Jan Philippé

        Department of Clinical Chemistry, Microbiology and Immunology, Ghent University, Belgium

    Prof. Dr. Bruno Verhasselt

        Department of Clinical Chemistry, Microbiology and Immunology, Ghent University, Belgium

    Prof. Dr. Kathleen Van Craenenbroeck

        Department of Biochemistry and Microbiology, Ghent University, Belgium

    Prof. Dr. Christophe Ampe

        Department of Biochemistry, Ghent University, Belgium

    Prof. Dr. Claude Cuvelier

        Department of Medical and Forensic Pathology, Ghent University, Belgium

    Prof. Dr. Rebecca Cardigan

        Department of Haematology, Cambridge University, United Kingdom

    Prof. Dr. Judith Cosemans

        Department of Biochemistry, Maastricht University, the Netherlands

PREFACE

I've found a beauty in seeing how complex and sophisticated, but logically these pathways have evolved. It's a challenge to get to know every single little piece of that puzzle. Worth to mention the membrane, a structure of which once was believed it was just a barrier to shield off the cytosolic fraction of a cell. Yet today many questions are open to resolve its contribution to cell signal transduction. If only we could miniaturize and take a walk on the membrane to behold its actions and movements. One thing is for sure, in a cell and on a membrane nothing happens without a reason.

SUMMARY

Pathogen inactivation technology (PIT) is developed to decrease transfusion transmitted infections. The methods on the market today use ultraviolet light illumination with or without a photosensitizer. The impact of these treatments on products for transfusion is not clear and therefore we thoroughly investigated the quality of blood products following PIT treatment.

In the first chapter, three different PIT developed for treatment of plasma are compared. The activity and concentration of plasma proteins was studied with a focus on ADAMTS13 as a sentinel molecule for relevant plasma components. The different PIT methods all affected ADAMTS13, FVIII and fibrinogen albeit to different degrees. The pathogen inactivation method using riboflavin (RF-PRT) as a photosensitizer had the largest impact on plasma which was caused by reactive oxygen. Our data were the first to show that removal of dissolved oxygen protected plasma proteins during RF-PRT treatment.

In the following chapters, we examined the influence of PIT on platelet concentrates. For this, platelet function was assessed in microfluidic flow chamber experiments. These indicated a decreased platelet function for all PIT compared to untreated controls. Additional experiments showed that the underlying mechanisms of platelet damage were different for each PIT however resulting in similar decreased thrombus formation in flow chambers.

In the last chapter, biochemical research on platelets treated with AS-PCT found a specific inhibition of the PI 3-kinase signal transduction pathway. This was caused by covalent binding of amotosalen to acyl chains of membrane phospholipids changing the overall membrane structure. This phenotype was also found in T lymphocytes following extracellular photopheresis in a patient being treated for graft-versus-host disease. So research initiated from the observation that platelet function is decreased following AS-PCT has uncovered a fine-tuning role for phospholipid acyl chains in the regulation of PI 3-kinase signal transduction.

SAMENVATTING

Pathogeen inactivatie technologie (PIT) is ontwikkeld om de kans op een transfusie overdraagbare infectie te verlagen. De methodes die momenteel operationeel zijn, maken gebruik van belichting al dan niet in combinatie met een fotosensitizer. De impact van deze behandelingen op de kwaliteit van transfusieproducten is niet altijd duidelijk en daarom onderzochten wij de kwaliteit van bloedproducten die behandeld werden met PIT.

In het eerste luik vergeleken we drie PIT voor de behandeling van plasma. De activiteit en concentratie van plasma eiwitten werd bestudeerd met onder andere ADAMTS13 als referentie-eiwit voor relevante plasma componenten. Uit deze studie bleek dat zowel ADAMTS13, FVIII als fibrinogeen bij de drie methodes aangetast waren. De pathogeen inactivatie methode die gebruik maakt van riboflavine (RF-PRT) als fotosensitizer, vertoonde de grootste impact, veroorzaakt door oxidatieve stress. Onze data waren de eerste om aan te tonen dat de schade aan plasma eiwitten beperkt kon worden door de opgeloste zuurstof vóór de RF-PRT behandeling te verwijderen.

Vervolgens onderzochten we de invloed van PIT op bloedplaatjesconcentraten. Eerst werd de functie van de bloedplaatjes met behulp van flow kamer experimenten bestudeerd. Deze toonden een daling in functionaliteit aan voor de drie methodes. Bijkomende functionele experimenten wezen echter op verschillende onderliggende mechanismen.

In het laatste onderdeel werd voor de bloedplaatjes behandeld met AS-PCT een specifiek defect in de PI 3-kinase signaal transductie cascade gevonden. Dit werd veroorzaakt door een covalente binding tussen amotosalen en de vetzuurzijketens van membraan fosfolipiden, met een verandering in de structuur van de celmembraan tot gevolg. Inhibitie van PI 3-kinase kon bovendien ook aangetoond worden in de T-lymfocyten van een graft-versus-host patiënt na behandeling met extracorporele fotoferese.

LIST OF ABBREVIATIONS

ADP	Adenosine diphosphate
Akt	Protein kinase B
AS	Amotosalen
AS-PCT	Amotosalon Photochemical Treatment (Intercept Blood System, Cerus Corp, Concord, CA)
Btk	Bruton's Tyrosine kinase
CalDAG-GEF1	Calcium and DAG-regulated guanine nucleotide exchange factor
cAMP	Cyclic adenosine monophosphate
CCI	Corrected Count Increment
CMV	Cytomegalovirus
COX-1	Cyclo-oxygenase 1
CPD	Citrate Phosphate Dextrose Solution
DAG	Diacylglycerol
ECP	Extracorporeal photopheresis
FcR	Fc receptor
GDP	Guanosine disphosphate
GPCR	G-protein coupled receptor
GTP	Guanosine triphosphate
GvhD	Graft-versus-host disease
HBV	Hepatitis B-Virus
HCV	Hepatitis C-Virus
HIV	Human Immunodeficiency Virus
HLA	Human Leukocyte Antigen
HPA	Human Platelet Antigen
IP3	Inositol 1,4,5- trisphosphate
ITAM	Immunoreceptor, tyrosine-based activation motif
LAT	Linker for activation of T cells
MBT	Methylene Blue Technology
NAT	Nucleid Acid Testing
Orai1	Calcium release-activated calcium channel protein 1
PAR	Protease-activated receptor
PAS	Platelet Additive Solution
PC	Phosphatidylcholine
PDK1	3-phosphoinositide-dependent protein kinase 1
PG	Phosphatidylglycerol
PH	Pleckstrin Homology
PI 3-kinase	Phosphatidylinositol 3-kinase
PIT	Pathogen inactivation technology
PKC	Protein kinase C
PLC	Phospholipase C
PI(3,4)P2	Phosphatidylinositol 3,4-bisphosphate
PI(3,4,5)P3	Phosphatidylinositol 3,4,5-trisphosphate
PI(4,5)P2	Phosphatidylinositol 4,5-bisphosphate
PTEN	Phosphatase and tensin homolog
RBC	Red Blood Cell
RF-PRT	Riboflavin Pathogen Reduction Technology (Mirasol Pathogen Reduction Technology, TerumoBCT, Lakewood, CO)
RhD	Rhesus D
ROS	Reactive oxygen species
RTK	Receptor tyrosine kinase
SARS	Severe Acute Respiratory Syndrome
SFK	Src family kinase
SH2	Src Homology 2
STIM1	Stromal interaction molecule 1
Syk	Spleen tyrosine kinase
TP	Thromboxane receptor
TTI	Transfusion Transmitted Infection
TXA2	Thromboxane A2
UVA	Ultraviolet A
UVC	Ultraviolet C
UV-C	Ultraviolet C Pathogen Inactivation (Theraflex UV-platelets, Macopharma, Tourcoing, France)
VWF	Von Willebrand factor

TABLE OF CONTENTS

PART 1
INTRODUCTION

1. THE PATHWAY OF BLOOD

1.1 COLLECTING BLOOD

1.1.1 DONOR RECRUITMENT AND SELECTION
The pathway of blood starts with the donor. In 2014 there were close to 185,000 donors that made it possible to collect 372,759 successful donations in Flanders. Bearing in mind that only 3% of the population donates blood while more than 70% will need blood in the course of their lives, donor recruitment is a very important aspect in the pathway of blood. Several awareness campaigns successfully recruited 41,339 new donors in 2014[1] **(Figure 1)**.

Figure 1: Campaign banner.
It is used to promote blood donation by the Red Cross-Flanders donor relation service.

In a first step, careful consideration of donor and patient health helps to minimize product wastage and to reduce risks inherent to transfusion. For this, a questionnaire is filled out by the candidate donor. The questionnaire is designed according to the medical donor selection guideline which follows European and Belgian legislation based on scientific evidence and recommendations of the Federal Agency for Medicines and Health Products, and the Superior Health Council. The filled in and signature confirmed questionnaire is analysed in a private consultation with a trained medical doctor who performs a basic medical anamnesis to assess donor well-being and risk behaviour carefully. This questionnaire and medical examination protects the donor by setting minimum thresholds of different criteria like haemoglobin levels and total blood volume by donor weight. On the other hand, these serve as first-line elimination tools to prevent transfusion transmittable disease[2,3]. The inquiry to risk behaviour like overseas travelling, ongoing or past medical treatments and specific sexual activities is intended to mitigate the risk for receiving patients. Furthermore, donor selection is important to minimize wastage of resources caused by collecting blood from unsuitable donors, exemplified by the 92 million worldwide donations and 13 million prospective donor deferrals due to anaemia and other medical conditions[4].

1.1.2 WHOLE BLOOD COLLECTION
Whole blood is the most common collection type, for which 87% of our donors are signing in. Before venepuncture, the phlebotomy site is disinfected to avoid contamination of the blood by skin bacteria[5]. The first 25mL is deviated to a sample bag and will be used for laboratory tests. Then, depending on the gender, weight and height of the donor, 470mL or 400mL blood is drawn into a specialized sealed and sterile bag containing Citrate Phosphate Dextrose Solution (CPD)[6] to prevent coagulation. The duration of the donation is 9 minutes, on average. Donors are allowed four whole blood donations a year, with minimally 60 days in between. After collection the unit is thermostatized to 20-22ºC in specially designed klimacontainers **(Figure 2)**. These are then transported to the manufacturing sites for blood component preparation[7].

Figure 2: Klimacontainer.
The klimacontainer is equipped with temperature sensors and keeps fresh whole blood at 20-22ºC.

1.1.3 APHERESIS

Another way to collect blood products is by apheresis. It is a more expensive and time consuming technology but only the desired components (plasma and/or platelets and/or red blood cells and/or granulocytes) are collected. It is less common than whole blood donation with about 11% of the donors signing in for plasmapheresis and roughly 2% for thrombopheresis[8]. Yet, these thrombopheresis products do account for 50% of the platelet concentrates produced in Flanders. A major advantage of apheresis is the increased flexibility towards the donor as (s)he can choose for only plasma or a combination of plasma and platelets. Because red blood cells are not collected with plasma- and thrombopheresis, the likelihood of developing post-donation anaemia, is very small allowing donation every two weeks. Apheresis allows to invite donors for targeted donation with specific human leukocyte antigen (HLA) and human platelet antigen (HPA) profiles for patients, refractory to certain phenotypes due to antibodies against HLA or HPA.

Depending on the donors height and weight, up to 650 mL plasma can be collected over 45–60 minutes in a plasmapheresis procedure. During this procedure, blood is collected in 4% sodium citrate anticoagulant and plasma is separated from cells and pumped into a collection bag. The cellular fraction is returned to the donor with 500mL of saline solution to replace the donated volume. In the Red Cross-Flanders, 20% of the collected plasma is obtained by plasmapheresis.

During dual apheresis of platelets and plasma an average of 350mL plasma and 5.5×10^{11} platelets is collected during a 60-100 minutes procedure. Like in plasmapheresis, the remainder cellular components are returned to the donor with 500mL of saline.

1.2 TESTING BLOOD

To prevent transfusion transmitted infections (TTI), the donor questionnaire and laboratory screening tests fulfil complementary roles. Laboratory tests are performed on every donation using the deviated blood sample that is taken in a separate pouch prior to donation. The Central Laboratory of the Belgian Red Cross-Flanders performs these tests which include serological tests, nucleid acid tests (NAT) and complete blood counting.

Serological tests are used to test the presence of hepatitis C-virus (HCV), hepatitis B-virus (HBV), human immunodeficiency virus (HIV) and Treponema pallidum (syphilis). Routine NAT is a multiplex-assay of a pooled sample of 6 donations to assess the presence of HIV-RNA, HCV-RNA and HBV-DNA. When this combined sample is positive, discriminatory experiments are performed on each of the six samples included to differentiate what specific donation and what virus is involved. Depending upon the results of the medical questionnaire, additional tests for Trypanosoma cruzi, malaria or hepatitis B core antibodies are conducted. Additional laboratory work includes blood group determination, irregular blood group antibodies and whole blood cell counting to measure hemoglobine, red blood cell, white blood cell and platelet counts[9].

1.3 PROCESSING BLOOD

Following collection, transportation and temporary storage, the whole blood is separated into two (red blood cells and plasma) or three (red blood cells, plasma and platelets) components **(Figure 3)**. This fate is linked to the type of container the blood was collected in. Blood is separated by centrifugation exploiting the differences in size and density of the blood constituents. During a 'hard spin' centrifugation, the red cells condense at the bottom of the container. The white blood cells and platelets sediment on top of these red cells, leaving plasma as a supernatant. Using an automated separator, red blood cells and plasma are transferred through top and bottom tubings, respectively until only the buffy coat remains in the original collection bag.
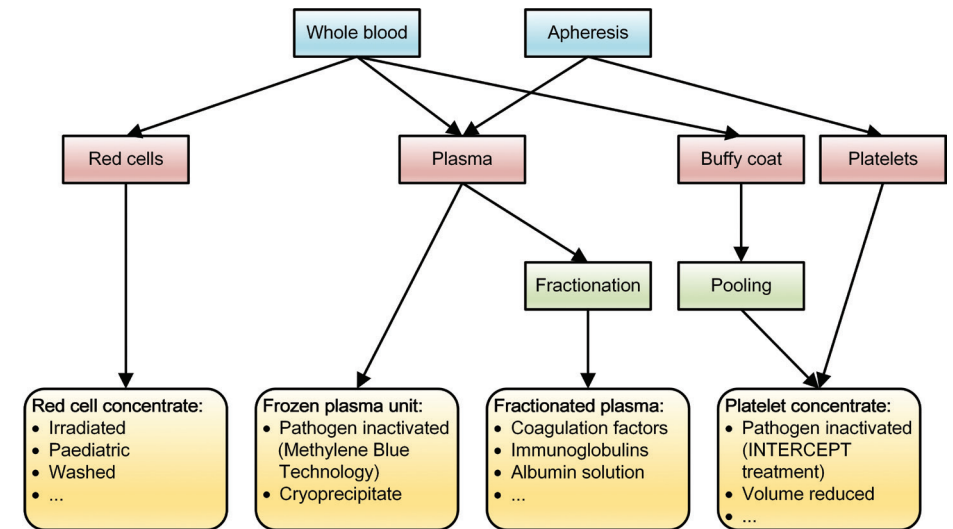
Figure 3: Blood processing. *Schematic of blood component routes in Red Cross-Flanders.*

1.3.1 RED BLOOD CELLS

After centrifugation and separation, leukocytes are removed by filtration (targeting $<1.0 \times 10^6$ leukocytes per unit) and an additive solution, saline-adenine-glucose-mannitol (SAGM) is added which supports preservation of red blood cell concentrates during 42 days of storage at 2-6°C[10]. The tubing connected to the storage bag contains red blood cells and is sealed in segments of approximately 5 cm in length. These are used as samples in the immunohematology laboratory for typing and cross matching prior to transfusion. An additional production step is 25-50 Gray gamma irradiation to prevent lymphocyte proliferation in the host[11]. Following this manipulation, red blood cell concentrate shelf life is shortened to 28 days, but these units can be transfused to

immunocompromised patients at risk of graft-versus-host disease (GvhD).

About 85 million red blood cell units are transfused worldwide[12] for the treatment of clinically significant anaemia. Anaemia occurs in a wide variety of diseases which can be acquired by malignancies or infection, or they can be inherited like in sickle cell disease. Furthermore, blood loss during surgery or after trauma is a common indication for red blood cell transfusion[13].

Some blood components are modified for specific indications and patient groups, like washed red blood cells for patients with recurrent severe allergic transfusion reactions or Cytomegalovirus (CMV) negative units for intrauterine red blood cell transfusions. Though, all transfusions should be ABO and Rhesus D (RhD) compatible and will raise the hemoglobin of an average size adult by 1g/dL for each red blood cell concentrate, helping the oxygen-carrying capacity to restore[14].

1.3.2 PLASMA

To maintain the quality, fresh plasma is frozen within 24 hours after collection. If not, labile clotting factors deteriorate and protein extraction is less productive. During the freezing process, a core temperature below -30ºC must be reached within one hour from the time freezing starts. Fresh frozen plasma is then sold to a fractionation centre where coagulation factors, immunoglobulins and albumin solutions are prepared by extraction from a pool of several thousand blood donations. The products obtained by fractionation are used to treat different disorders. Coagulation factors are used for treatment and prophylaxis to prevent bleeding in patients with a clotting disorder, linked to a specific coagulation factor deficiency, like haemophilia A (Factor VIII) or B (Factor IX) or von Willebrand Disease (VWF-FVIII concentrate)[15]. The immunoglobulin fraction is used for protein replacement therapy for immune deficient patients who have decreased or abolished antibody production capabilities, for example patients with idiopathic thrombocytopenic purpura or Kawasaki disease[16]. The albumin fraction is used to treat conditions associated with pronounced hypoproteinemia like nephrotic syndrome or extensive and serious burns[17].

Some of the collected plasma is not sold for fractionation, but is treated instead with a photochemical pathogen inactivation method to obtain pathogen inactivated plasma. To this purpose, remainder cells and debris are removed by filtration prior to the Methylene Blue Technology treatment (MBT, Macopharma, Tourcoing, France or Baxter International Inc, Deerfield, IL). After the addition of methylene blue (final concentration 0.8 to 1.2μM), the units are illuminated with visible light (630nm). The photo-activated methylene blue then damages nucleic acids preventing proliferation of pathogens and donor derived leukocytes. Finally, methylene blue is removed by a second filtration step and the units are frozen and preserved at -30ºC.

Methylene blue pathogen inactivated plasma contains all coagulation factors and additionally serum salts, sugars, fats, hormones and vitamins. This blood product is used for patients with a coagulopathy who are bleeding or at risk of bleeding, and where a specific therapy or factor concentrate is not appropriate or unavailable. For instance, to treat thrombotic thrombocytopenic purpura or when several labile plasma coagulation factors need to be replaced, i.e. during massive transfusion[18,19].

1.3.3 PLATELETS

Platelet concentrates are prepared from apheresis or from pooling of buffy coats. The main difference between these products is the multitude of exposure to donor material by the host. To produce buffy coat pooled platelet concentrates, five to six buffy coats of the same ABO blood group are pooled and supplemented with platelet additive solution (PAS)(SSP+, Macopharma). A 'soft spin' centrifugation step sediments the residual red and white blood cells while the platelets largely remain suspended in the plasma/PAS supernatant. This platelet rich supernatant is transferred to a platelet bag through automated separators. After pathogen inactivation, the platelets are stored at 22 ± 2ºC under continuous, gentle agitation in a storage container composed of semipermeable plastic to allow exchange of metabolic gas. Some countries allow storage for 7 days while others for 4 days. Belgian legislation (2005) allowed extended storage to seven days in the case a validated system for bacterial growth was in place (which was the case in Flanders since 1998). However, the internal medical committee of our organisation questioned the quality of PAS stored platelets preserved for longer than five days and opted not to implement a seven day storage time. When pathogen inactivation was introduced in 2009 in the southern part of Belgium, a seven day shelf life was introduced for PI platelets. However in 2009, following an advice of the Superior Health Council of Belgium concerning the therapeutic efficiency of pathogen inactivated platelet concentrates, the Federal Agency for Medicines and Health Products issued a recommendation to limit storage time to five days (and an minimal content of 3 x 10^{11} platelets per product) because of eight cases of cerebral hemorrhage (of which two were fatal) shortly after PIT implementation.

Worldwide, 4 million platelet concentrates are transfused each year. They can be used for therapeutic treatment of patients with bleeding due to functional abnormal platelets or severely decreased platelet concentration. On the other hand, platelets can also be administered prophylactically to mitigate the risk of bleeding in patients with rapidly falling or low platelet counts secondary to cancer, chemotherapy, bone marrow failure or other primary conditions[18,20].

1.3.4 PATHOGEN INACTIVATION OF BLOOD COMPONENTS

As mentioned before, the donor questionnaire and the prevailing exclusion criteria are the first instrument to avoid TTIs. In conjunction with laboratory screening of known pathogens, it reduces the risk of TTI dramatically and has rendered transfusion increasingly safe. Today the residual risk for viral TTIs is decreased to 1/1,467,000 for HIV, 1/1,149,000 for HCV[21] and 1/282,000 for HBV[22]. For bacterial TTIs however, it are mainly the platelet concentrates that are vulnerable as their storage temperature is high enough for germ growth (22 ± 2ºC), with an estimated risk of 1/2-3,000. These bacterial TTIs are the major cause of transfusion related morbidity and mortality because transfusion-related bacterial sepsis (1/20-50,000) can be fatal in 10% of cases[23]. Besides the known viral and bacterial TTIs, the emerging pathogens like Chagas disease, Dengue, Chikungunya-virus, West Nile virus and Severe Acute Respiratory Syndrome (SARS) are a weighty argument to consider implementation of pathogen inactivation of blood components[24].

Emerging pathogens are in the spotlight, because tests are not routinely available and often very expensive. Besides, the large biological diversity of (opportunistic) pathogens infecting humans, makes implementation of tests for each of these unrealistic. Several pathogen inactivation technologies (PIT) are available for the treatment of blood components[25]. An overview is given in **Table 1**. For platelet concentrates and plasma three of these methods use ultraviolet light (UV) illumination in combination with an exogenously added photosensitizer to damage nucleic acids and one uses UV-C illumination alone[26]. These methods are not suitable to treat RBC containing blood products because the optical properties of densely packed hemoglobin requires very high doses of light. Some companies are developing a different approach suitable to treat RBC concentrates and whole blood[27,28].

	Solvent-detergent (SD) method	Methylene Blue technology	UVC technology	Riboflavin/UV technology	Amotosalen/UVA technology	S-303 technology
Blood component	Plasma	Plasma	Platelets	Plasma / Platelets	Plasma / Platelets	Red blood cells
Technology	Chemical	Photochemical	Photochemical	Photochemical	Photochemical	Chemical
Active compound	Trinitrobutyl phosphate and Triton X-100	Methylene Blue	/	Riboflavin	Amotosalen (S-59)	S-303
Wavelength	/	Visible light	UVC	Broad spectrum	UVA	/
Additional step	Fitration	Filtration	/	/	Filtration	Glutathione
Mechanism	Membrane disruption	Nucleic acids damage by reactive oxygen	Nucleic acids damage by pyrimidine dimer formation	Nucleic acids damage by reactive oxygen and cross-linking	Nucleic acids damage by cross-linking	Nucleic acids damage by cross-linking
Status **PLASMA**	Used in 32 countries FDA approved in 2013	Used in 15 countries	/	Used in 11 countries CE mark class IIb	Used in 13 countries CE mark class III FDA approved in 2014	/
PLATELETS	/	/	Phase III clinical trial CE mark class IIb	Used in 18 countries CE mark class Iib	Used in 22 countries CE mark class III FDA approved in 2014	/
RED BLOOD CELLS	/	/	/	/	/	Phase III clinical trial
Clinical trials **PLASMA**	No difference in clinical efficacy	Reduced effectivity: required more exchanges	/	Trials ongoing	No difference: recovery, tolerance and efficacy OK	/
PLATELETS	/	/	/	Reduced CCI: primary endpoint not met*	Reduced CCI*	/
RED BLOOD CELLS	/	/	/	/	/	Trials ongoing

Cfr 1.3.4.2 for more details

Table 1: Overview of the available pathogen inactivation technologies for blood components[25,28-30]

1.3.4.1. PLASMA

Different bench-top technologies applicable to single units of plasma are available. The Mirasol Riboflavin (vitamin B2) pathogen reduction technology[31] (RF-PRT, TerumoBCT, Lakewood, CO) with broad spectrum UV light, INTERCEPT amotosalen (S59) photochemical treatment[32] (AS-PCT, Cerus Corp, Concord, CA, USA) with UVA, and THERAFLEX Methylene Blue Technology[33] (MBT, Macopharma) with visible light are used to treat plasma products. The mechanisms of action described by these suppliers is that the chemical sensitizers intercalate in helical regions of RNA and DNA and form irreversible adducts and cross-links with pyrimidines following photoexcitation. Consequently, replication of cells/viruses is prevented. Although these treatments provide additional safety for fresh plasma products, they degrade product quality to some degree. This has been demonstrated by our group in an in vitro paired study comparing all three methods[34].

1.3.4.2 PLATELETS

RF-PRT and AS-PCT were originally developed and are most widely known for the treatment of platelet concentrates. Besides these two, a third method (THERAFLEX UV-PLTs, UV-C, Macopharma) uses short-wavelength UVC light in the absence of exogenously added photosensitizer[35]. As with plasma, the product quality of platelet concentrates after treatment is a subject of research and debate. *In vitro* assays have investigated the matter but conflicting reports require a critical read of available results[36-41]. For example, Apelseth T.O. et al concluded a generally reduced *in vitro* quality of platelets treated with AS-PCT[36], while Hechler B et al state that they have similar functional, morphologic and proteomic characteristics[37]. However, in the latter one, AS-PCT treated platelets were washed and resuspended in Tyrode's buffer before testing.

As of April 2015 platelet concentrates prepared by our facilities are all treated with pathogen inactivation (AS-PCT) compliant to the Royal Decree of June 17th, 2013. Belgium was the first country to adopt legislation on pathogen inactivation for platelet concentrates, despite delays in implementation caused by a number of issues during the course of the past years. These events are summarized in **Table 2** and were influenced by the outcomes of the clinical trials over time. Ten completed trials comparing pathogen inactivated platelets with standard platelets were analysed by a Cochrane review published in 2013[42]. Nine trials assessed AS-PCT (1312 patients) and one RF-PRT (110 patients). Trials of multiple pathogen inactivated platelets showed a significant shorter transfusion interval and the participants required 7% more platelet transfusions. The corrected count increments at 1 and at 24 hours were significantly lower following pathogen inactivated platelet transfusions compared to standard platelets. Furthermore, the meta-analysis demonstrated no differences in mortality, clinical significant bleeding or severe bleeding between treatment arms. Five trials, however, reported a significant increase in 'any bleeding' in the pathogen inactivated platelets arm using a fixed-effect model (favouring standard platelets). The conflicting results of these two analysis makes it difficult to interpret. It shows the need for studies with reliable design, relevant endpoints and sufficient statistical power.

The hemovigilance data of Belgium suggest that Intercept PIT reduces bacterial transfusion-transmitted infections. More than 150 000 pathogen inactivated platelet concentrates have been transfused since 2009. None of them provoked bacterial transfusion-transmitted infections. In the same time period, 4 bacterial transfusion-transmitted infections were reported in approximately 186 000 standard platelet transfusions.

1.3.4.3 RED BLOOD CELLS

For the red blood cell concentrates a different approach is needed. Their greater viscosity and the absorption spectrum of haemoglobin prohibits the use of illumination. The S-303 pathogen and leukocyte inactivation system includes glutathione as a quencher for oxidative side-effects[27]. The compound S-303 acts as a pathogen inactivator in the intracellular compartment where it targets and cross-links nucleic acids to prevent further replication. After this, a breakdown product S-300 is formed and rapidly degraded. The quenching glutathione is included to minimize extracellular reactions with common nucleophiles. Treatment solution and breakdown products are partially removed by centrifugation before storage. This method is under development by Cerus Corporation and phase III clinical trials are ongoing[43].

Table 2: Chronological series of decisive events during and following the mandatory implementation of PIT for platelets in Belgium (2009).

Date	Authority	Decision or recommendation	Reason
2005/02/01	RD	Platelet concentrates can be stored for 7 days, provided bacterial screening or PIT	
2009/06/28	RD	National mandatory implementation of PIT on platelets starting July 2010	SHC recommends national mandatory implementation of PIT on platelets
2009/11/16	FAMHP/ SHC	Platelets treated with PIT should at least contain 3×10^{11} platelets and shelf-life limited to 5 days	Hemovigilance annals reports 8 registered hemorrhage cases despite transfusion of platelets treated with PIT (Int), including 2 deaths by cerebral hemorrhage.
2010/06/13	RD	National mandatory implementation of PIT on platelets postponed until July 2011	Further advice on clinical efficacy of photochemical PIT required
2010	FAMHP		Hemovigilance annals reports 4 registered hemorrhage cases despite of transfusion of PIT treated platelets (Int), including 1 death by cerebral hemorrhage.
2011/07/29	BRC-F BE	Cessation of PIT (Mir) implementation at BRC-F BE	Perforation of bags by breaking pen shatter: registered frequency of leakages in the final PRPC >1/500
2011/06/01	SHC	SHC recommends national mandatory implementation of PIT on platelets, extensive hemovigilance analysis and repeats restrictions to product content and shelf-life	FAMHP seeked advice on clinical efficacy of photochemical methods
2011/06/28	RD	National mandatory implementation of PIT on platelets is postponed until July 2013	
2012/12/24	BRC-F BE	Premature abortion of validation for routine implementation of PIT on platelets	>50% of products (Mir) fail quality control during validation
2013/06/17	RD	National mandatory implementation of PIT on platelets is postponed until July 2015	

PIT=Pathogen inactivation technology; RD=Royal Decree; Federal Government decision; SHC=Superior Health Council; the scientific advisory body of the Federal Public Service of Health, Food Chain Safety and Environment; FAMHP=Federal Agency for Medicines and Health Products; the competent authority responsible for the quality, safety and efficacy of medicines and health products; BRC-F BE=Belgian Red Cross-Flanders Blood Service; Belgian Regional Blood Establishment; Int=Intercept Blood System; amotosalen and ultraviolet A light treatment ; Mir=Mirasol Pathogen Reduction Technology; riboflavin and broad spectrum ultraviolet light treatment.

2. PLASMA

2.1 PLASMA: THE LIQUID COMPONENT OF OUR BLOOD

This pale yellow liquid part of anticoagulated blood, remains after separation from the cellular components as described above. It makes up about 55% of the body's total blood volume. Beside water as its main constituent, plasma contains low molecular weight (glucose, the whole set of amino acids, nucleotides, vitamins, hormones, fatty acids, lipids, etc.) and high molecular weight components (peptides, proteins, saccharides, etc), dissolved gases and products of the metabolism. Furthermore, plasma contains ions which are essential for several biological processes and the maintenance of a constant pH. The plasma transports nutrients to the cells of various organs, and waste products to the kidneys, liver and lungs. It carries red blood cells, white blood cells and platelets, transporting oxygen, providing an immune response, and delivering clotting agents[44,45], respectively.

2.2 THE PLASMA PROTEOME

The thousands of proteins, which are dissolved in plasma are divided in different categories, each with its own properties and function[46].

2.2.1 ALBUMIN

This multifunctional, non-glycosylated, negatively charged plasma protein comprises 50% of the total plasma protein content. With only 66kDa, it is a relative small protein compared to other plasma proteins[47]. Albumin is synthesized in the liver. It contains three homologous domains and each consists of two separate helical subdomains, connected by random coil[48]. Albumin possesses extraordinary ligand binding properties and thereby transports a diversity of molecules[49]. Because of its abundance, its carrier function is important in pharmacokinetics of many drugs, influencing efficacy and rate of delivery[50]. Furthermore, at high concentration and strong negative charge, albumin is responsible for around 70% of plasma oncotic pressure and therefore plays a pivotal role in modulating the distribution of fluid between compartments[51].

It has not been clearly determined whether there is a threshold concentration of albumin below which its oncotic function is compromised to a clinically relevant degree. There is, however, a consensus that oncotic activity remains physiologically adequate at values of albumin ≥ 2g/dL and total proteins ≥ 3.5g/dL. Hypoalbuminemia can occur in acute conditions like hemorrhagic shock and major surgery or in chronic states, like liver cirrhosis and

nephrotic syndrome. It may have life-threatening effects as it results in extravascular fluid accumulation or increased concentrations of protein-bound drugs in the unbound form, leading to either adverse effects or rapid metabolism and decreased efficacy[52]. Solution of albumin is prepared in the fractionation centre from the plasma of healthy donors. When volume deficiencies have been demonstrated and the use of a colloid is indicated, albumin is infused in order to restore and maintain the blood circulation volumes [53].

2.2.2 GLOBULIN
Although globulins make up a smaller fraction (36%) of blood plasma protein and include protein carriers, enzymes, gamma globulin and immunoglobulins. Globulins are actually subdivided into four major categories: gamma globulin, alpha-1 globulin, alpha-2 globulin, and beta globulin. The former one contains immunoglobulins and is the specific group of plasma proteins that functions as antibodies providing protection against disease on a cellular level. The alpha and beta globulins primarily act as transporters for fat soluble vitamins, hormones and lipids[45].
Immunoglobulins prepared at the fractionation centre from the plasma of healthy donors, is used as an 'immunomodulatory' agent in an increasing number of immune and inflammatory disorders[54]. Intravenous globulin therapy is either a substitution therapy in the case of primary immunodeficiency syndroms or a immunomodulatory therapy in the case of allogeneic bone marrow transplant or Kawasaki disease[55].

2.2.3 COAGULATION PROTEINS
The coagulation proteins are the core components of the coagulation system; the complex interplay of reactions resulting in the conversion of soluble fibrinogen to insoluble fibrin fibers[56]. Two key players relevant for transfusion are fibrinogen and factor VIII.
Fibrinogen is a 340kDa glycoprotein comprising 4% of the total plasma protein content at a concentration of 2g/L to 4g/L[57]. It consist of two disulfide-linked monomers, each containing three different polypeptide chains, Aα, Bβ and Cγ[58]. In the coagulation cascade, fibrinogen is converted to fibrin when thrombin cleaves off the peptides A and B from the amino-terminal segments of the fibrinogen Aα-and Bβ-chains. Soluble fibrinogen is thus converted into fibrin monomers, which can form insoluble fibrin polymers and a network of fibrin fibers catalyzed by the action of (activated) FXIII. This cohesive network also provides a temporary support for wound healing[59]. In transfusion medicine, plasma-derived fibrinogen concentrate is the replacement therapy of choice in patients with afibrinogenemia. It is virally inactivated, a smaller infusion volume is needed and the risk of allergic reactions is lower compared to the use of cryoprecipitate or FFP[60].
Factor VIII participates in the middle phase of the intrinsic pathway of blood coagulation where it functions as a cofactor in the factor IXa-mediated conversion of factor X to factor Xa. It is synthesized as a single polypeptide chain, but circulates in plasma as a two-chain

molecule non-covalently linked to von Willebrand factor. Factor VIII circulates in plasma in an inactive form that is proteolytically cleaved by factor Xa and/or thrombin in the presence of calcium and negatively charged phospholipids, to yield factor VIIIa[61]. Mutations in the *factor VIII* gene can result in hemophilia A[62], a mild to severe bleeding disorder. A replacement therapy with intravenously delivered plasma-derived FVIII concentrates, aimed at correcting the coagulation factor deficiency in the case of, or in order to prevent, bleeding in patients with hemophilia A. As with the fibrinogen replacement therapy described above, this specific and viral-inactivated product is the source of choice over cryoprecipitate or FFP[63].

2.2.4 REGULATORY PROTEINS
Other plasma proteins are regulatory proteins, such as enzymes, proenzymes and hormones. One of those enzymes is ADAMTS13. It circulates as an active enzyme in plasma at a concentration of approximately 5nM[64] and cleaves VWF multimers, decreasing their avidity for platelet GPIb-IX-V complex[65]. A deficiency in ADAMTS13 causes thrombotic thrombocytopenic purpura which is a rare systemic disorder where ultra-large VWF multimers cause accumulation of platelet microthrombi in the (micro)vasculature. These lead to thrombotic occlusion of small blood vessels and platelet consumption with severe thrombocytopenia. Disseminated multi-organ ischemia ultimately leads to death if untreated[66]. In transfusion medicine, this disease is treated by plasma exchange in order to replenish ADAMTS13[67].

3. PLATELETS

3.1 PLATELETS: THE SMALLEST CELLS IN BLOOD

Circulating platelets have a life span of approximately 8 to 9 days and about 30% of platelets are residing in spleen and liver, resulting in an average turnover of 10^{11} platelets each day in a healthy adult[68]. The platelet precursor cell, called the megakaryocyte, originates from the bone marrow and is differentiated out of hematopoietic stem cells. One megakaryocyte at 50-100μm in diameter, can produce 2000 to 5000 platelets of 2-5μm[69]. Platelets are considered the smallest operating cells in circulating blood and adopt a discoid morphology while resting, but following activation they quickly change shape by extending filopodia and increasing their surface by more than 400%[70] **(Figure 4)**. Platelets are anucleate but contain distinct mitochondria, a dense tubular system, a highly specialized cytoskeleton and unique granules. Numerous proteins and biologically active molecules are stored in these granules that can be released during activation. The normal platelet count in human peripheral anticoagulated blood is 150,000 to 400,000 per microliter of blood[71]. In response to vascular damage, platelets form a plug to stop bleeding. They adhere to subendothelial matrix proteins like collagen and VWF. Following binding, platelets activate through a complex series of (signal transduction) events caused by triggering receptors. This results in shape change, granule secretion, integrin activation, aggregation and support of coagulation[72]. Recently, researchers in the Brass group demonstrated that platelet activation is not uniform throughout the hemostatic plug. Local variations in environmental chemistry and different elements of the platelet-signalling network work in concert to produce marked differences in the platelet activation state thereby regulating a single tailored hemostatic response to injury[73].
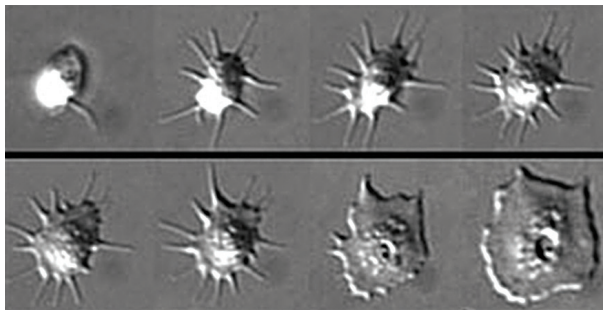
Figure 4: Platelet spreading. A differential interference contrast microscopic image series of a human platelet activating and spreading on a surface of immobilized fibrinogen[74].

3.2 SIGNAL TRANSDUCTION PATHWAYS IN PLATELET PLUG FORMATION

3.2.1 PLATELET ADHESION TO THE INJURED VESSEL WALL

The formation of thrombi at sites of vascular damage is the result of a concerted action of diverse signal transduction pathways **(Figure 5)**. This sequence initiates when the subendothelial extracellular matrix is exposed to blood. The mechanism for initial tethering and platelet adhesion to the exposed subendothelial matrix is influenced by the localized rheological conditions and prevailing flow rates[75]. At high shear ($>600s^{-1}$) encountered in (small) arteries, vascular VWF binds through the A1 and A3 domain to collagen fibres in the injured vessel wall, creating a landing strip for fast flowing platelets[76,77]. Circulating erythrocytes push platelets towards the vessel wall where a dynamic process of transient interactions between the platelet GPIb/IX/V complex and immobilized VWF decelerates platelets, allowing firm binding to collagen with GPVI and integrin $\alpha_2\beta_1$, and to VWF with integrin $\alpha_{IIb}\beta_3$. At low shear rates ($<600s^{-1}$) platelets can directly bind to damaged vessel wall proteins like collagen, fibronectin and laminin[78].

### 3.2.2 PLATELET ACTIVATION AND AGGREGATION

Following adhesion, co-ordinated signal transduction events occur downstream of multiple agonist receptors of which the most relevant are those responding to collagen, thrombin, adenosine diphosphate (ADP) and thromboxane A2 (TXA_2).

3.2.2.1 A CASCADE OF EVENTS STARTS WITH COLLAGEN BINDING

When platelets adhere to collagen fibres, a signal transduction cascade starts from GPVI activation **(Figure 6)**. This glycoprotein couples to a disulphide-linked Fc receptor (FcR) γ-chain homodimer in the cytoplasmic membrane. When GPVI clusters are formed, Src family tyrosine kinases Fyn and Lyn phosphorylate the immunoreceptor, tyrosine-based activation motif (ITAM) of the FCR γ-chain. This creates a docking site for the tandem Src Homology 2 (SH2) domains of Syk. The binding of this tyrosine kinase initiates a signal transduction cascade that leads to the formation of a linker for activation of T cell (LAT) signalosome and following activation of one of the major effector enzymes, phospholipase C (PLC) γ2[79]. Phospholipases hydrolyze phosphatidylinositol 4,5-bisphosphate (PI(4,5)P_2) to form diacylglycerol (DAG) and inositol 1,4,5- trisphosphate (IP$_3$). The latter diffuses through the cytosol and binds IP$_3$ receptors in the dense tubular system (DTS) which results in Ca^{2+} release into the cytosol. When the calcium pool in the DTS is depleted, a second rise of cytosolic Ca^{2+} is achieved by stromal interaction molecule 1 (STIM1) which triggers calcium entry from the extracellular compartment via calcium release-activated calcium channel protein 1 (Orai1). The simultaneously generated glyceride DAG is a lipid signal transduction molecule essential for localization and activation of protein kinases C (PKC). These play pivotal roles

in cytoskeleton reorganization through phosphorylation of its major substrate, pleckstrin[80], and in platelet granule secretion by elevating the inhibitory effect of cytohesin-2[81]. Rap1 calcium and DAG-regulated guanine nucleotide exchange factor 1 (CalDAG-GEF1) is another effector downstream of DAG and calcium elevations important in integrin $\alpha_{IIb}\beta_3$ activation[82]. This integrin makes a dramatic conformational change in its extracellular domain enabling the crucial interaction with fibrinogen to substantiate interplatelet binding[83]. Another pathway following receptor tyrosine kinase (RTK) activation involves phosphatidylinositol 3-kinase (PI 3-kinase). The PI 3-kinase family all catalyse phosphorylation of (phospho)inositides on the 3' position of the inositol ring. There are three classes, based on their structure and lipid substrate preferences. Class I is divided into 2 subclasses of which

Class IA represents heterodimers of a catalytic (p110α, p110β or p110δ) and regulatory subunit (p85α, P85β, p55α, p55γ or p50α) and class IB consist of heterodimers built from one catalytic subunit (p110γ) associating with either of three regulatory subunits p101 or p84/87. Class II PI 3-kinases catalyse the production of PI3P and PI(3,4)P$_2$. Finally, Class III PI 3-kinases form PI3P out of PI[84]. The class IA is activated downstream of tyrosine kinases which results in the transient formation of phosphatidylinositol 3,4,5-trisphosphate (PI(3,4,5)P$_3$) and phosphatidylinositol 3,4-bisphosphate (PI(3,4)P$_2$)[85]. Cytosolic kinases with pleckstrin homology (PH) domains like Protein kinase B (Akt) and Bruton's Tyrosine kinase (Btk) bind to these products and in turn are phosphorylated. The precise mechanisms of Akt, Btk or other PH-dependent kinases in regulating platelet activation are poorly understood[86].
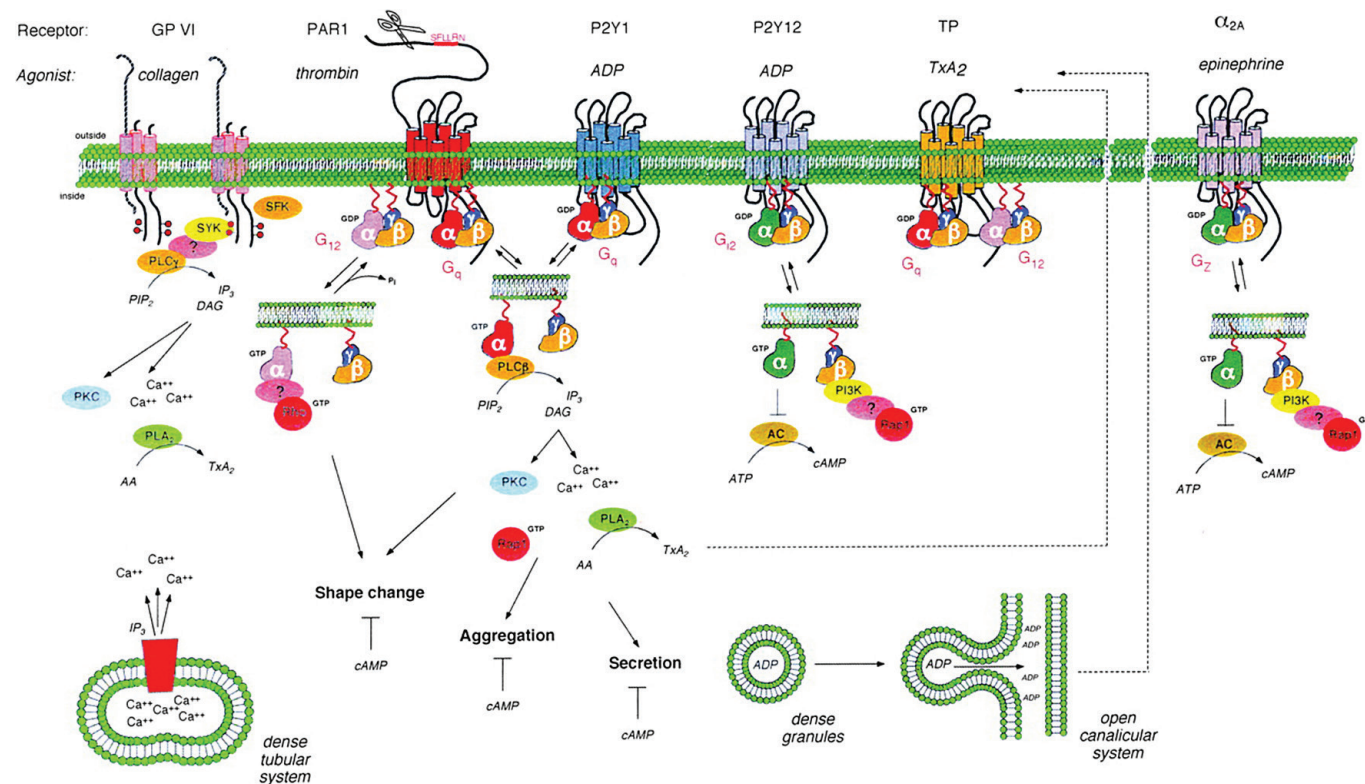
Figure 5: Overview of signal transduction during platelet plug formation[87].

3.2.2.2 EXPANDING ACTIVATION WHEN THROMBIN COMES ALONG

Thrombin activates platelets at concentrations below 0.1nM making it the most potent platelet agonist. Thrombin signals through protease-activated receptors (PAR), more specifically PAR1 and PAR4 on human platelets. Activation occurs when thrombin cleaves the extended PAR N-terminus, exposing a de novo N-terminus which functions as a tethered ligand for self-activation. PARs are G-protein-coupled receptors (GPCR), which are 7-transmembrane domain proteins transmitting signals through heterotrimeric G proteins. These consist of a guanine-nucleotide binding subunit , which is non-covalently linked to β and γ subunits. In the resting state, G_α is guanosine disphosphate (GDP) bound and associates with β and γ. Upon agonist engagement, GDP exchanges for guanosine trisphosphate (GTP) on G_α which causes dissociation from $G_{\beta\gamma}$. Downstream signal transduction specificities depend on the G protein subtype these receptors are coupled to[88].

PAR1 and PAR4 are both activated by thrombin and there is considerable overlap in signal transduction through activation of G_q, G_i and $G_{12/13}$ coupled isoforms. Yet, PAR1 and PAR4 have different roles in platelet activation. PAR1 causes an acute and short-lived reaction in response to low thrombin concentrations, while PAR4 causes a slower but sustained platelet activation only in response to high thrombin concentrations[89,90].

The signal transduction pathway through G_q causes PLCβ activation and consequent DAG and IP_3 formation[91]. The IP_3 secondary messenger stimulates Ca^{2+} mobilization. The subsequent increase in intracellular Ca^{2+} concentration activates or potentiates multiple proteins, including actin-myosin, calmodulin, NO synthases and calcium-dependent proteases. One of those is the exchange factor CalDAG-GEF1 which leads to integrin activation, TXA_2 synthesis and granule secretion[92]. Furthermore, the elevation of intracellular Ca^{2+} concentration stimulates the phosphorylation of certain PKC isoforms by DAG[93].

$G_{12/13}$ signals through Rho guanine nucleotide exchange factors, activating Rho kinase which phosphorylates and inhibits myosin light chain phosphorylation and contraction of actin. This leads to platelet shape change and granule secretion[94].

Finally, the signalling molecules of the G_i family are important for cyclic adenosine monophosphate (cAMP) concentration decreases through inhibition of adenylyl cyclase. Decreasing cAMP concentration is one of the primary mechanisms supporting sustained platelet activation through the P2Y12 receptor. Furthermore, the PI 3-kinase-Akt axis is downstream of G_i activation and cooperates sustained platelet responses[95].

3.2.2.3 AUTOCRINE AND PARACRINE ACTIVITIES OF ADP AND TXA_2

Compared to thrombin, platelet self-generated ADP and TXA_2 are less potent agonists by themselves, but are nonetheless very important synergistic activators absolutely required for efficient recruitment of platelets to the site of injury. Stimulation of P2Y1 and P2Y12 by ADP reinforces integrin $\alpha_{IIb}\beta_3$ inside-out activation and consolidates its interplatelet binding function[96]. It thus stabilizes the hemostatic plug through synergy with other platelet agonists[97]. P2Y12 is G_i coupled and marginally present on the resting cytoplasmic membrane. But upon activation, an inducible pool of P2Y12 receptors is exposed[98]. Besides inhibition of adenylyl cyclase, P2Y12 plays a crucial role in PI 3-kinase signal transduction[99]. P2Y1 on the other hand, is mainly G_q-coupled, resulting in PLC activation[100].
Like ADP, TXA_2 is a weak agonist by itself, but amplifies initial stimuli. TXA_2 is produced through the conversion of arachidonic acid by the cyclo-oxygenase 1 (COX-1) pathway and diffuses through the cytoplasmic membrane to bind thromboxane receptors (TP). TP is coupled to both G_q and $G_{12/13}$[101].
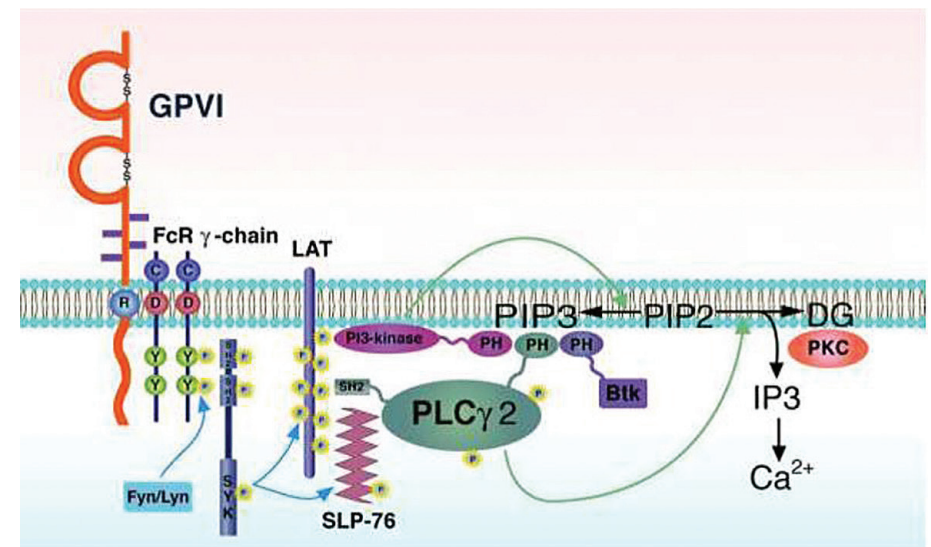
Figure 6: GPVI signal transduction pathway. Phosphorylation of the FcR-chain by Fyn/lyn kinases is followed by activation of Syk. This in turn phosphorylates the LAT signalosome resulting eventually in central PLC2 and PI 3-kinase activation, leading to increased concentrations of cytosolic ionized calcium and PI(3,4,5)P$_3$ formation, respectively[102]

3.2.2.4 AGGREGATION AND THROMBUS STABILIZATION THROUGH OUTSIDE-IN SIGNALLING

The above described agonist-dependent intracellular signal transduction pathways stimulate the binding of key regulatory proteins to the cytoplasmatic tail of integrins, which for example induces the transformation of integrin $\alpha_{IIb}\beta_3$ from a 'resting' state to an 'activated' state. A key requirement for this so-called inside-out signalling is the binding of talin and kindlin to the membrane proximal half of the β_3 cytoplasmic domain[103]. The following unclasping of the transmembrane and cytoplasmic domains of α_{IIb} and β_3 increases the affinity for subsequent ligands, like fibrinogen and VWF. When these multimeric ligands bind the receptor, avidity is increased through clustering of integrin $\alpha_{IIb}\beta_3$ molecules[104] **(Figure 7).** This causes outside-in signal transduction because signalling complexes proximal to the cytoplasmic tails of integrin $\alpha_{IIb}\beta_3$ are assembled. The Src kinases that are constitutively bound to the β_3 cytoplasmic tail in the cytoplasm are activated, clustered, unclamped and phosphorylated, which eventually leads to additional recruitment and phosphorylation of signalling and scaffolding proteins like Src and Syk protein tyrosine kinases[105], RhoA[106], PLCγ2[107], PI 3-kinase[108] and Rap1b[109] amplifying platelet spreading, granule secretion, stabilization and clot retraction[106,110].
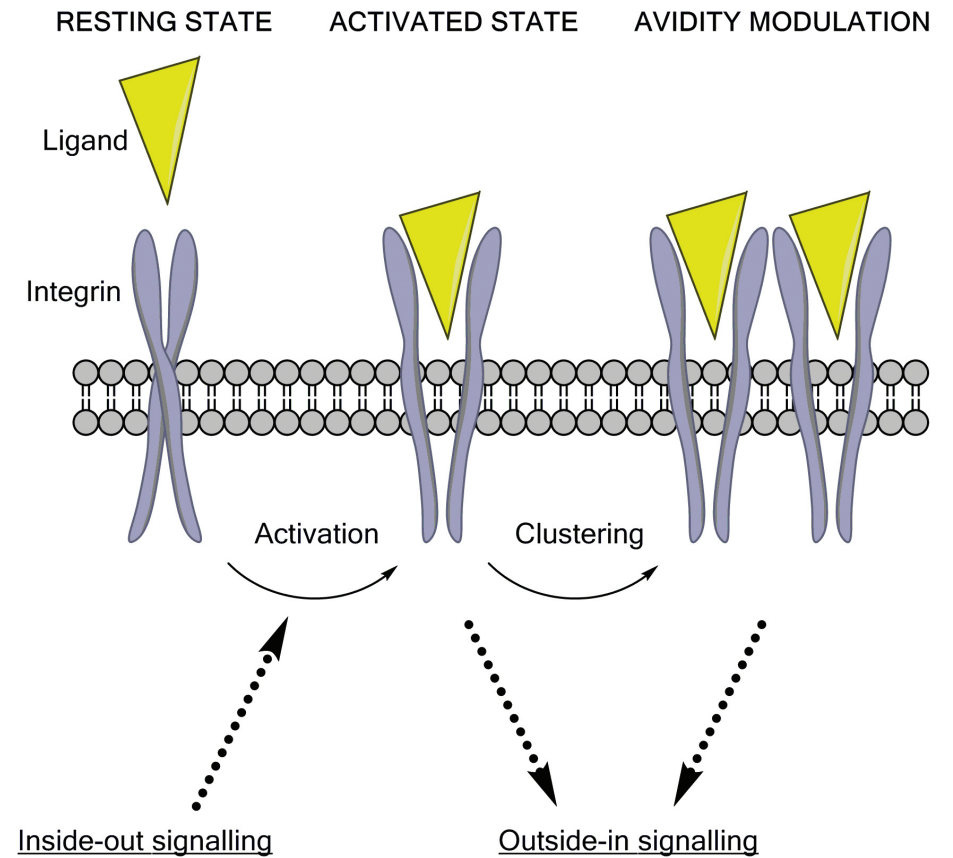

Figure 7: Inside-out and outside-in signal transduction of the platelet integrin receptor

4. CELL MEMBRANE AS SIGNAL ORGANIZER

4.1 CELL MEMBRANE COMPONENTS

The reigning fluid mosaic three-dimensional model of the cellular cytoplasmic membrane was devised in 1972 by Singer and Nicolson[111]. **(Figure 8)** In this model, the cell membrane is a discontinuous fluid bilayer of amphipathic phospholipids in which lipophilic proteins are (partially) embedded. Phospholipids spontaneously arrange back-to-back to thermodynamically stabilize hydrophobic acyl chains by shielding these from the surrounding watery environment. This biochemical property enables cells to segregate internal constituents from the extracellular environment
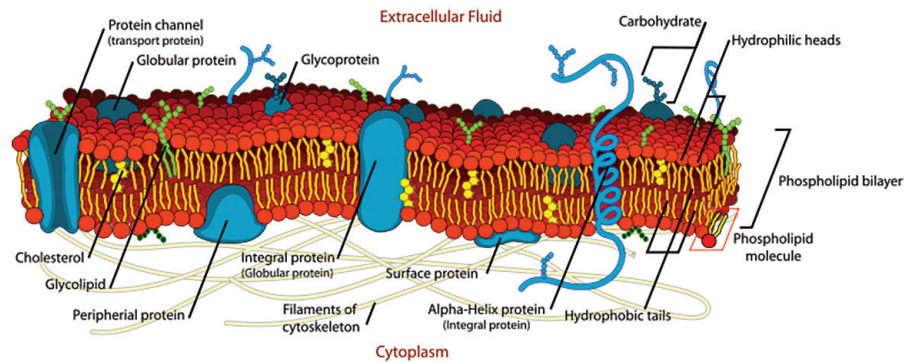

Figure 8: Fluid mosaic model. Cell membranes share a common structural organization of phospholipid bilayer with associated proteins[112].

Cell membrane constituting phospholipids are variable by their polar head groups which differ in size and electric charge. Common polar head groups are glycerol, ethanolamine, choline, inositol and serine. Eukaryotic cells typically bear 45-55% phosphatidylcholine, 15-25% phosphatidylethanolamine, 10-15% phosphatidylinositol, 5-10% sphingomyelin, 2-10% phosphatidylserine, 1-2% phosphatidylglycerol and 1-2% phosphatidic acid[113]. An important additional level of phospholipid variability is caused by the number of hydrophobic acyl chains (one, two or three), the acyl chain length and the number of double bonds or so-called unsaturations in the acyl chain[114]. Next to phospholipids, the cytoplasmic membrane harbours proteins, carbohydrates and sterols (mainly cholesterol). Within the lipid bilayer, cholesterol lines up approximately parallel to the acyl chains of the lipids with its hydrophilic hydroxyl group situated near the polar interface and the short hydrocarbon tail towards the nonpolar centre. Local cholesterol concentration is important for mechanical stability and fluidity of the membrane[115].

Proteins constitute between 25% to 75% of the dry mass of cell membranes and are therefore of major importance both to the membrane biophysical properties as well as to its relation with the intra- and extracellular biological environment. Membrane dwelling proteins are diverse in composition, function and in their interaction with the membrane which can be weak in peripheral proteins or strong in integral proteins[116].

4.2 CELL MEMBRANE ARCHITECTURE

The cell membrane is a site where important cellular processes are carried out ranging from controlled transmembrane trafficking and surveillance to mechanical sensing. By its architecture, that is, the organization of constituents in space and time, it orchestrates these processes carefully. The membrane is separated in large and smaller compartments **(Figure 9)** depending on the actin cytoskeleton, protein complexes and lipid packing. The first one, the actin cytoskeleton, dynamically associates with the cell membrane through interactions with integral membrane proteins, phospholipids and bridging molecules, forming compartments of roughly 40 to 300nm in diameter[117,118]. The second type of cell membrane domain, dynamic protein complexes, are generally between 3 and 10nm in diameter and can be subdivided in three types: oligomers of membrane-anchored proteins[119], coat-protein-facilitated domains (endocytosis and exocytosis)[120], and scaffolding-protein-induced protein complex domains, assembling more than two molecules[121]. Finally, compartments of 2 to 20nm in diameter are formed by the organization of the (phospho)lipids. The formation of these microdomains (sometimes called 'rafts') is regulated by the size of the polar headgroup of phospholipids which is small (e.g. phosphatidylglycerol) or large (e.g. phosphatidylinositol), and by the acyl side chains. Single double bonds in the hydrophobic core cause kinks in the chain because of their cis conformation, thereby physically pushing away vicinal molecules influencing hydrophobic core packing[122]. The two characteristics (head group and acyl chain), both determine the overall three dimensional shape of a phospholipid and the extent to which the membrane displays "imperfections" in the geometrical tightness, so-called lipid packing defects (LPD). For instance, tightly packed and highly ordered lipid microdomains are composed of phospho- and sphingolipids containing mainly saturated acyl chains, with "cavities" that are filled with sterols[123]. Less tightly packed disordered microdomains exist of mono- and polyunsaturated acyl chains and less (chole)sterol. This suborganization restricts and permits access of specific proteins allowing spatiotemporal organization of membrane-dependent cellular processes[124]. Modulation of signal transduction and associated lipid and protein interactions along the cell membrane surface is also influenced by the electrostatic environment. For example, the tetravalent acid $PI(4,5)P_2$ can be attracted by cationic (membrane-associated) molecules, because of the negative charges on the inositol ring. On the other hand, acidic phospholipids will repulse molecules with negatively charged domains[125].
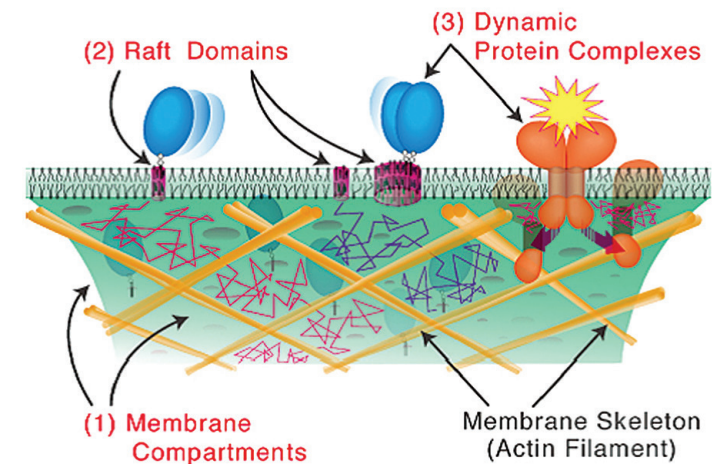
Figure 9: Membrane architecture. The microdomains (2) can vary from 2 to 20nm in diameter while the dynamic protein complexes (3) vary from 3 to 10nm. Both are accommodated in the membrane-skeleton-induced compartments (1) which vary from 40 to 300nm in diameter. Depending on the interactions between lipids and proteins and their architectural behavior, molecules have different diffusion abilities in the cell membrane[118].

4.3 CELL MEMBRANE RELAYING SIGNAL TRANSDUCTION

The phosphorylated phosphatidylinositol molecules or phosphoinositides are present in the cell membrane in small amounts. For instance, $PI(4,5)P_2$ comprises 0.5-1% of the total phospholipid content. Despite this, PI are of great importance as scaffolding molecules and nucleation centres in virtually all living eukaryotic species[126]. Following GPCR and RTK signal transduction there are two well described, known fates for $PI(4,5)P_2$. (1) PLC enzymes hydrolyze this inositide to yield IP_3 and DAG, and (2) PI 3-kinase phosphorylate the 3' position to yield $PI(3,4,5)P_3$. The concentration of $PI(3,4,5)P_3$ thus transiently rises, and functions as a nucleation centre for signalosomes to build on in a spatiotemporally restricted manner. As described earlier, the PI 3-kinase family contains three classes. For this work, Class I enzymes are most relevant. These phosphorylate $PI(4,5)P_2$ and $PI(4)P$ to yield $PI(3,4,5)P_3$ and $PI(3,4)P_2$ respectively. Both $PI(3,4,5)P_3$ and $PI(3,4)P_2$ are potent scaffolding molecules that regulate cell growth, replication, survival, proliferation and motility in a plethora of cell types throughout biology[127]. More specific, they coordinate the spatiotemporal function of effector proteins which bind via so-called PH domains. Abundantly expressed effector proteins are Btk and Akt[128]. For instance, Akt translocates from the cytosol to where $PI(3,4,5)P_3$ is formed at the inner leaflet of the cell membrane binding to the negatively charged pocket via the PH domain. Then the PH- containing enzyme 3-phosphoinositide-dependent protein kinase 1 (PDK1) phosphorylates Akt at T308[129]. Next, phosphorylated Akt in turn phosphorylates a diversity of substrates which can regulate energy metabolism, cell survival, cell cycle progression, or differentiation depending on the tissue and the signaling context[130].

5. REFERENCES

1   http://www.rodekruis.be/jaarverslag/2014.

2   Wet betreffende bloed en bloedderivaten van menselijke oorsprong. (1994).

3   Eder, A., Goldman, M., Rossmann, S., Waxman, D. & Bianco, C. Selection criteria to protect the blood donor in North America and Europe: past (dogma), present (evidence), and future (hemovigilance). *Transfus Med Rev* **23**, 205-220, doi:10.1016/j.tmrv.2009.03.003 (2009).

4   Organization, W. H. *Blood Donor Selection. Guidelines on Assessing Donor Suitability for Blood Donation.* (2012).

5   McDonald, C. P. Bacterial risk reduction by improved donor arm disinfection, diversion and bacterial screening. *Transfus Med* **16**, 381-396, doi:10.1111/j.1365-3148.2006.00697.x (2006).

6   Roback JD, G. B., Harris T, Hillyer CD. AABB Technical Manual. Vol. 17th (2011).

7   Vanaudenaerde D, V. L., Hintjens P, van den Hoogen P, Coene J, Compernolle V, Ceulemans J. Development of a novel device to improve whole blood cooling and storage at mobile collections and during transportation to the processing center. *Vox Sanguinis* **105 (Suppl. 1)**, 124 (2013).

8   http://www.rodekruis.be/jaarverslag/2014/kerncijfers/372759-geslaagde-donaties/.

9   *http://www.dienstvoorhetbloed.be/DVB-Channel/Bloedinstelling-Nederlands/ Bloedvoorziening/Bloedtesten/Bloedgroepbepaling-Centraal-Laboratorium.html.*

10   Hogman, C. F., Hedlund, K. & Sahlestrom, Y. Red cell preservation in protein-poor media. III. Protection against in vitro hemolysis. *Vox Sang* **41**, 274-281 (1981).

11   Guidelines on gamma irradiation of blood components for the prevention of transfusion-associated graft-versus-host disease. BCSH Blood Transfusion Task Force. *Transfus Med* **6**, 261-271 (1996).

12   Carson, J. L. et al. Red blood cell transfusion: a clinical practice guideline from the AABB*. *Ann Intern Med* **157**, 49-58, doi:10.7326/0003-4819-157-1-201206190-00429 (2012).

13   Liumbruno, G., Bennardello, F., Lattanzio, A., Piccoli, P. & Rossetti, G. Recommendations for the transfusion of red blood cells. *Blood Transfus* **7**, 49-64, doi:10.2450/ 2008.0020-08 (2009).

14   Dienst voor het Bloed, R. K. V. Productinformatiebrochure. (2006).

15   Peyvandi, F., Garagiola, I. & Seregni, S. Future of coagulation factor replacement therapy. J *Thromb Haemost* **11 Suppl 1**, 84-98, doi:10.1111/jth.12270 (2013).

16   Jolles, S., Sewell, W. A. & Misbah, S. A. Clinical uses of intravenous immunoglobulin. *Clin Exp Immunol* **142**, 1-11, doi:10.1111/j.1365-2249.2005.02834.x (2005).

17 *http://www.caf-dcf-redcross.be/.*

18 Liumbruno, G. et al. Recommendations for the transfusion of plasma and platelets. *Blood Transfus* **7**, 132-150, doi:10.2450/2009.0005-09 (2009).

19 Roback, J. D. *et al.* Evidence-based practice guidelines for plasma transfusion. *Transfusion* **50**, 1227-1239, doi:10.1111/j.1537-2995.2010.02632.x (2010).

20 Haematology;, B. C. f. S. i. & Force, B. T. T. Guidelines for the use of platelet transfusions. *British Journal of Haematology* **122**, 10-23, doi:10.1046/j.1365-2141.2003.04468.x (2003).

21 Zou, S. et al. Prevalence, incidence, and residual risk of human immunodeficiency virus and hepatitis C virus infections among United States blood donors since the introduction of nucleic acid testing. *Transfusion* **50**, 1495-1504, doi:10.1111/j.1537-2995.2010.02622.x (2010).

22 Zou, S. *et al.* Current incidence and residual risk of hepatitis B infection among blood donors in the United States. *Transfusion* **49**, 1609-1620, doi:10.1111/j.1537-2995.2009.02195.x (2009).

23 Funk, M. B. *et al.* Transfusion-Transmitted Bacterial Infections - Haemovigilance Data of German Blood Establishments (1997-2010). *Transfus Med Hemother* **38**, 266-271, doi:10.1159/000330372 (2011).

24 Dodd, R. Y. Emerging pathogens and their implications for the blood supply and transfusion transmitted infections. *Br J Haematol* **159,** 135-142, doi:10.1111/bjh.12031 (2012).

25 Prowse, C. V. Component pathogen inactivation: a critical review. *Vox Sang* **104**, 183-199, doi:10.1111/j.1423-0410.2012.01662.x (2013).

26 Picker, S. M. Current methods for the reduction of blood-borne pathogens: a comprehensive literature review. *Blood Transfus* **11**, 343-348, doi:10.2450/2013.0218-12 (2013).

27 Henschler, R., Seifried, E. & Mufti, N. Development of the S-303 Pathogen Inactivation Technology for Red Blood Cell Concentrates. *Transfus Med Hemother* **38**, 33-42, doi:10.1159/000324458 (2011).

28 Schlenke, P. Pathogen Inactivation Technologies for Cellular Blood Components: an Update. *Transfus Med Hemother* **41**, 309-325, doi:10.1159/000365646 (2014).

29 Salunkhe, V., van der Meer, P. F., de Korte, D., Seghatchian, J. & Gutierrez, L. Development of blood transfusion product pathogen reduction treatments: a review of methods, current applications and demands. *Transfus Apher Sci* **52**, 19-34, doi:10.1016/j.transci.2014.12.016 (2015).

30 Seghatchian, J. & Putter, J. S. Pathogen inactivation of whole blood and red cell components: An overview of concept, design, developments, criteria of acceptability and storage lesion. *Transfusion and Apheresis Science* **49**, 357-363, doi:10.1016/j.transci.2013.07.023.

31 Smith, J. & Rock, G. Protein quality in Mirasol pathogen reduction technology-treated, apheresis-derived fresh-frozen plasma. *Transfusion* **50**, 926-931, doi:10.1111/j.1537-2995.2009.02517.x (2010).

32 Ciaravino, V., McCullough, T., Cimino, G. & Sullivan, T. Preclinical safety profile of plasma prepared using the INTERCEPT Blood System. *Vox Sang* **85**, 171-182 (2003).

33 Hornsey, V. S., Drummond, O., Young, D., Docherty, A. & Prowse, C. V. A potentially improved approach to methylene blue virus inactivation of plasma: the Maco Pharma Maco-Tronic system. *Transfus Med* **11**, 31-36, doi:10.1046/j.1365-3148.2001.00282.x (2001).

34 Coene, J. *et al.* Paired analysis of plasma proteins and coagulant capacity after treatment with three methods of pathogen reduction. *Transfusion* **54**, 1321-1331, doi:10.1111/trf.12460 (2014).

35 Kallenbach, N. R., Cornelius, P. A., Negus, D., Montgomerie, D. & Englander, S. Inactivation of viruses by ultraviolet light. *Curr Stud Hematol Blood Transfus*, 70-82 (1989).

36 Apelseth, T. O. *et al.* In vitro evaluation of metabolic changes and residual platelet responsiveness in photochemical treated and gamma-irradiated single-donor platelet concentrates during long-term storage. *Transfusion* **47**, 653-665, doi:10.1111/j.1537-2995.2007.01167.x (2007).

37 Hechler, B. *et al.* Preserved functional and biochemical characteristics of platelet components prepared with amotosalen and ultraviolet A for pathogen inactivation. *Transfusion* **53**, 1187-1200, doi:10.1111/j.1537-2995.2012.03923.x (2013).

38 Zeddies, S. *et al.* Pathogen reduction treatment using riboflavin and ultraviolet light impairs platelet reactivity toward specific agonists in vitro. *Transfusion* **54**, 2292-2300, doi:10.1111/trf.12636 (2014).

39 Terada, C., Mori, J., Okazaki, H., Satake, M. & Tadokoro, K. Effects of riboflavin and ultraviolet light treatment on platelet thrombus formation on collagen via integrin alphaIIbbeta3 activation. *Transfusion* **54**, 1808-1816, doi:10.1111/trf.12566 (2014).

40 Verhaar, R. *et al.* UV-C irradiation disrupts platelet surface disulfide bonds and activates the platelet integrin alphaIIbbeta3. *Blood* **112**, 4935-4939, doi:10.1182/blood-2008-04-151043 (2008).

41 Sandgren, P., Tolksdorf, F., Struff, W. G. & Gulliksson, H. In vitro effects on platelets irradiated with short-wave ultraviolet light without any additional photoactive reagent using the THERAFLEX UV-Platelets method. *Vox Sang* **101**, 35-43, doi:10.1111/j.1423-0410.2010.01454.x (2011).

42 Butler, C. *et al.* Pathogen-reduced platelets for the prevention of bleeding. *Cochrane Database Syst Rev* **3**, Cd009072, doi:10.1002/14651858.CD009072.pub2 (2013).

43 Leibacher, J. *et al.* Quality parameters of red blood cells treated with Intercept pathogen inactivation system using S-303: a phase III clinicla trial in cardiac surgery patients. *Vox Sanguinis* **109** (Suppl. 1), 194 (2015).

44 Yawn, D. H. in *Encyclopædia Britannica Online* (Encyclopædia Britannica Inc., 2016).

45 Schaller, J., Gerber, S., Kaempfer, U., Lejon, S. & Trachsel, C. *Human Blood Plasma Proteins: Structure and Function.* (John Wiley & Sons, 2008).

46 Nanjappa, V. *et al.* Plasma Proteome Database as a resource for proteomics research: 2014 update. *Nucleic Acids Res* **42**, D959-965, doi:10.1093/nar/gkt1251 (2014).

47 Evans, T. W. Review article: albumin as a drug—biological effects of albumin unrelated to oncotic pressure. Alimentary Pharmacology & Therapeutics 16, 6-11, doi:10.1046/j.1365-2036.16.s5.2.x (2002).

48 Carter, D. C. & Ho, J. X. Structure of serum albumin. *Adv Protein Chem* **45**, 153-203 (1994).

49 Fasano, M. *et al.* The extraordinary ligand binding properties of human serum albumin. *IUBMB Life* **57**, 787-796, doi:10.1080/15216540500404093 (2005).

50 Schmidt, S., Gonzalez, D. & Derendorf, H. Significance of protein binding in pharmacokinetics and pharmacodynamics. *J Pharm Sci* **99**, 1107-1122, doi:10.1002/jps.21916 (2010).

51 Fanali, G. *et al.* Human serum albumin: from bench to bedside. *Mol Aspects Med* **33**, 209-290, doi:10.1016/j.mam.2011.12.002 (2012).

52 Liumbruno, G., Bennardello, F., Lattanzio, A., Piccoli, P. & Rossettias, G. Recommendations for the use of albumin and immunoglobulins. *Blood Transfus* **7**, 216-234, doi:10.2450/2009.0094-09 (2009).

53 Boldt, J. Use of albumin: an update. *British Journal of Anaesthesia* **104**, 276-284, doi:10.1093/bja/aep393 (2010).

54 Mandell, B. F. Intravenous gamma-globulin therapy. *J Clin Rheumatol* **2**, 317-324 (1996).

55 Jolles, S., Sewell, W. & Misbah, S. Clinical uses of intravenous immunoglobulin. *Clin Exp Immunol* **142**, 1-11, doi:10.1111/j.1365-2249.2005.02834.x (2005).

56 Palta, S., Saroa, R. & Palta, A. Overview of the coagulation system. *Indian J Anaesth* **58**, 515-523, doi:10.4103/0019-5049.144643 (2014).

57 Tennent, G. A. *et al.* Human plasma fibrinogen is synthesized in the liver. *Blood* **109**, 1971-1974, doi:10.1182/blood-2006-08-040956 (2007).

58 Mosesson, M. W. Fibrinogen and fibrin structure and functions. *Journal of Thrombosis and Haemostasis* **3**, 1894-1904, doi:10.1111/j.1538-7836.2005.01365.x (2005).

59 Laurens, N., Koolwijk, P. & de Maat, M. P. Fibrin structure and wound healing. *J Thromb Haemost* **4**, 932-939, doi:10.1111/j.1538-7836.2006.01861.x (2006).

60 Tziomalos, K., Vakalopoulou, S., Perifanis, V. & Garipidou, V. Treatment of congenital fibrinogen deficiency: overview and recent findings. *Vasc Health Risk Manag* **5**, 843-848 (2009).

61 Fay, P. J. Factor VIII structure and function. *Int J Hematol* **83**, 103-108, doi:10.1532/ijh97.05113 (2006).

62 Franchini, M. & Mannucci, P. M. Past, present and future of hemophilia: a narrative review. *Orphanet J Rare Dis* **7**, 24, doi:10.1186/1750-1172-7-24 (2012).

63 Morfini, M., Coppola, A., Franchini, M. & Di Minno, G. Clinical use of factor VIII and factor IX concentrates. *Blood Transfus* **11**, s55-63, doi:10.2450/2013.010s (2013).

64 Feys, H. B. et al. ADAMTS-13 plasma level determination uncovers antigen absence in acquired thrombotic thrombocytopenic purpura and ethnic differences. *Journal of Thrombosis and Haemostasis* **4**, 955-962, doi:10.1111/j.1538-7836.2006.01833.x (2006).

65 Dong, J.-f. *et al.* ADAMTS-13 rapidly cleaves newly secreted ultralarge von Willebrand factor multimers on the endothelial surface under flowing conditions. *Blood* **100**, 4033-4039, doi:10.1182/blood-2002-05-1401 (2002).

66 Hovinga, J. A. K. & Lämmle, B. Role of ADAMTS13 in the pathogenesis, diagnosis, and treatment of thrombotic thrombocytopenic purpura. *ASH Education Program Book* **2012**, 610-616, doi:10.1182/asheducation-2012.1.610 (2012).

67 Tsai, H. M. Thrombotic Thrombocytopenic Purpura: A Thrombotic Disorder Caused by ADAMTS13 Deficiency. *Hematol Oncol Clin North Am* **21**, 609-v, doi:10.1016/j.hoc.2007.06.003 (2007).

68 Harker, L. A. *et al.* Effects of megakaryocyte growth and development factor on platelet production, platelet life span, and platelet function in healthy human volunteers. *Blood* **95**, 2514-2522 (2000).

69 Deutsch, V. R. & Tomer, A. Megakaryocyte development and platelet production. *Br J Haematol* **134**, 453-466, doi:10.1111/j.1365-2141.2006.06215.x (2006).

70 White, J. G. in *Platelets (Third Edition)* (ed Alan D. Michelson) 117-144 (Academic Press, 2013).

71 Ghoshal, K. & Bhattacharyya, M. Overview of platelet physiology: its hemostatic and nonhemostatic role in disease pathogenesis. *ScientificWorldJournal* **2014**, 781857, doi:10.1155/2014/781857 (2014).

72 Ruggeri, Z. M. & Jackson, S. P. in P*latelets (Third Edition)* (ed Alan D. Michelson) 399-423 (Academic Press, 2013).

73 Stalker, T. J. *et al.* Hierarchical organization in the hemostatic response and its relationship to the platelet-signaling network. *Blood* **121**, 1875-1885, doi:10.1182/blood-2012-09-457739 (2013).

74 *http://www.bioch.ox.ac.uk/aspsite/index.asp?pageid=595, <http://www.bioch.ox.ac.uk/aspsite/index.asp?pageid=595> (*

75 Cosemans, J. M., Angelillo-Scherrer, A., Mattheij, N. J. & Heemskerk, J. W. The effects of arterial flow on platelet activation, thrombus growth, and stabilization. *Cardiovasc Res* **99**, 342-352, doi:10.1093/cvr/cvt110 (2013).

76 van der Plas, R. M. e*t al.* Binding of von Willebrand factor to collagen type III: role of specific amino acids in the collagen binding domain of vWF and effects of neighboring domains. *Thromb Haemost* **84**, 1005-1011 (2000).

77 Rand, J. H., Wu, X. X., Potter, B. J., Uson, R. R. & Gordon, R. E. Co-localization of von Willebrand factor and type VI collagen in human vascular subendothelium. *Am J Pathol*

142, 843–850 (1993).

78 Baumgartner, H. R. The role of blood flow in platelet adhesion, fibrin deposition, and formation of mural thrombi. *Microvasc Res* **5**, 167–179 (1973).

79 Watson, S. P., Auger, J. M., McCarty, O. J. & Pearce, A. C. GPVI and integrin alphaIIb beta3 signaling in platelets. *J Thromb Haemost* **3**, 1752–1762, doi:10.1111/j.1538-7836.2005.01429.x (2005).

80 Lian, L. *et al*. Loss of pleckstrin defines a novel pathway for PKC-mediated exocytosis. *Blood* **113**, 3577–3584, doi:10.1182/blood-2008-09-178913 (2009).

81 van den Bosch, M. T., Poole, A. W. & Hers, I. Cytohesin-2 phosphorylation by protein kinase C relieves the constitutive suppression of platelet dense granule secretion by ADP-ribosylation factor 6. *J Thromb Haemost* **12**, 726–735, doi:10.1111/jth.12542 (2014).

82 Crittenden, J. R. *et al.* CalDAG-GEFI integrates signaling for platelet aggregation and thrombus formation. *Nat Med* **10**, 982–986, doi:10.1038/nm1098 (2004).

83 Ma, Y. Q., Qin, J. & Plow, E. F. Platelet integrin alpha(IIb)beta(3): activation mechanisms. *J. Thromb Haemost* **5**, 1345–1352, doi:10.1111/j.1538-7836.2007.02537.x (2007).

84 Leevers, S. J., Vanhaesebroeck, B. & Waterfield, M. D. Signalling through phosphoinositide 3-kinases: the lipids take centre stage. *Current Opinion in Cell Biology* **11**, 219–225, doi:10.1016/s0955-0674(99)80029-5 (1999).

85 Watson, S. P., Auger, J. M., McCarty, O. J. T. & Pearce, A. C. GPVI and integrin IIb3 signaling in platelets. *Journal of Thrombosis and Haemostasis* **3**, 1752–1762, doi:10.1111/j.1538-7836.2005.01429.x (2005).

86 Woulfe, D. S. Akt signaling in platelets and thrombosis. *Expert Rev Hematol* **3**, 81–91, doi:10.1586/ehm.09.75 (2010).

87 Brass, L. F. Thrombin and platelet activation. *Chest* **124**, 18S–25S, doi:10.1378/chest.124.3_suppl.18S (2003).

88 Oldham, W. M. & Hamm, H. E. Heterotrimeric G protein activation by G-protein-coupled receptors. *Nat Rev Mol Cell Biol* **9**, 60–71, doi:10.1038/nrm2299 (2008).

89 Khan, A., Li, D., Ibrahim, S., Smyth, E. & Woulfe, D. S. The physical association of the P2Y12 receptor with PAR4 regulates arrestin-mediated Akt activation. *Mol Pharmacol* **86**, 1–11, doi:10.1124/mol.114.091595 (2014).

90 Holinstat, M. *et al.* PAR4, but not PAR1, signals human platelet aggregation via Ca^{2+} mobilization and synergistic P2Y12 receptor activation. *J Biol Chem* **281**, 26665–26674, doi:10.1074/jbc.M602174200 (2006).

91 Brass, L. F., Hoxie, J. A. & Manning, D. R. Signaling through G proteins and G protein-coupled receptors during platelet activation. *Thromb Haemost* **70**, 217–223 (1993).

92 Brass, L. F. & Joseph, S. K. A role for inositol triphosphate in intracellular Ca2+ mobilization and granule secretion in platelets. *Journal of Biological Chemistry* **260**, 15172–15179 (1985).

93 Harper, M. T. & Poole, A. W. Diverse functions of protein kinase C isoforms in platelet

activation and thrombus formation. *Journal of Thrombosis and Haemostasis* **8**, 454–462, doi:10.1111/j.1538-7836.2009.03722.x (2010).

94 Klages, B., Brandt, U., Simon, M. I., Schultz, G. & Offermanns, S. Activation of G12/G13 results in shape change and Rho/Rho-kinase-mediated myosin light chain phosphorylation in mouse platelets. *J Cell Biol* **144**, 745–754 (1999).

95 Woulfe, D. S. Platelet G protein-coupled receptors in hemostasis and thrombosis. *J Thromb Haemost* **3**, 2193–2200, doi:10.1111/j.1538-7836.2005.01338.x (2005).

96 Guidetti, G. F., Canobbio, I. & Torti, M. PI3K/Akt in platelet integrin signaling and implications in thrombosis. *Adv Biol Regul* **59**, 36–52, doi:10.1016/j.jbior.2015.06.001 (2015).

97 Packham, M. A. & Mustard, J. F. Platelet aggregation and adenosine diphosphate/adenosine triphosphate receptors: a historical perspective. *Semin Thromb Hemost* **31**, 129–138, doi:10.1055/s-2005-869518 (2005).

98 Haberstock-Debic, H., Andre, P., Mills, S., Phillips, D. R. & Conley, P. B. A clopidogrel-insensitive inducible pool of P2Y12 receptors contributes to thrombus formation: inhibition by elinogrel, a direct-acting, reversible P2Y12 antagonist. *J Pharmacol Exp Ther* **339**, 54–61, doi:10.1124/jpet.111.184143 (2011).

99 Kauffenstein, G. *et al.* The P2Y12receptor induces platelet aggregation through weak activation of the IIb3integrin – a phosphoinositide 3-kinase-dependent mechanism. *FEBS Letters* **505**, 281–290, doi:10.1016/s0014-5793(01)02824-1 (2001).

100 Mahaut-Smith, M. P., Ennion, S. J., Rolf, M. G. & Evans, R. J. ADP is not an agonist at P2X(1) receptors: evidence for separate receptors stimulated by ATP and ADP on human platelets. *Br J Pharmacol* **131**, 108–114, doi:10.1038/sj.bjp.0703517 (2000).

101 FitzGerald, G. A. Mechanisms of platelet activation: Thromboxane A2 as an amplifying signal for other agonists. *The American Journal of Cardiology* **68**, B11–B15, doi:10.1016/0002-9149(91)90379-y (1991).

102 Versteeg, H. H., Heemskerk, J. W., Levi, M. & Reitsma, P. H. New fundamentals in hemostasis. *Physiol Rev* **93**, 327–358, doi:10.1152/physrev.00016.2011 (2013).

103 Tadokoro, S. *et al.* Talin binding to integrin beta tails: a final common step in integrin activation. *Science* **302**, 103–106, doi:10.1126/science.1086652 (2003).

104 Shattil, S. J., Kashiwagi, H. & Pampori, N. Integrin signaling: the platelet paradigm. *Blood* **91**, 2645–2657 (1998).

105 Obergfell, *A. et al.* Coordinate interactions of Csk, Src, and Syk kinases with [alpha]IIb[beta]3 initiate integrin signaling to the cytoskeleton. *J Cell Biol* **157**, 265–275, doi:10.1083/jcb.200112113 (2002).

106 Leng, L., Kashiwagi, H., Ren, X. D. & Shattil, S. J. RhoA and the function of platelet integrin alphaIIbbeta3. *Blood* **91**, 4206–4215 (1998).

107 Wonerow, P., Pearce, A. C., Vaux, D. J. & Watson, S. P. A critical role for phospholipase Cgamma2 in alphaIIbbeta3-mediated platelet spreading. *J Biol Chem* **278**,

37520-37529, doi:10.1074/jbc.M305077200 (2003).

108 Canobbio, I. et al. Genetic evidence for a predominant role of PI3Kbeta catalytic activity in ITAM- and integrin-mediated signaling in platelets. *Blood* **114**, 2193-2196, doi:10.1182/blood-2009-03-208074 (2009).

109 Zhang, G. *et al.* Distinct roles for Rap1b protein in platelet secretion and integrin alphaIIbbeta3 outside-in signaling. *J Biol Chem* **286**, 39466-39477, doi:10.1074/jbc.M111.239608 (2011).

110 Estevez, B., Shen, B. & Du, X. Targeting integrin and integrin signaling in treating thrombosis. *Arterioscler Thromb Vasc Biol* **35**, 24-29, doi:10.1161/atvbaha.114.303411 (2015).

111 Singer, S. J. & Nicolson, G. L. The fluid mosaic model of the structure of cell membranes. *Science* **175**, 720-731 (1972).

112 *https://en.wikipedia.org/wiki/Cell_membrane.*

113 van Meer, G., Voelker, D. R. & Feigenson, G. W. Membrane lipids: where they are and how they behave. *Nat Rev Mol Cell Biol* **9**, 112-124, doi:10.1038/nrm2330 (2008).

114 Simons, K. & Sampaio, J. L. Membrane organization and lipid rafts. *Cold Spring Harb Perspect Biol* **3**, a004697, doi:10.1101/cshperspect.a004697 (2011).

115 Wassall, S. R. & Stillwell, W. Polyunsaturated fatty acid-cholesterol interactions: domain formation in membranes. *Biochim Biophys Acta* **1788**, 24-32, doi:10.1016/j.bbamem.2008.10.011 (2009).

116 Green, D. & Vanderkooi, G. in *Colloidal and Morphological Behavior of Block and Graft Copolymers* (ed GuntherE Molau) Ch. 8, 101-112 (Springer US, 1971).

117 Bezanilla, M., Gladfelter, A. S., Kovar, D. R. & Lee, W. L. Cytoskeletal dynamics: a view from the membrane. *J Cell Biol* **209**, 329-337, doi:10.1083/jcb.201502062 (2015).

118 Kusumi, A. et al. Membrane mechanisms for signal transduction: the coupling of the meso-scale raft domains to membrane-skeleton-induced compartments and dynamic protein complexes. *Semin Cell Dev Biol* **23**, 126-144, doi:10.1016/j.semcdb.2012.01.018 (2012).

119 Duarte, J. M., Biyani, N., Baskaran, K. & Capitani, G. An analysis of oligomerization inter faces in transmembrane proteins. *BMC Structural Biology* **13**, 1-11, doi:10.1186/1472-6807-13-21 (2013).

120 Parton, R. G. & del Pozo, M. A. Caveolae as plasma membrane sensors, protectors and organizers. *Nat Rev Mol Cell Biol* **14**, 98-112 (2013).

121 Hall, R. A. & Lefkowitz, R. J. Regulation of G protein-coupled receptor signaling by scaffold proteins. *Circ Res* **91**, 672-680 (2002).

122 Bigay, J. & Antonny, B. Curvature, lipid packing, and electrostatics of membrane organelles: defining cellular territories in determining specificity. *Dev Cell* **23**, 886-895, doi:10.1016/j.devcel.2012.10.009 (2012).

123 Brown, D. A. & London, E. Structure and function of sphingolipid- and cholesterol-rich membrane rafts. *J Biol Chem* **275**, 17221-17224, doi:10.1074/jbc.R000005200 (2000).

124 Simons, K. & Ikonen, E. Functional rafts in cell membranes. *Nature* **387**, 569-572, doi:10.1038/42408 (1997).

125 Trimble, W. S. & Grinstein, S. Barriers to the free diffusion of proteins and lipids in the plasma membrane. *J Cell Biol* **208**, 259-271, doi:10.1083/jcb.201410071 (2015).

126 Di Paolo, G. & De Camilli, P. Phosphoinositides in cell regulation and membrane dynamics. *Nature* **443**, 651-657, doi:10.1038/nature05185 (2006).

127 Vanhaesebroeck, B., Stephens, L. & Hawkins, P. PI3K signalling: the path to discovery and understanding. *Nat Rev Mol Cell Biol* **13**, 195-203, doi:10.1038/nrm3290 (2012).

128 Vanhaesebroeck, B., Guillermet-Guibert, J., Graupera, M. & Bilanges, B. The emerging mechanisms of isoform-specific PI3K signalling. *Nat Rev Mol Cell Biol* **11**, 329-341, doi:10.1038/nrm2882 (2010).

129 Liao, Y. & Hung, M. C. Physiological regulation of Akt activity and stability. *Am J Transl Res* **2**, 19-42 (2010).

130 Balla, T. Phosphoinositides: tiny lipids with giant impact on cell regulation. *Physiol Rev* **93**, 1019-1137, doi:10.1152/physrev.00028.2012 (2013).

PART 2
RESEARCH OBJECTIVES

Transfusion transmitted infections are a considerable threat to global blood supplies. The implementation of preventive measures like screening tests and donor questionnaires have decreased the risk substantially. However, emerging pathogens and bacterial contamination of platelets still remain a concern for blood safety. Pathogen inactivation technology adds a layer of safety to the latter. The efficacy of pathogen inactivation to prevent replication of viruses, bacteria and protozoa has been investigated extensively. However, many questions are still open concerning the consequences of pathogen inactivation technologies to blood product quality and function.

For plasma, the solvent/detergent treatment was developed in the early 1980s. Nowadays, several bench-top pathogen inactivation technologies are available. Coene *et al*[1] previously compared the impact of Mirasol Riboflavin (vitamin B2) pathogen reduction technology, INTERCEPT amotosalen (S59) photochemical treatment and THERAFLEX Methylene Blue Technology on plasma units. A significant decrease in the activity of fibrinogen, FII, FV, FVIII, FIX and FXI was found. Following this work, we investigated the molecular mechanism causing decreased activity of protein in plasma treated by Mirasol in particular, because the decrease was the largest in that case. We focused on the proteolytic enzyme ADAMTS13 which is important for the treatment of thrombotic thromobyctopenic purpura (RESULTS § 1.1)

Next, we investigated the off-target effects on platelets caused by pathogen inactivation. In the past decade the behavior of pathogen inactivation treated platelets has been assessed using many *in vitro* assays like light transmission or impedance aggregometry, flow cytometry, thromboelastography, cone-and-plate viscometry and blood gas analysis. However, it

is not entirely clear what this implies for platelet behavior in general or the context of hemostasis. We approached this question by setting up a comprehensive platelet function test with hydrodynamic shear and real-time analysis of platelet deposition onto immobilized collagen (RESULTS § 2.1) This microfluidic flow chamber model is then used together with traditional platelet function experiments to evaluate the impact of pathogen inactivation on platelet concentrates in a paired study in function of storage time. (RF-PRT and AS-PCT in RESULTS § 3.1; UV-C in RESULTS § 3.2) Finally, a critical analysis of AS-PCT is done to examine what biochemical defects impact platelet function. (RESULTS § 3.3)

1. Coene, J., *et al.* Paired analysis of plasma proteins and coagulant capacity after treatment with three methods of pathogen reduction. *Transfusion* **54**, 1321-1331 (2014).

PART 3
RESULTS

1. PATHOGEN INACTIVATION OF PLASMA

1.1 OXYGEN REMOVAL DURING PATHOGEN INACTIVATION WITH RIBOFLAVIN AND UV LIGHT PRESERVES PROTEIN FUNCTION IN PLASMA FOR TRANSFUSION INTRODUCTION

Oxygen removal during pathogen inactivation with riboflavin and UV light preserves protein function in plasma for transfusion

H. B. Feys,[1] B. Van Aelst,[1] K. Devreese,[2] R. Devloo,[1] J. Coene,[3] P. Vandekerckhove[3] & V. Compernolle[1,3]

[1]Transfusion Research Center, Belgian Red Cross-Flanders, Ghent, Belgium
[2]Coagulation Laboratory, Ghent University Hospital, Ghent, Belgium
[3]Blood Service of the Belgian Red Cross-Flanders, Mechelen, Belgium

INTRODUCTION

Fresh frozen plasma (FFP) is used clinically to replenish isolated coagulation factors deficiencies, to reverse the effect the warfarin, and to treat the dilution coagulopathy that occurs with massive bleeding [1]. Plasma exchange, requiring large quantities of donor plasma, has become the treatment of choice in patients suffering from thrombotic thrombocytopenic purpura. Like other blood components for transfusion, FFP inherently carries a risk of pathogen transmission [2,3] which can be reduced by various treatment methods. Solvent/detergent (S/D) treatment efficiently kills enveloped viruses and was licensed in Europe in 1991 and recently in the United Sates. The process includes pooling of multiple donations increasing patient exposure to donor material [4]. In the last couple of decades bench-top alternatives have been developed allowing treatment of single donations and effectiveness against non-enveloped viruses. These methods are commonly based on light energy treatment of individual component bags in the presence of a dissolved chemical photosensitizer. Photosensitizers are exogenously added molecules which interact with nucleic acids to various extents and react upon photoexcitation to induce strand breakage or cross-linking, thereby irreversibly preventing replication [4]. Methylene Blue [5] (Macopharma, Tourcoing, France or Baxter International Inc, Deerfield, IL) treated plasma is used in some European countries but requires freezing or additional filtering to release or remove cytoplasm-borne pathogens, respectively. 'Newer' photosensitizers include amotosalen [6,7] (or S-59, Cerus Corporation, Concord, CA) which does not require a freezing step and riboflavin [8] (or vitamin B2, Terumo BCT, Lakewood, CO) which is a naturally occurring vitamin and therefore does not require cumbersome removal from plasma products following treatment. Both amotosalen and riboflavin initially were described for inactivation of pathogens in platelet concentrates, but have since also been validated for treatment of single plasma units [6,9].

Pathogen inactivation treatment of plasma involves risks of losing valuable material through processing and/or affecting the constituents required for efficient transfusion [10]. There are few sufficiently powered studies that have evaluated clinical efficacy of pathogen reduced plasma [11,12], therefore evaluation of plasma quality is principally based on *in vitro* analysis of (labile) coagulation factors. From our previous paired analysis on the effects of the three photosensitizer-based methods [13], we concluded that coagulation factor loss is most pronounced in riboflavin treatment, though compensated to some extent by its low volume loss. Inversely, the methylene blue and amotosalen methods affect the constituent proteins less but are associated with larger volume losses.

The present work reveals the mechanism underlying the protein loss in riboflavin-based pathogen inactivation showing a significant role for reactive oxygen species and suggesting significant improvement by removal of dissolved oxygen prior to treatment.

METHODS

PATHOGEN INACTIVATION METHODS

For comparison of methods, paired samples were used following a pool and split design which joined and mixed five single plasma units followed by an equal split per pathogen inactivation method [13].

Plasma for methylene blue (MB) treatment [14] (Macotronic, Macopharma) is passed over a 0.65μm membrane filter and a dry MB tablet while being transferred to an illumination bag. The plasma containing approximately 1μM MB is exposed to a light dose of $180J/cm^2$ by illumination for about 20 minutes with long wavelength light (mainly 590nm). Next, the treated plasma is led over an auxiliary filter to remove residual MB.

Plasma for riboflavin (RF) treatment [15] (Mirasol, Terumo BCT) is mixed with 35mL RF solution (final concentration approximately 50μM) and transferred to an illumination bag which is subsequently illuminated with a UV (265-370nm) light dose of 6.24J/mL. Finally, the treated plasma is transferred to the storage bag.

Plasma for amotosalen (AS) treatment [16] (Intercept, Cerus) is led through a pouch containing 15mL AS solution (final concentration approximately 150μM). A UV (320-400nm) light dose of $3J/cm^2$ is delivered followed by an auxiliary adsorption step to reduce residual AS.

ADAMTS13 ACTIVITY AND ANTIGEN DETERMINATION

ADAMTS13 enzyme activity was measured using the fluorogenic substrate FRETS-VWF73 (AnaSpec, Fremont, CA, USA) [17] with modifications [18]. Normal human pooled plasma (NHP) (n=21) was used as a reference and EDTA at 10mM as a negative control. The final mixture contained 50mM 4-(2-hydroxyethyl)-1-piperazineethanesulfonic acid (HEPES) buffer, pH 7.4 supplemented with 1mM $CaCl_2$, 1μM $ZnCl_2$, 4.2mM 4-(2-Aminoethyl) benzenesulfonyl fluoride hydrochloride (Sigma-Aldrich) and 2μM FRETS-VWF73. Fluorescence intensity was measured every 150 seconds for 90 minutes at 25°C in a microplate reader (Infinite F200 Pro, Tecan, Männedorf, Switzerland) equipped with a 340nm excitation and 448nm emission filter. Product formation rates were determined relative to NHP.

A sandwich enzyme-linked immunosorbent assay (ELISA) (Imubind, American Diagnostica, Greenwich, CT, USA) was used to measure ADAMTS13 antigen, following the instructions of the provider. Detection of bound antigen is through a goat anti-human IgG antibody labeled with a streptavidin-horseradish peroxidase (HRP) which reacts with the perborate-3,3'-5,5'-tetramethylbenzidine (TMB) substrate to generate a blue colored solution. After acid addition to stop colorimetric development, absorbance was measured at 450nm in a microplate reader.

ELECTROPHORESIS AND WESTERN BLOTTING

Sodium Dodecyl Sulfate PolyAcrylamide Gel Electrophoresis (SDS-PAGE) was performed on stain-free precast TGX gel, 7.5% (Bio-rad, Hercules, CA, USA) in a 2-Amino-2-hydroxyme-thyl-propane-1,3-diol Tris –glycine buffered system (25mM Tris, 192mM Glycine, 0.1% (w/v) SDS). Plasma samples were diluted twenty-fold in phosphate buffered saline (PBS) containing 137mM NaCl, 2.7mM KCl, 10mM Na_2HPO_4, 2mM KH_2PO_4, pH 7.4 and non-reducing sample buffer containing 60mM Tris-HCl, 10% (v/v) glycerol, 2% (v/v) SDS and 0.01% (w/v) bromophenolblue. NHP was used as a negative control. As a positive control, NHP was incubated with 250U/mL urokinase-type plasminogen activator (Sigma-Aldrich, St Louis, MO, USA) overnight at 37°C, followed by addition of 100µM Amiloride hydrochloride hydrate (Sigma-Aldrich, St Louis, MO, USA) to stop proteolysis. Transfer was on nitrocellulose blotting sandwiches for Turbo™ (Bio-rad, Hercules, CA, USA). After incubation with anti-ADAMTS-13 primary antibody[19] (kind gift of Dr. JTB Crawley, Imperial College London), HRP-labeled goat anti-rabbit (Jackson ImmunoResearch, West Grove, PA, USA) and chemiluminiscence (Thermo Fisher Scientific, Rockford, IL, USA) were used to detect bound antibody. Gel images were developed on a digital imager (ChemiDoc MP System, Bio-rad, Hercules, CA, USA) and analyzed by Image Lab (Bio-rad, Hercules, CA, USA).

SUPEROXIDE ANION MEASUREMENTS

As a reporter for oxidative stress[20] 170µM nitroblue tetrazolium (NBT) (Merck, Darmstadt, Germany) was mixed with 5µM riboflavin (RF) and 0.5mM ethylenediaminetetraacetic acid (EDTA) (both Acros Organics, Geel, Belgium) in phosphate buffered saline (PBS, pH 7.4) in a polyolefin platelet illumination and storage bag (Terumo BCT). In order to specifically scavenge O_2^-, superoxide dismutase (SOD) (Sigma-Aldrich, St Louis, MO) was added to 100U/mL. Following PIT according to standard operating protocols in a Mirasol illuminator (Terumo BCT), formazan formation was measured by absorbance at 550nm in a regular spectrophotometer (UV-3100PC, VWR International, Radnor, PA). For dynamic range purposes, a lead-up experiment using a serial dilution of RF in the same assay conditions **(Figure S1)** indicated that 5µM of RF resides in the linear portion of the dose-response relationship. All samples, bags and equipment were kept shaded from ambient light at all times and air bubbles were removed manually by applying physical pressure.

DEGASIFICATION PROCEDURE

Molecular oxygen gas dissolves in aqueous solutions according to Henry's law depending on partial gas pressure and solubility. To remove dissolved oxygen from buffer solutions or plasma, a small tube carrying pressurized inert nitrogen gas (Air Liquide, Paris, France) at 40kPa was introduced in polyolefin storage bags and mixed for 20 minutes at room temperature in the dark. Following this procedure, oxygen concentrations were decreased to levels unable to oxidize resorufin **(Figure S2)** in the alkaline 'blue bottle' oxygen reporter system containing 0.5M KOH and 0.2M D-glucose (all Acros Organics). Measurements by micro-Clark electrode potentiometry (Lazar Laboratories, Los Angeles, CA) indicated that the residual oxygen pressure in the bags was 540±169Pa (mean±SEM, n=3) **(Figure S3)**.

FACTOR VIII AND FIBRINOGEN

FVIII activity (%) was measured in a one-stage activated partial thromboplastin time based clotting assay with factor deficient plasma. Fibrinogen activity was measured by the Clauss method and both analyses were performed in duplicate on a STA-R Evolution apparatus with tools and reagents from Diagnostica Stago (Asnières, France).

CARBONYLATION

Carbonyl content was determined by spectrophotometric analysis of dinitrophenylhydrazone as described by Dalle-Donne et al[21]. In brief, samples containing 2mg protein were supplemented with 10mM 2,4-dinitrophenylhydrazine (DNPH) (Sigma-Aldrich) in 2M HCl (final concentrations) and incubated at room temperature with shaking for one hour in shaded vials. Parallel samples only contained vehicle (2M HCl) to determine background. Next, trichloroacetic acid (VWR International) in water was added to a final 10% (m/v) followed by gentle mixing and 10 minute incubation on ice. Precipitated proteins were centrifuged at 2,000*g* for 10 minutes at 4°C followed by resuspension of the pelleted fraction in 6M guanidine hydrochloride (GuHCl) in water. Excess unreacted DNPH was removed by desalting column chromatography over a 6M GuHCl pre-equilibrated spin column (Zeba™, Thermo Fisher Scientific). Absorbance of dinitrophenylhydrazone in the flow-through fraction was determined by spectrophotometry at 370nm and values were corrected for background. An extinction coefficient of $22,000M^{-1}cm^{-1}$ was used for determination of carbonyl quantity. Finally, the flow-through samples were analyzed for protein concentration by BCA assay to enable expression of carbonylation as mole per milligram protein.
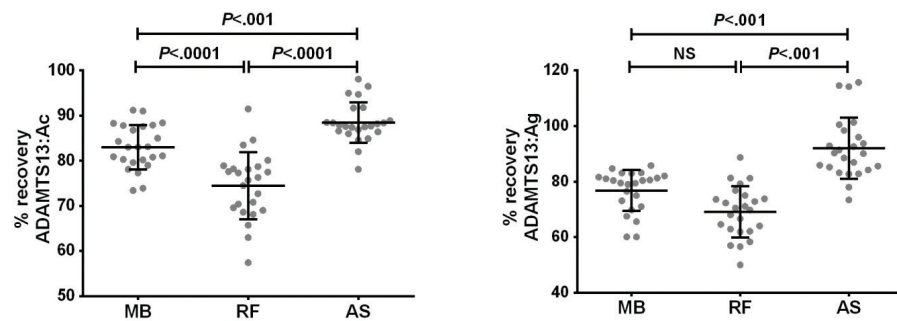
STATISTICAL ANALYSIS

Statistical analysis used standard algorithms from Prism 5.04 software (GraphPad, La Jolla, CA) including one-way repeated measures ANOVA with Bonferroni or Dunn's post-tests, t-test and Mann-Whitney U-tests for comparison of means. Estimation of Gaussian distribution used Shapiro-Wilk or Kolgomorov-Smirnov tests.

RESULTS

ADAMTS13 IN PATHOGEN INACTIVATION

Plasma exchange or infusion is the standard treatment for thrombotic thrombocytopenic purpura (TTP)[22], a thrombotic microangiopathy caused by severe ADAMTS13 deficiency. ADAMTS13 content in plasma products is well studied, but the effects of pathogen inactivation were never compared in paired samples. Therefore, ADAMTS13 activity and antigen were measured in three photosensitizer-based pathogen inactivation methods as part of a prior comprehensive study by our group[13].

Figure 1 indicates the percentage recovery which relates final to initial ADAMTS13 values and is a measure for retention over the entire pathogen inactivation procedure. Recovery percentages hence take into account all procedural steps including volume loss which is prominent in MB but absent in the RF methodology. Yet, **Figure 1** shows that RF treatment is not necessarily superior in retaining ADAMTS13 than MB or AS. This is explained by a significant decrease of ADAMTS13 antigen and function (by activity) of 29% and 23%, respectively in RF **(Figure 2)**. Taken together, significant ADAMTS13 (functional) enzyme is lost in both MB and RF, but volume loss accounts for decreases in the former while molecular changes contribute most to the latter. Recovery is most sustained by AS treatment.
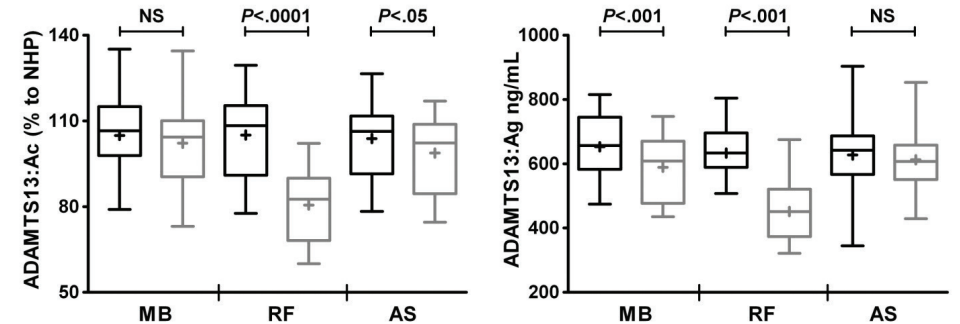
ADAMTS13 IS NOT CLEAVED NOR DIRECTLY INHIBITED BY RIBOFLAVIN

In order to explain the ADAMTS13 molecular changes in RF-based pathogen inactivation, we hypothesized that the plasma treatment causes collateral serine protease activation. It is known that ADAMTS13 is variably susceptible to proteolytic degradation and subsequent inactivation by serine proteases, including factor Xa, thrombin or plasmin[19,23]. However, despite substantial loss of the intact full length ADAMTS13 molecule in western blot analysis **(Figure 3)**, no increase in smaller immunoreactive fragments characteristic for proteolytic breakdown is seen.
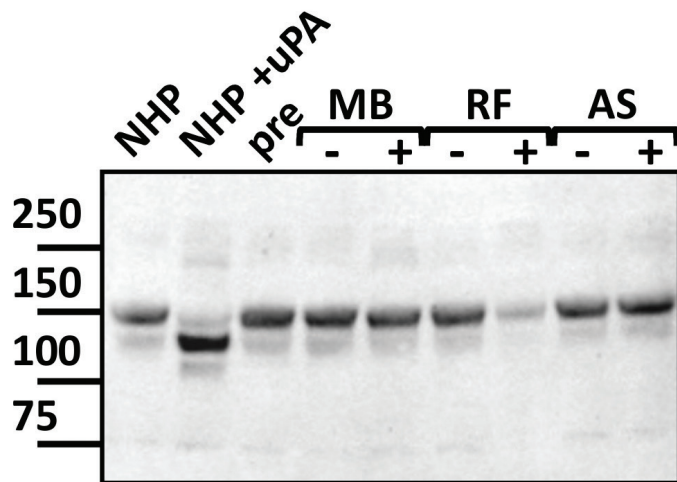
In addition, VWF73 proteolysis is not directly inhibited by RF at concentrations used in pathogen inactivation **(Figure S4)** indicating no direct binding of RF to ADAMTS13.

Figure 1: Percentage recovery of ADAMTS13 in three pathogen reduction methods. The percentage of AD-AMTS13 activity (top) or antigen (bottom) retained in the final bag relative to the starting amount is depicted in function of each photochemical pathogen reduction method. It takes into account several procedural steps including molecular degradation as well as volume loss. Individual data are shown as dots, dataset mean as a horizontal line and standard deviation as whiskers. Statistics indicated on top were generated by repeated measures one-way ANOVA with Bonferroni multiple comparison testing (n=24).

Figure 2: ADAMTS13 activity and antigen are affected most by RF-based pathogen reduction. ADAMTS13 activity (top) and antigen (bottom) absolute concentrations were determined in plasma sampled from paired bags before (black boxes) and after (grey boxes) pathogen reduction treatment with either MB, RF or AS. Box edges represent standard deviations, median (horizontal line) and mean (+). Whiskers indicate data range (n=24). Statistical results of repeated measures one-way ANOVA with Bonferroni multiple comparison testing are indicated above each dataset.

SUPEROXIDE ANIONS ARE GENERATED DURING PATHOGEN INACTIVATION WITH RIBOFLAVIN

Next, we hypothesized that the molecular changes in ADAMTS13 are caused by oxidation promoted by newly generated ROS. Oxidative stress during RF-based pathogen inactivation was directly measured by (colorless) NBT reduction to blue formazan. In buffer, significant formazan formation is seen upon illumination of 5µM RF in a Mirasol apparatus **(Figure 4)**. To dissect the nature of the reactive species involved, the specific superoxide scavenging enzyme SOD was added. A significantly lower signal is seen in the presence of 100U/mL SOD indicating that a considerable portion of NBT reduction is caused by O_{2-} which can be scavenged by SOD. Superoxide anion radicals are formed when dissolved molecular oxygen $(O_{2,aq})$ accepts the excess energy from photochemically excited sensitizers. Indeed, when the $O_{2,aq}$ concentration is experimentally lowered by nitrogen gas sparging, the O_{2-} related NBT reduction can no longer be diverted using SOD **(Figure 4)**. Instead, NBT reduction is now established through non-oxygen and most probably direct electron transfer from excited photosensitizer molecules to the reporter. These data show that photosensitized RF transfers its excitation energy to $O_{2,aq}$ when present, generating O_{2-} in the exact conditions used for pathogen inactivation of blood components.

Figure 4: Pathogen reduction conditions of RF and light generate O_{2-} depending on $O_{2,aq}$. *The nitroblue tetrazolium redox indicator is converted to formazan which absorbs at 550nm upon reduction by superoxide or its derivatives. The absorbance in blood component storage bags before (open bars) and after (closed bars) pathogen reduction with 5µM RF in a Mirasol apparatus is shown. Addition of 100U/mL SOD indicates the specific presence of O_{2-} molecules. These are generated in function of $O_{2,aq}$ availability as is shown when ambient partial pressures ('nor') of $O_{2,aq}$ are experimentally lowered ('low') by nitrogen gas sparging. Means (n=5) with standard error of the mean as error bars are depicted.*

Figure 3: ADAMTS13 is not proteolyzed but partially degraded. *Plasma samples before (-) or after (+) pathogen reduction were analyzed in SDS PAGE with western blotting for ADAMTS13 protein. An equal amount of protein was loaded in each lane. As negative and positive controls for enzymatic proteolysis, untreated (NHP) or urokinase (NHP+u-PA) incubated paired plasma samples were loaded. The sample prior to thawing for pathogen reduction (pre) is also included. Molecular weight references are indicated to the left in kilodaltons.*

OXIDATIVE DAMAGE CAN BE PREVENTED BY LOWERING DISSOLVED MOLECULAR OXYGEN

Superoxide anions and its derived radicals are highly reactive and not selective, therefore not restricting its effects to ADAMTS13. To assess disseminated oxidative damage on plasma proteins, total carbonylation levels were determined **(Figure 5)**. Carbonyl groups (both aldehydes and ketones) are irreversibly added to protein by many different oxidative mechanisms[24] including reactions with advanced glycation and lipid end-products as well as metal-catalyzed (Fenton-like chemistry) reactions. The data show that in the presence of normal $O_{2,aq}$ concentrations generic oxidation of proteins is prominent following RF-PRT. However, when $O_{2,aq}$ is experimentally lowered by inert gas sparging this damage is prevented **(Figure 5)**. This shows a direct role of $O_{2,aq}$ in modification of proteins present in plasma.

Because some proteins in donorplasma are specifically relevant in the context of coagulopathies, these were investigated in more detail with respect to RF-PRT in the presence or absence of $O_{2,aq}$. **Figure 6** shows that ADAMTS13 activity, fibrinogen concentration and FVIII:C are significantly better retained when the donorplasmas are pretreated with nitrogen gas to reduce $O_{2,aq}$.
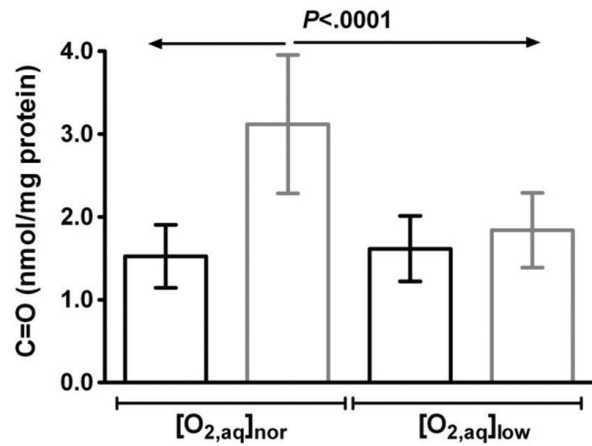
Figure 5: Disseminated oxidative damage of plasma proteins. *Carbonyl content of protein molecules is determined by chromogenic derivatization on paired samples (n=7) taken from plasma bags before (black bars) and after (grey bars) pathogen reduction with RF without plasma pretreatment ($[O_{2,aq}]_{nor}$) or following oxygen reduction ($[O_{2,aq}]_{low}$) by inert gas purging. Data are expressed as mean molar carbonyl content per unit of mass protein and standard deviations are indicated by whiskers. Statistics compared means by repeated measures one-way ANOVA using Bonferonni multiple comparison post testing.*

DISCUSSION

Photochemical treatment of biological material affects the (functional) integrity of the constituents to various degrees. This has been demonstrated for plasma with all three available methods for blood product processing and most specifically using intrinsically labile factors like FVIII[10]. However, the molecular basis for the observed effect is unclear and novel insights should allow optimization of current methods to deliver better blood products to patients.

From our experiments measuring ADAMTS13 in treated plasma it is clear that the largest biomolecular damage is seen with RF-PRT when compared to MB and AS. These specific data corroborate well with the observed changes in other unrelated coagulation factors during PIT[13]. Although clinically not investigated to date, plasma products containing fewer active ADAMTS13 may in theory be less efficient to treat TTP. Remission might be achieved more slowly or only following administration of a larger volume which may in turn increase typical risks of plasma exchange or plasma infusion like fluid overload or citrate-induced hypocalcemia. Some might argue that the difference in ADAMTS13 concentration is not that relevant when taking into account the seemingly low threshold of ADAMTS13 activity required for achieving remission of TTP[25], but clinical studies are lacking to confirm either statement.

Although adverse effects of photochemistry on coagulation factors have been reported before, there are no data describing the underlying phenomenon that damages plasma biomolecules. Using the ADAMTS13 susceptibility to RF-PRT as a readout, a series of experiments sought to identify the cause. First, direct riboflavin inhibition of ADAMTS13 function was investigated as a potential bias in the readout. Using the FRETS-VWF73 based ADAMTS13 activity assay, no direct effect of RF on the enzyme function could be detected. Next, random activation of zymogens was hypothesized relating the observed functional and effective decrease in ADAMTS13 to its previously reported susceptibility to serine proteases[23]. In a western blotting experiment known to be sensitive to proteolytic bands of ADAMTS13[19], no increased breakdown could be detected following RF-PRT despite a significantly weaker intensity of the full length band of ADAMTS13.
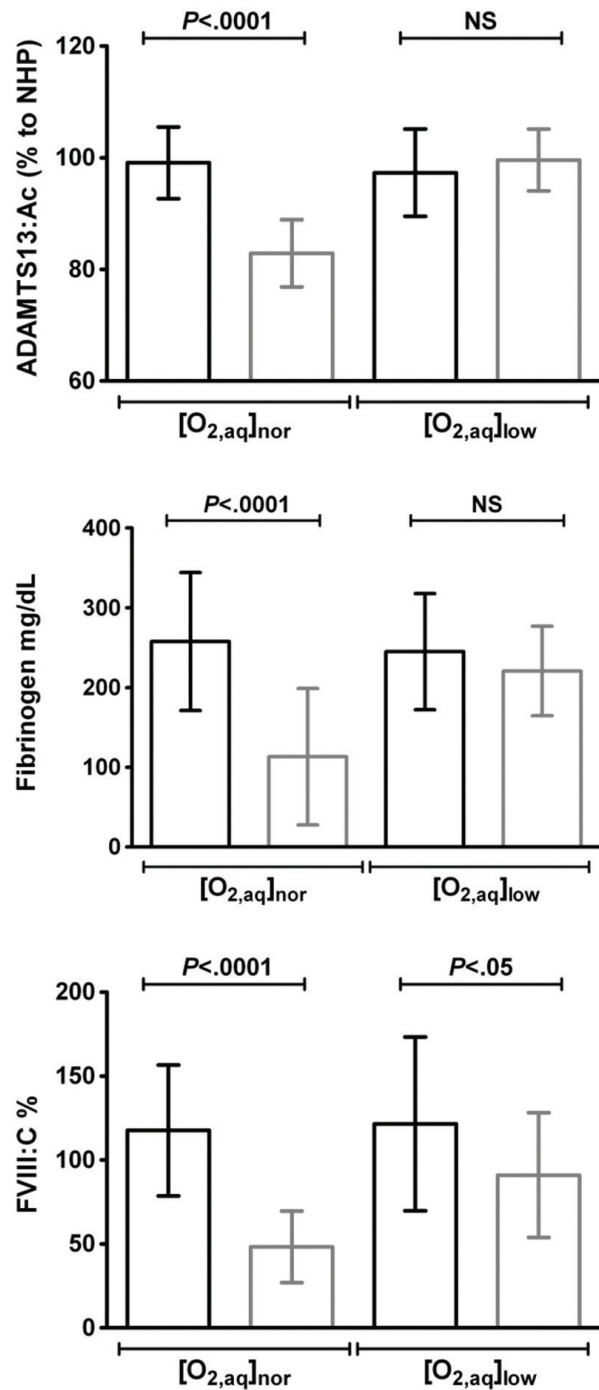
Figure 6: Dissolved molecular oxygen underlies damage to ADAMTS13, fibrinogen and FVIII during pathogen reduction with riboflavin. ADAMTS13 activity, fibrinogen and FVIII levels were determined in paired samples taken from plasma bags before (black bars) and after (grey bars) pathogen reduction with RF without plasma pretreatment ($[O_{2,aq}]_{nor}$) or with oxygen reduction ($[O_{2,aq}]_{low}$) by inert gas purging. Bars represent means and whiskers standard deviations (n=7). Statistics compared means by repeated measures one-way ANOVA using Bonferonni multiple comparison post testing

Next, the role of increased oxidative stress was investigated by using the redox reporter NBT[20]. Riboflavin and ultraviolet light have been used for decades in chemistry laboratories as an easy and inexpensive model system for the generation and investigation of superoxide anions and singlet oxygen. However, in the specific context of pathogen inactivation it is unknown if and to what extent ROS are produced. To investigate this, blood product bags that would otherwise contain donor plasma were filled with buffered NBT redox reporter and treated with RF pathogen inactivation. An oxidative response in function of RF dose could be detected, indicating dose dependent increase of redox potential in the exact setting of bench-top plasma pathogen inactivation. By addition of the specific superoxide scavenger SOD, the reporter was significantly less reduced demonstrating that substantial amounts of superoxide anion were driving the NBT redox reaction during the process of RF pathogen inactivation.

Since ROS react with multiple targets in an unspecific fashion, generic damage to the plasma content was investigated by measurement of carbonyl modifications to plasma protein. Carbonylation is irreversible and can be detected and quantified by chemical derivatization in solution. Indeed, following RF mediated pathogen inactivation, a significant increase in protein carbonyl content is seen. This might also explain the observed decrease of anti-ADAMTS13 binding in western blot **(Figure 3)** as epitopes may be directly affected by these or other molecular modifications induced by ROS.

Nonetheless, our data show that the damage to the product can be bypassed through performing the pathogen inactivation procedure in a hypoxic environment. First, when the NBT redox reporter experiment with and without SOD was repeated in hypoxic conditions we found that the RF-mediated NBT redox reaction was no longer driven by superoxide. This shows that in the absence of dissolved oxygen photo-excited RF intermediates are still able to reduce NBT and possibly other targets (like pathogen nucleic acids) but that the superoxide production is severely hampered. Secondly, in such hypoxic conditions the disseminated carbonylation of protein also was efficiently rescued as shown in **figure 5**. Finally, the earlier reported specific damage to FVIII, fibrinogen and ADAMTS13 can be rescued eventually resulting in higher yields of these clinically significant factors.

Taken together, our data show that UV light excitation of RF in the practical context of pathogen inactivation transfers energy to dissolved molecular oxygen, generating superoxide anion. This and other reactive species not only cause protein carbonylation but may potentially also induce fatty acid peroxidation chain reactions in lipids[26], auxiliary modifications in proteins[27] (eg

nitrosylation) and glycation of carbohydrates[28]. Therefore, superoxide and other ROS generated during pathogen inactivation likely contribute to the biostatic action of pathogen inactivation technologies by effectively damaging pathogen biomolecules[29] as an indirect effect of RF excitation. However, this is not the sole pathogen inactivation mechanism[30] because direct damage of nucleic acids by excited RF is also likely to be involved since direct irreversible oxidative chemistry by photo-excited RF has been demonstrated[31] as well as direct (non-covalent) binding of RF to nucleic acids[32]. Therefore performing the pathogen inactivation procedure in hypoxic conditions may still adequately affect pathogenic nucleic acids with the important advantage of avoiding random damage in the product caused by ROS.

The same phenomenon may apply to platelet concentrates treated with Mirasol technology because recent work by the Australian Red Cross[33] indicates that platelet lysates from concentrates treated with RF pathogen inactivation have increased carbonylation levels as well as a rise in the advanced lipid end product 4-hydroxy-2-nonenal. It is unclear if performing pathogen inactivation of platelets in the absence of dissolved molecular oxygen can rescue the observed biomolecular damage without compromising the cell's metabolic housekeeping. Anoxia causes metabolic damage in platelets[34] and therefore the beneficial effects of such pretreatment in the setting of pathogen inactivation may be balanced out. Despite this, the entire process of illumination only takes a couple of minutes which may allow to effectively remove and resupply oxygen without significantly disturbing platelet metabolism and gas exchange. If feasible, this would prove a major technological step forward in safekeeping blood products during pathogen inactivation. Pathogen inactivation is an important step forward in the aim to reduce transmission of disease by transfusion of blood products. Our experimental work indicates that the delicate balance to conserve blood product integrity while ensuring a high safety level may benefit from working in hypoxic conditions, at least for plasma but maybe also for platelets.

AUTHORSHIP CONTRIBUTIONS

HBF and VC designed research; VC, JC and PV contributed critical analytical tools, reagents, samples or data; BVA, RD, KD and HBF performed research and collected data; BVA, RD, VC, KD and HBF analysed and interpreted data; BVA and HBF performed statistical analyses; HBF wrote the manuscript; all authors critically reviewed and amended the manuscript. VC has primary responsibility for final content.

REFERENCES

1 O'Shaughnessy, D. F. *et al.* Guidelines for the use of fresh-frozen plasma, cryoprecipitate and cryosupernatant. *Br J Haematol* **126**, 11-28, doi:10.1111/j.1365-2141.2004.04972.x (2004).

2 Dodd, R. Y. Emerging pathogens and their implications for the blood supply and transfusion transmitted infections. *Br J Haematol* **159**, 135-142, doi:10.1111/bjh.12031 (2012).

3 Allain, J. P. *et al.* Transfusion-transmitted infectious diseases. *Biologicals* **37**, 71-77, doi:10.1016/j.biologicals.2009.01.002 (2009).

4 Pelletier, J. P., Transue, S. & Snyder, E. L. Pathogen inactivation techniques. *Best Pract Res Clin Haematol* **19**, 205-242, doi:10.1016/j.beha.2005.04.001 (2006).

5 Hornsey, V. S., Drummond, O., Young, D., Docherty, A. & Prowse, C. V. A potentially improved approach to methylene blue virus inactivation of plasma: the Maco Pharma Maco-Tronic system. *Transfus Med* **11**, 31-36, doi:10.1046/j.1365-3148.2001.00282.x (2001).

6 Ciaravino, V., McCullough, T., Cimino, G. & Sullivan, T. Preclinical safety profile of plasma prepared using the INTERCEPT Blood System. *Vox Sang* **85**, 171-182 (2003).

7 Lin, L. *et al.* Photochemical inactivation of viruses and bacteria in platelet concentrates by use of a novel psoralen and long-wavelength ultraviolet light. *Transfusion* **37**, 423-435 (1997).

8 Ruane, P. H. *et al.* Photochemical inactivation of selected viruses and bacteria in platelet concentrates using riboflavin and light. *Transfusion* **44**, 877-885, doi:10.1111/j.1537-2995.2004.03355.x (2004).

9 Smith, J. & Rock, G. Protein quality in Mirasol pathogen reduction technology-treated, apheresis-derived fresh-frozen plasma. *Transfusion* **50**, 926-931, doi:10.1111/j.1537-2995.2009.02517.x (2010).

10 Benjamin, R. J. & McLaughlin, L. S. Plasma components: properties, differences, and uses. *Transfusion* **52 Suppl 1**, 9S-19S, doi:10.1111/j.1537-2995.2012.03622.x (2012).

11 Mintz, P. D. *et al.* Photochemically treated fresh frozen plasma for transfusion of patients with acquired coagulopathy of liver disease. *Blood* **107**, 3753-3760, doi:10.1182 blood-2004-03-0930 (2006).

12 Bartelmaos, T. *et al.* Plasma transfusion in liver transplantation: a randomized, double-blind, multicenter clinical comparison of three virally secured plasmas. *Transfusion* **53**, 1335-1345, doi:10.1111/j.1537-2995.2012.03895.x (2013).

13 Coene, J., Devreese, K., Sabot, B., Compernolle, V. & Vandekerckhove, P. Comparitive in vitro evaluation of the plasma quality for three methods of pathogen reduction [abstract]. *Transfusion* **52**, 53A-54A. Abstract SP52., doi:DOI: 10.1111/j.1537-2995.2012.03833_1.x (2012).

14 Seghatchian, J., Struff, W. G. & Reichenberg, S. Main Properties of the THERAFLEX MB-Plasma System for Pathogen Reduction. *Transfus Med Hemother* **38**, 55-64, doi:10.1159/000323786 (2011).

15 Bihm, D. J. *et al.* Characterization of plasma protein activity in riboflavin and UV light-treated

fresh frozen plasma during 2 years of storage at –30 degrees C. *Vox Sang* **98**, 108–115, doi:10.1111/j.1423-0410.2009.01238.x (2010).

16 Irsch, J., Pinkoski, L., Corash, L. & Lin, L. INTERCEPT plasma: comparability with conventional fresh-frozen plasma based on coagulation function––an in vitro analysis. *Vox Sang* **98**, 47–55, doi:10.1111/j.1423-0410.2009.01224.x (2010).

17 Kokame, K., Nobe, Y., Kokubo, Y., Okayama, A. & Miyata, T. FRETS-VWF73, a first fluorogenic substrate for ADAMTS13 assay. *Br J Haematol* **129**, 93-100, doi:10.1111/j.1365-2141.2005.05420.x (2005).

18 Anderson, P. J., Kokame, K. & Sadler, J. E. Zinc and calcium ions cooperatively modulate ADAMTS13 activity. *J Biol Chem* **281**, 850-857, doi:10.1074/jbc.M504540200 (2006).

19 Crawley, J. T. *et al.* Proteolytic inactivation of ADAMTS13 by thrombin and plasmin. *Blood* **105**, 1085-1093, doi:10.1182/blood-2004-03-1101 (2005).

20 Gibson, S. L., Cohen, H. J. & Hilf, R. Evidence against the production of superoxide by photoirradiation of hematoporphyrin derivative. *Photochem Photobiol* **40**, 441-448 (1984).

21 Dalle-Donne, I., Rossi, R., Giustarini, D., Milzani, A. & Colombo, R. Protein carbonyl groups as biomarkers of oxidative stress. *Clinica Chimica Acta* **329**, 23-38, doi:10.1016 s0009-8981(03)00003-2 (2003).

22 Rock, G., Shumak, K. H., Sutton, D. M., Buskard, N. A. & Nair, R. C. Cryosupernatant as replacement fluid for plasma exchange in thrombotic thrombocytopenic purpura. Members of the Canadian Apheresis Group. *Br J Haematol* **94**, 383-386 (1996).

23 Feys, H. B. *et al.* Inactivation of ADAMTS13 by plasmin as a potential cause of thrombotic thrombocytopenic purpura. *J Thromb Haemost* **8**, 2053-2062, doi:10.1111/j.1538-7836.2010.03942.x (2010).

24 Levine, R. L., Wehr, N., Williams, J. A., Stadtman, E. R. & Shacter, E. Determination of carbonyl groups in oxidized proteins. *Methods Mol Biol* **99**, 15-24, doi:10.1385/1-59259-054-3:15 (2000).

25 Moake, J. L. Thrombotic thrombocytopenic purpura: the systemic clumping "plague". *Annu Rev Med* **53**, 75-88, doi:10.1146/annurev.med.53.082901.103948 (2002).

26 Niki, E. Lipid peroxidation: physiological levels and dual biological effects. *Free Radic Biol Med* **47**, 469-484, doi:10.1016/j.freeradbiomed.2009.05.032 (2009).

27 Suzuki, Y. J., Carini, M. & Butterfield, D. A. Protein carbonylation. *Antioxid Redox Signal* **12**, 323-325, doi:10.1089/ars.2009.2887 (2010).

28 Singh, R., Barden, A., Mori, T. & Beilin, L. Advanced glycation end-products: a review. *Diabetologia* **44**, 129-146, doi:10.1007/s001250051591 (2001).

29 Maisch, T. *et al.* The role of singlet oxygen and oxygen concentration in photodynamic inactivation of bacteria. *Proc Natl Acad Sci U S A* **104**, 7223-7228, doi:10.1073 pnas.0611328104 (2007).

30 Kumar, V. *et al.* Riboflavin and UV-light based pathogen reduction: extent and consequence of DNA damage at the molecular level. *Photochem Photobiol* **80**, 15-21,

doi:10.1562/2003-12-23-RA-036.1 (2004).

31 Dardare, N. & Platz, M. S. Binding affinities of commonly employed sensitizers of viral inactivation. *Photochem Photobiol* **75**, 561-564 (2002).

32 Kasai, H., Yamaizumi, Z., Berger, M. & Cadet, J. Photosensitized formation of 7,8-dihydro-8-oxo-2'-deoxyguanosine (8-hydroxy-2'-deoxyguanosine) in DNA by riboflavin: a nonsinglet oxygen-mediated reaction. *J Am Chem Soc* **114**, 9692-9694, doi:10.1021/ja00050a078 (1992).

33 Johnson, L. & Marks, D. Mirasol pathogen reduction technology modulates platelet oxidative stress [abstract]. *Vox Sang* **105**, 65-299. Abstract P-195. (2013).

34 Kilkson, H., Holme, S. & Murphy, S. Platelet metabolism during storage of platelet concentrates at 22 degrees C. *Blood* **64**, 406-414 (1984).

SUPPLEMENTARY FIGURES
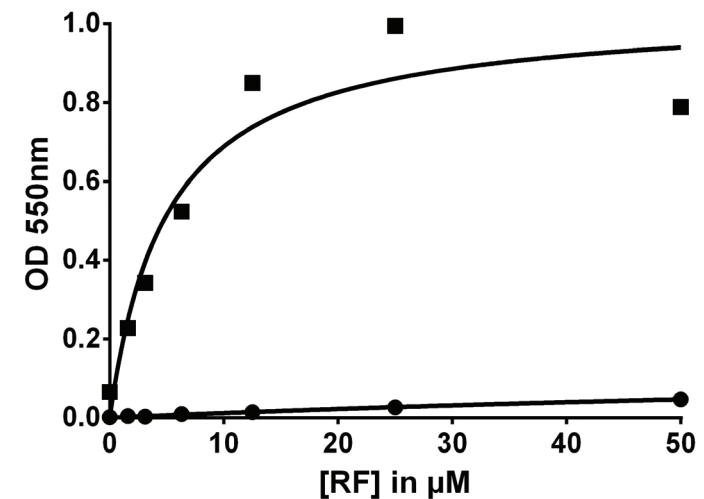
Figure S1: Reduction of nitrobluetetrazolium (NBT) by Mirasol illumination of various RF concentrations. *Nitroblue tetrazolium reduction to formazan derivatives was measured by spectrophotometry following (■) illumination of storage bags in a Mirasol illuminator in the presence of varying concentrations of riboflavin (RF) in PBS with EDTA. Absorbance values of each paired sample before illumination (●) is also shown. This experiment allows selection of an RF concentration in the linear part for dynamic range purposes.*
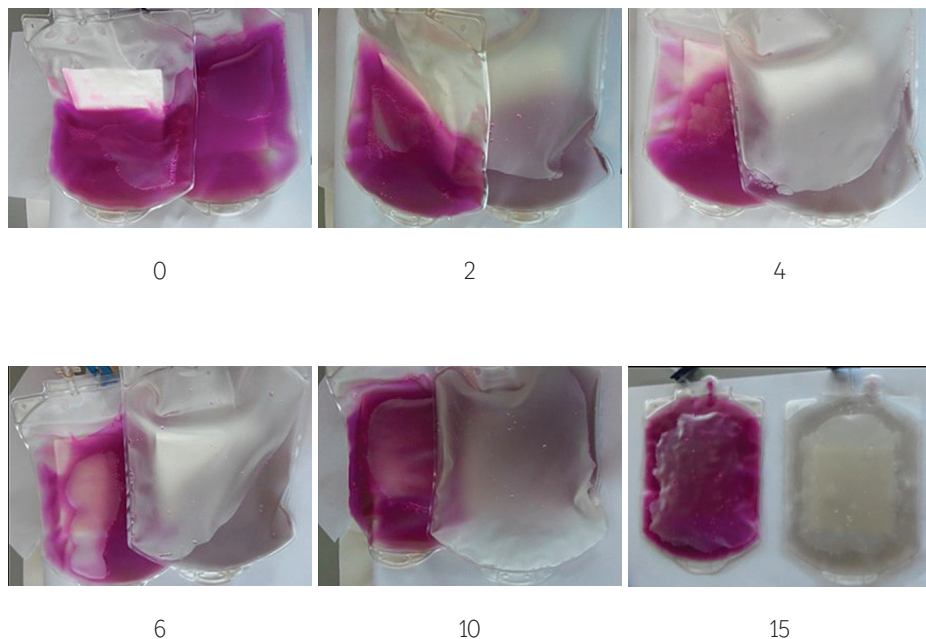
Figure S2: Nitrogen gas sparging effectively decreases dissolved oxygen in illumination bags. *The classical 'blue bottle experiment' used the resazurin-resorufin redox relationship to report the presence of dissolved molecular oxygen (pink) or not (transparent) in bags sparged with nitrogen gas (right) or not (left) during constant orbital agitation. Values below panels indicate sparging times in minutes. Following 15 minutes of sparging, sufficient molecular oxygen was removed from the bag to prevent reporter oxidation*
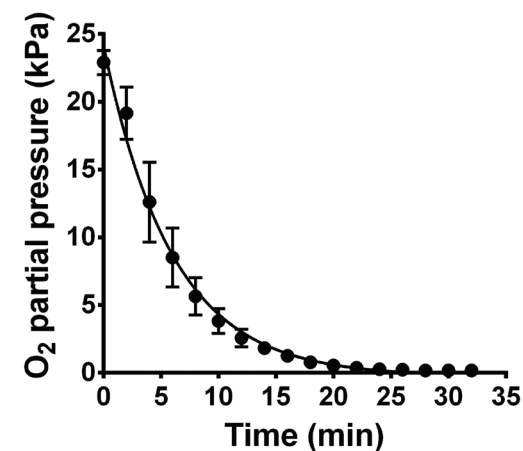
Figure S3: Partial pressure of dissolved oxygen in plasma decreases in function of N_2 sparging time. *Plasma bags containing 250mL single donor plasma was sparged with 0.5bar of dry gaseous N_2 under continuous mixing. A Clark-type oxygen sensing microelectrode was suspended in the bag content for continuous potentiometric recording. The data are depicted in kilopascal (kPa) and represent means with standard deviations of three independent experiments.*
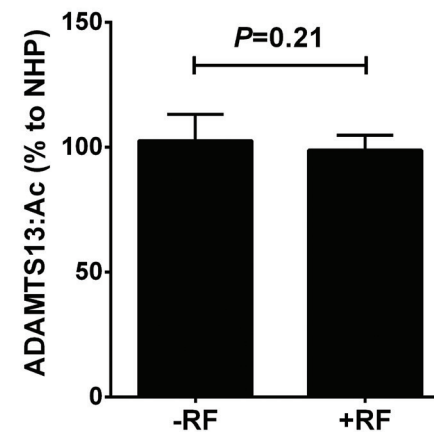
Figure S4: ADAMTS13 is not directly inhibited by RF. *ADAMTS13 activity was measured in paired plasma samples (n=9) in the presence (+RF) or absence (-RF) of 50µM riboflavin. Activity is expressed relative to an unrelated NHP. A paired two tailed t-test was used for comparison of means.*

2. POWERFUL RESEARCH TOOL TO INVESTIGATE THE FUNCTION OF PLATELETS

2.1 MICROFLUIDIC FLOW CHAMBERS USING RECONSTITUTED BLOOD TO MODEL HEMOSTASIS AND PLATELET TRANSFUSION *IN VITRO*

Video Article
Microfluidic Flow Chambers Using Reconstituted Blood to Model Hemostasis and Platelet Transfusion *In Vitro*

Britt Van Aelst[1], Hendrik B. Feys[1], Rosalie Devloo[1], Philippe Vandekerckhove[2,3,4], Veerle Compernolle[1,2,4]

[1]Transfusion Research Center, Belgium Red Cross-Flanders
[2]Blood Service, Belgium Red Cross-Flanders
[3]Department of Public Health and Primary Care, Catholic University of Leuven
[4]Faculty of Medicine and Health Sciences, University of Ghent

INTRODUCTION

Hemostasis requires the combined and regulated activity of cells, proteins, ions and tissues in a restricted spatiotemporal context[1]. Uncontrolled activity may lead to hemorrhage or thrombosis and morbidity or mortality in a spectrum of disorders related to blood coagulation. A microfluidic flow chamber experiment is a challenging technique that mimics hemostasis *in vitro*. This approach allows investigation of the complex interplay of processes that take part in hemostasis with a leading role for blood platelets.

Following vascular injury, platelets adhere to the exposed subendothelial matrix (glyco) proteins to prevent blood loss. Following adhesion, platelets activate and aggregate in response to auto- and paracrine signaling which finally leads to the formation of a platelet network, stabilized by fibrin and resulting in a firm, wound sealing thrombus[2]. Unlike most other platelet function tests, experiments with flow chambers take into account the physical parameter of blood flow and therefore the influence of rheology on the participating cells and biomolecules[3,4].

Flow chamber experiments have generated landmark insights in hemostasis and thrombosis by varying key parameters that influence hemostatic (sub)processes including the adhesive matrix, rheology and flow profiles, cellular composition, presence of toxins or drugs, ionic strength and many more. In the past two decades, low throughput flow chamber experiments requiring large sample volumes (10-100mL) have evolved to microfluidic chambers often consisting of small parallel-plate chambers and including modern technology for perfusing whole blood at controlled wall shear conditions[5]. Microscaling has significantly increased assay throughput mostly because the hardware setup has simplified and less (blood) volume is required, rendering the experiment more accessible and versatile. For instance, blood from small laboratory animals can now be used without the need to sacrifice animals. Blood samples of genetically modified mice have thus aided in the identification of key molecules promoting or inhibiting hemostasis and in novel basic insights [6].

Specialized research laboratories often still use custom made flow chambers for instance from polydimethylsiloxane (PDMS)[7] that polymerizes on lithographed molds which can be blueprinted by software. The resulting chamber is inexpensive, disposable and can be easily disassembled for post hoc analysis. Furthermore, basically any design of vessels, including bifurcations or sharp turns can be built on command. This advantage is also its downside since standardization was already the primary problem with flow chamber experiments, and PDMS custom made chambers have not aided this. On top of this particular issue, coating (conditions), fluorescent probes, anticoagulant, temperature and time between sampling and analysis are all poorly standardized[8]. Standardization of these variables is challenging, but nonetheless required to permit comparison of results between laboratories. This topic is the major subject of the International Society on Thrombosis and Haemostasis in Scientific and Standardization subcommittee on Biorheology[9,10].

Platelet concentrates (PC) are transfused in patients suffering from various diseases that cause thrombocytopenia and/or bleeding. But platelets in PC are known to desensitize, especially in function of storage time[11], a deterioration process linked to ageing and commonly referred to as platelet storage lesion. It is sometimes claimed that such platelets restore in circulation once transfused[12], but evidence for this is scarce. Furthermore, the functionality of platelets making up a PC is not routinely tested because the relationship between such assays and therapeutic or prophylactic efficacy is unclear[13]. Microfluidic flow chambers offer a means to investigate platelet function in PC to optimize the chain of manipulations between collection and issuing. It is a powerful research tool for direct (paired) comparisons of PC as we have previously published[14,15] and is described here.

PROTOCOL

This protocol follows the institutional ethical guidelines for research on human samples and informed consent was obtained from all donors involved. Approval for the experiments described here was obtained from the institutional review board of the Antwerp University Hospital. **Note:** Temperature indications are always room temperature, unless specified.

1. PREPARATION FLOW CHAMBER SET UP

1.1 PREPARING LANES, TUBING AND PINS

1.1.1 Vortex the collagen suspension vigorously and dilute 1/20 in the isotonic glucose solution supplied by the provider to a final concentration of 50µg/mL.
Note: We use equine tendon collagen, mainly made up of type I fibrils. The equine collagen type I is often referred to as "Horm" collagen and is the golden standard for this type of assay[9] for both historical as well as biological reasons. Human type III collagen can also be used, but the fibrils coat less well and the platelet response is not as strong. Other coating surfaces can also be used, for example von Willebrand Factor (VWF), fibrinogen, fibronectin, laminin, vitronectin, thrombospondin-1 or combinations of these[16].

1.1.2 Take a new disposable biochip from the provider's container. The dimensions of the biochips used here are 0.4W X 0.1H X 20L in mm.

1.1.3 Pipet 0.8µL into the lane(s) of the microfluidic biochip on one end of the chip and mark as outlet. Make sure that the lane is filled 5/6th with the collagen containing coating solution prepared in 1.1.1. Ensure that there are no air bubbles.
Note: Channels are partially coated to avoid accumulation of collagen fibers at the entrance of the channel (see discussion).

1.1.4 Incubate at 4°C for 4h or overnight in a humidified and closed container.

1.1.5 Block the coated channels by pipetting blocking buffer (1.0% (w/v) bovine serum albumin and 0.1% (w/v) glucose in 10mM 4-(2-hydroxyethyl)-1-piperazineethanesulfonic acid (HEPES) buffered saline (HBS; 0.9% (w/v) NaCl, pH 7.4) at the other end and mark as inlet. Make sure that the lane is completely filled with the blocking buffer avoiding air bubbles.

1.1.6 Cut tubing at equal length (12cm). Use one per lane and connect each tubing with a pin. For example, an experiment comparing two conditions, run in duplicate will require four tubing stretches and four pins to be prepared.

1.1.7 Rinse the tubing with distilled water using a syringe and a 26G needle or the accompanying connectors.

1.1.8 Saturate the tubing with blocking buffer. Store in a closed and humidified container for a minimum of 1h.

1.2 PREPARING PUMP AND MANIFOLD

1.2.1 Rinse the pump and manifold with distilled water, remove air bubbles.

1.2.2 Aspirate the blocking buffer out of the biochip lane(s) using the fixed 10µL tip at the outlet. Clean the surface of the biochip with a precision dust free wipe and denatured alcohol to remove prints and dust.

1.2.3.Fix the biochip on an automated microscope stage. If more than one lane is used simultaneously in one run, connect the eight-lane manifold splitter to the biochip outlet.
Note: The eight-lane manifold splitter is a piece of hardware **(Figure S1)** connected to the pump and the biochip. It allows operation of all available (eight) lanes on a biochip or a combination of lanes which can be operator-defined in the accompanying software.

1.2.4.Use the pins in the tubing to fix them in the biochip inlet. Place the other end of the tubing (without pin) in a 1.5mL conical test tube filled with HBS. Rinse all tubing and their connected lanes with 1mL HBS using the pump, so as to remove remainder blocking buffer and poorly adhering collagen.

2. PREPARATION OF BLOOD SAMPLES

2.1 COLLECTION AND SEPARATION OF FRESH WHOLE BLOOD FROM A HEALTHY VOLUNTEER.[17]

2.1.1 Collect the first milliliters of blood in an evacuated tube containing Ethyl-enediaminetetraacetic acid (EDTA) as an anticoagulant and exclusively use this sample for complete blood count (CBC) with an automated hematology analyzer.

2.1.2 Collect a volume of blood in a suitable anticoagulant using evacuated tubes. Standard anticoagulants for flow chamber experiments are heparin or hirudin when fibrin formation is not part of the study protocol and sodium citrate when it is.
Note: Heparin was used as an anticoagulant for all the experiments described in the results.
Note: The amount of blood depends on the number of experiments to be performed. Approximately 1 tube (7mL) for 3 lanes.

2.1.3 Place the tubes on a rotator pending blood reconstitution.
Note: The assay should be completed within 3 hours of phlebotomy.

2.1.4 Centrifuge for 15 minutes at 250g to prepare platelet rich plasma (PRP). Do not use the centrifuge break to prevent disturbance of the loosely packed pellet.

2.1.4.1 When more than one tube was collected, pool the blood in a single conical centrifugation tube.
Note: Centrifugation can be done more slowly or less long, depending on the PRP yield and differential cell "contamination" preferred.

2.1.5 Remove and discard the PRP and buffy coat yielding packed red blood cells with few platelets.
Note: The platelet count in the packed red cell fraction is $13\pm5\times10^3$ per μL (mean$\pm$SD, n=12) on average in our hands.

2.2. BLOOD RECONSTITUTION

2.2.1 Thaw blood group AB (Rhesus D negative) plasma at 37°C for 5 minutes and 20 seconds per 4mL.

2.2.2 Determine the hematocrit of the packed red blood cells prepared in 2.1.5 using an automated hematology analyzer.

2.2.3 Determine the platelet concentration in the blood bank prepared platelet concentrate that will be used to reconstitute the red cell fraction above.

2.2.4 Calculate the volume of packed red blood cells and platelet concentrate that will yield 40% hematocrit and 250×10^3 platelets/μL in a 1mL sample.
Note: Other target titers of cells can be set arbitrarily, depending on the study protocol.

2.2.5 Transfer packed red blood cells and plasma into a fresh tube using a clipped pipet tip and add platelet concentrate until a sample volume of 1mL is reached.
Note: Depending on the variables studied, the plasma fraction should be equal in all reconstituted samples because plasma has a significant influence on thrombus formation rate. For instance, repeated freeze-thawing or plasma taken from different donors or on different anticoagulants may influence the result.

2.2.6 Mix the reconstituted blood gently by inverting and perform a CBC.

2.2.7 Prepare a "blank" control sample in which the volume of platelet fraction is replaced by the same volume of 0.9% (m/v) sodium chloride in water to determine the concentration of endogenous platelets (i.e. non-blood bank platelets) in the reconstituted blood using a CBC.

2.3 LABELING

2.3.1 Pipet 1mL reconstituted blood in a test tube containing 1μL 5mM Calcein AM (5μM final concentration).
Note: Other cell dyes can be used[14].

2.3.2 Mix gently by inverting.

2.3.3 Incubate for 5min at 37°C prior to use.

3. PERFUSION ASSAY

3.1   Focus the objective on the collagen fibers adhered at the bottom of the lanes. Ideally, use phase-contrast or differential interference contrast (DIC) settings for this focusing strategy. Select 'Set current Z for selected tile regions' in the experiment software to digitally fix the selected Z-positions.

3.2   Select a region of interest (ROI) in the lane (xy) in the experiment software of the microscope that will be recorded during the experiment.
Note: The ROI can be any surface area arbitrarily chosen within a perfusion lane. It is advisable not to analyze thrombus formation close to the in- and outlet of a lane so to avoid side effects of the variable flow profile in that region, even though this is relatively small. The ROI surface area should contain a significant number of platelets or thrombi to allow leveling of the signal. In this protocol the ROI is a digitally stitched aggregate of three equally sized side-by-side images resulting in 0.62mm^2 in the middle of the 2cm long lane.

3.3   Mix the samples gently by inverting and position these next to the biochip on the automated stage.

3.4   Place the tubing that is connected with the inlet of the biochip in the test tubes containing the reconstituted blood samples.

3.5   Launch the pump at 50dyne/cm^2 (or other shear stresses as desired) for those channels linked to test tubes containing the reconstituted blood samples using the software of the pump.
Note: Other shear stresses can be used.

3.6   Record images every 15 seconds for 5 minutes in real-time using the acquisition and experiment software of the microscope.
Note: Other time series can be used depending on the experimental set-up.
Note: We generally use a 100X magnification (10X objective and 10X lenses), but higher (or lower) magnification can easily be used as an alternative.

4. WASH OUT

4.1 Wash out all tubing attached to the outlet and connected to the multichannel manifold or pump using distilled water, followed by sodium hypochlorite (bleach) 0.5% (v/v) and finally 0.1M NaOH in water. Discard the tubing pinned to the biochip inlet as hazardous waste.

5. DATA ANALYSIS

5.1 DETERMINE THROMBUS GROWTH KINETICS WITH THE IMAGE ANALYSIS SOFTWARE. THE FOLLOWING COMMANDS ARE SPECIFIC FOR ZEN2012.

5.1.1 Open the plugin *Image Analysis* to determine the surface coverage of the platelets.

5.1.2 Set the fluorescence threshold in the *Analyze Interactive* tab to define the pixel intensity that correlates with a positive signal, i.e. an adhered platelet or adhering platelets.

5.1.3 Use *Create Tables* to automatically generate a spreadsheet that will contain the separate surface areas (in μm^2) of those "objects" containing pixels with a signal between the selected thresholds. This is performed for each time point.
Note: Once fluorescence thresholds have been chose, the analysis software automatically detects 'objects' in the view field that fulfill the criteria. These objects are thrombi, small platelet aggregates or single platelets and cover a number of pixels. Every object is listed in the spreadsheet separately.

5.1.4 Save these spreadsheets in xml format and open them in a spreadsheet program for further calculations.

5.1.5 Total the surface areas of the selected objects by summation and divide the result by the total area of the measurement field (μm^2). This will yield the relative surface coverage (%). Do so for every time point.
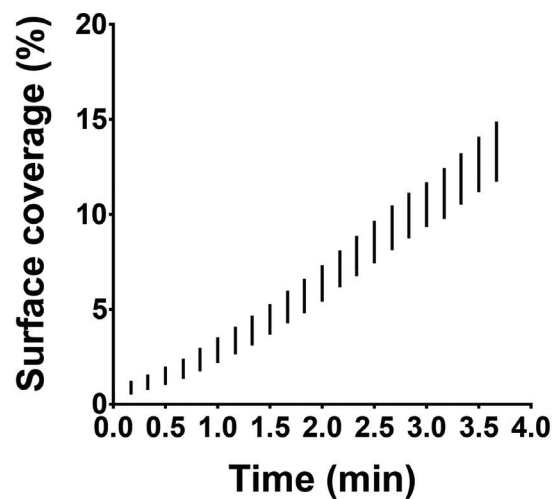
5.1.6 Plot these surface coverages in function of the perfusion time and calculate the slope by linear regression, yielding the thrombus growth kinetic of that particular condition.

RESULTS

To demonstrate intra-assay variation, three identical reconstituted whole blood samples were perfused simultaneously over collagen coated surfaces **(figure 1)**. This resulted in a coefficient of variation of 8.7%. This statistic suggests acceptable intra-assay and intralaboratory variation permitting reliable comparison between related samples.
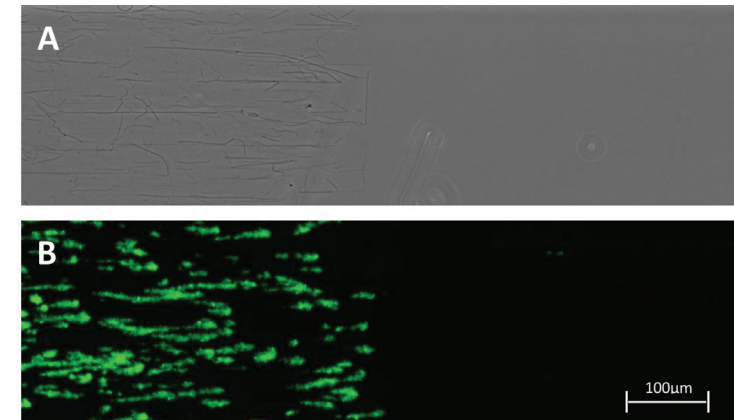
The inlet of the commercial flow chamber we describe here is perpendicular to the measurement chamber and this can cause slightly turbulent instead of laminar flow at that point. Especially in experiments without anticoagulation this may cause clogging because of the increased contact time between the blood and the immobilized agonist. The clogged inlet can confound the readout downstream in the chamber. Therefore, the setup was optimized by partially coating the flow chamber **(figure 2)** leaving the inlets devoid of platelet agonist, thereby avoiding untimely activation of primary and secondary hemostasis. Partial coating of adhesive surfaces is moreover successfully used by other research groups in the field[16]. In addition, this straightforward practical trick is an asset to study the "transition" zone where blood flowing over the non-reactive (uncoa-

ted) surface continues over the reactive (coated) portion.

Transfusion was simulated by reconstituting blood with the deficient component. To this purpose, anticoagulated whole blood from a healthy donor was rendered thrombocytopenic by differential centrifugation and PC platelets were added to increase platelet counts. An important question here was what platelet count to aim for? In most cases, real-life transfusions do not result in normalization of platelet counts in the thrombocytopenic patient. Rather a value above a certain threshold is aimed for, although the exact target value is ill-defined[18]. To understand the influence of varying platelet counts on microfluidic flow chambers outcomes in the context of blood reconstitution, several reconstitutions were performed with decreasing platelet concentrations **(figure 3)**. As expected, lower platelet counts resulted in less adhesion in function of perfusion time. Therefore, within a given study, platelet counts should be standardized to permit comparison between sample conditions[19]. The mere fact that there is fewer adhesion when platelet counts are low does however not imply that the assay cannot be used to measure platelet deposition in thrombocytopenic samples because microscopy and camera settings can be adapted to increase sensitivity. Finally, in most cases, the thrombocytopenic sample used for reconstitution contains remainder autologous platelets which resembles the situation in most transfusion demanding patients[18]. It is currently unclear if and what the role of autologous platelets is in the context of transfusion with allogeneic platelets but is an interesting question for future research.


Figure 1: Intra-assay variation in microfluidic flow chamber experiments. Microfluidic flow chamber experiments were performed on immobilized collagen at 50dynes/cm². All three identical reconstituted whole blood samples were perfused in parallel and at the same time. The results are shown as range (whiskers) for surface coverage in function of perfusion time.


Figure 2: Partially coated channel. (A) Collagen fibers visualized by phase contrast microscopy were found only in the coated region. (B) A snapshot after 5 minutes of perfusion with a Calcein AM labeled reconstituted whole blood sample pumped at 50dynes/cm² is shown. Both images were taken at a 100X magnification.
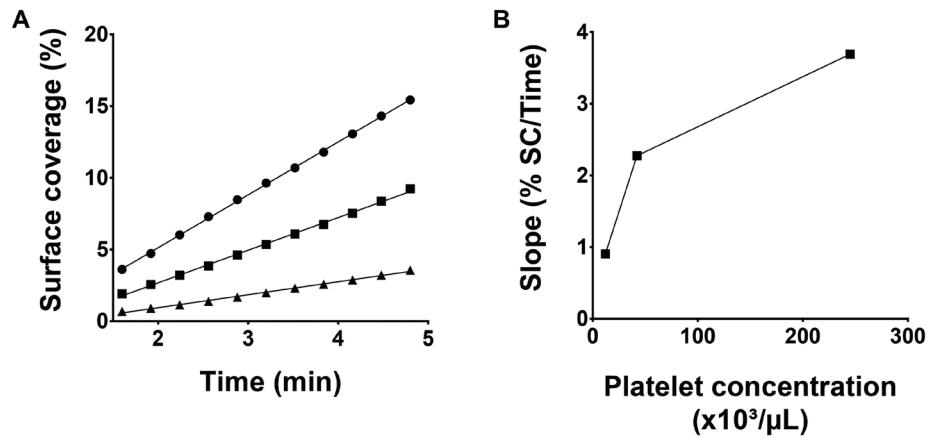
Figure 3: Thrombus growth kinetics depend on platelet counts in reconstituted blood. (A) Blood was reconstituted using a blood bank platelet concentrate yielding different platelet concentrations: 245x10³/µL (●), 42x10³/µL (■) and 12x10³/µL (▲). Microfluidic flow chamber experiments with collagen coated channels were performed simultaneously for all three samples at a shear stress of 50dynes/cm². (B) The slopes calculated by linear regression of the raw data in panel A are depicted.

Following collection of blood from healthy voluntary donors, whole blood is often cooled to and kept at constant room temperature prior to component preparation. Platelets are however sensitive to temperature changes. **Figure 4** shows the effect of decreased temperatures after blood collection and during perfusion. Thrombi were found to build more slowly when the blood was cooled to room temperature **(figure 4A)** compared to an identical (paired) sample kept at 37°C throughout the study **(figure 4B)**.

In circulation, platelets bind to vessel injury sites in conditions of elevated wall shear stress. Varying shear rates in microfluidic flow chambers coated with VWF/fibrinogen resulted in differences for total platelet adhesion at end point **(figure 5A)** and for thrombus growth kinetics **(figure 5B)**.
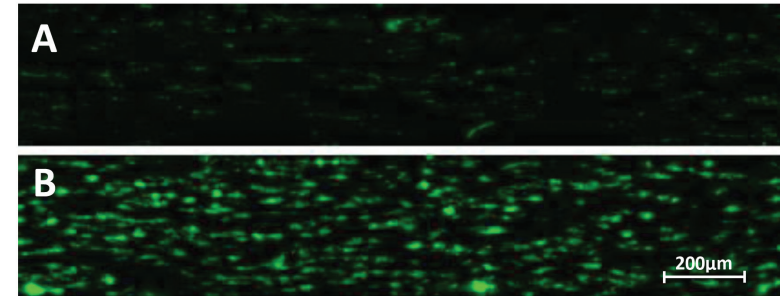

Figure 4: Temperature and microfluidic flow chambers. Whole blood collected in heparin vacutainers was preserved for 15 minutes in a water bath at room temperature (A) or at 37°C (B). Microfluidic perfusion on immobilized collagen at a shear stress of 50dynes/cm² was performed. Snap shots at end point (5 minutes perfusion) are depicted.

Finally, to demonstrate how microfluidic flow chambers can be used to investigate PC used for transfusion, thrombus growth kinetics in function of PC storage was investigated. All variables in sample preparation and experimental set-up were standardized throughout the study period. Hence, the sole variable parameter was PC storage time. **Figure 6** indicates decreasing thrombus growth in function of storage time demonstrating the effect of platelet storage lesion on hemostasis in vitro.

DISCUSSION

Microfluidic flow chamber experiments are an excellent tool to investigate platelet function in flowing blood and are used to evaluate hemostasis *in vitro* in varying experimental contexts. Despite poor interlaboratory standardization[9], we demonstrate that within our laboratory the experimental variation is acceptable. This allows to reliably compare (paired) samples within a given study. This was validated using the well documented phenomenon of platelet storage lesion, which is a detrimental consequence of platelet storage in blood bank conditions[11]. Furthermore, we recently published the impact of three available pathogen inactivation technologies on PC platelet function in microfluidic flow chambers following reconstitution of blood[14,15].

A

B
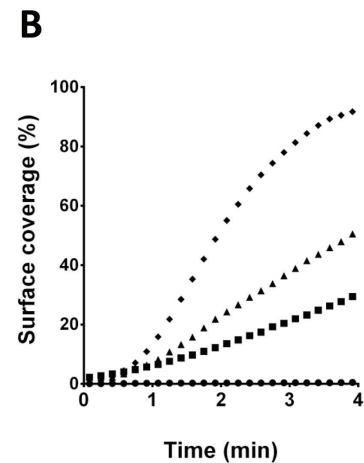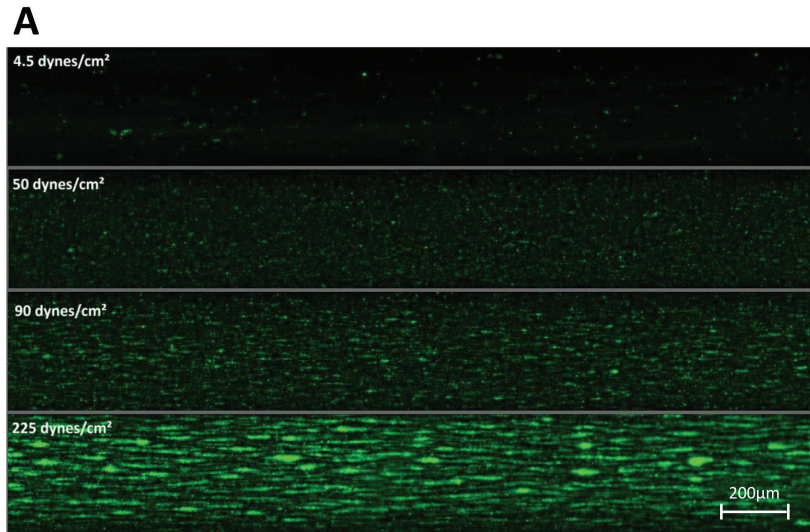
Figure 5: Role of shear stress on platelet adhesion to immobilized VWF/fibrinogen. (A) Four identical, calcein AM labeled, reconstituted whole blood samples were perfused over a VWF/fibrinogen coated surface with variable shear stress: 4.5dynes/cm² (●), 50dynes/cm² (■), 90dynes/cm² (●) and 225dynes/cm² (♦). After 3 minutes of perfusion, a snap shot was taken of all four channels. (B) Surface coverages in function of time of the samples described in (A) are shown illustrating differences in thrombus growth kinetics.

Platelets respond differently when biophysical and –chemical parameters are varied[19]. Therefore, shear stress, cell number and cellular composition, temperature, coating, anticoagulant and many more factors can be modified within this protocol depending on the research question. This protocol uses only commercially available hard- and software tools, allowing other laboratories to perform a similar assay. For basic research purposes this can be a disadvantage especially because the available hardware is less versatile than custom-made setups. The assay in itself is robust but reproducibility suffers from biological and temporal variation. Therefore, assay samples need to be paired as much as possible and study sizes should be sufficiently large. Samples also need to be paired in time, because reconstituted blood can only be stored for a short time.
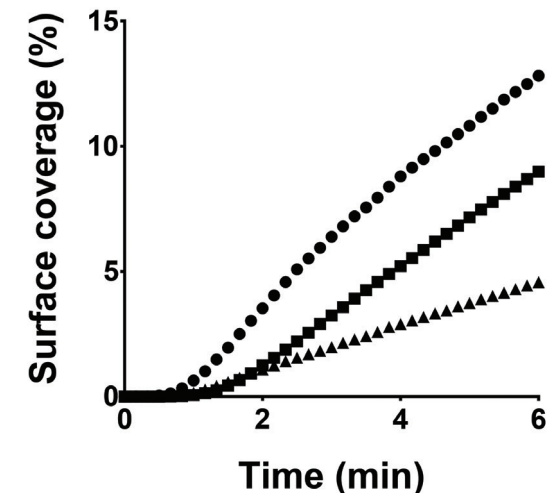
Figure 6: Thrombus formation of platelet concentrates in function of storage time. All microfluidic flow chamber experiments were performed under standardized conditions on collagen coated surfaces at a shear rate of 50dynes/cm². Blood was reconstituted with platelet samples of the same concentrate tested in duplicate on day three (●), seven (■) and ten (▲) post donation. Surface coverages in function of perfusion time are depicted.

Although microfluidic flow chambers for platelet function studies have boosted the research field, caution should be taken to overinterpret the platelet dependence on blood rheology. First, the rectangular shape of the flow chamber is not physiologic, but the best we have to allow optical focusing on growing thrombi. Second, blood vessels are not made of plastic and the influence of blood vessel elasticity on platelet function can therefore not be studied in this protocol. Third, the

heart causes pulsatile flow, while syringe pumps are more linear (although also slightly pulsatile). Finally, fibrillar type I collagen is the standard material used for platelet studies under flow, which is of animal origin. Of note however, fibrillar type I collagen and clinical results for platelet function correlate well in many cases as shown by decades of experience in (light transmission) aggregom-etry[20,21].

There are many assays to study platelet function[22]. Most of these address one or a couple of platelet features while putting platelets to work in (models of) hemostasis. Real time imaging of thrombus formation as demonstrated here is the most inclusive, to date. This means most aspects of the platelet's response to vessel injury are included. Unique advantages are the inclusion of blood flow and the presence of all blood cells. The assay is sensitive to the currently used drugs for antiplatelet therapy[23] as well as to genetic changes resulting in aberrant platelet function[24]. This demonstrates its value as a relevant indicator of platelet function. The comprehensive nature of this assay nonetheless also implies that it is less analytical than those assays measuring specific features of the platelet's response. Effects of blood banking manipulations on platelet concen-trates can therefore by picked up by flow chamber assays, but to interpret what causes them, addi-tional analysis is required. For instance, our data indicate that temperature significantly influences platelet adhesion in microfluidic flow chambers. But additional detailed analysis has shown that refrigerated platelets change shape and cluster GPIbα receptors[25].

The versatility of the adhesive surface permits to study different reactive platelet substrates or combinations thereof. Recent work by De Witt et al[16] demonstrated the relevance of substrate definition to platelet systems biology. Moreover, the combination of varying shear rates in func-tion of the substrate is important because binding of platelets to immobilized VWF will require high shear rates, while this is less important for binding to collagen. Therefore, depending on the research question, choices can be made on what substrates and their respective flow rates are to be included.

In conclusion, we present a protocol for microfluidic flow chamber experiments to study platelet function in the context of blood banking and transfusion medicine. Standardization efforts are ongoing[9,10,26-28] and most of these recommendations are included in the protocol presented. The reconstitution of blood is a model for transfusion but additional validation work should indicate the relevance to clinical outcomes.

AUTHORSHIP CONTRIBUTIONS

BVA, HBF and VC designed research; VC and PV contributed critical analytical tools, reagents, or samples and facilitated research; BVA and RD performed research and collected data; BVA, RD, VC, and HBF analyzed and interpreted data; BVA, RD, and HBF performed statistical analyses; BVA and HBF wrote the manuscript; and all authors critically reviewed and amended the manuscript.

REFERENCES

1. Broos, K., Feys, H.B., De Meyer, S.F., Vanhoorelbeke, K. & Deckmyn, H. Platelets at work in primary hemostasis. *Blood Rev* **25**, 155-167 (2011).
2. Stalker, T.J., *et al.* Hierarchical organization in the hemostatic response and its relationship to the platelet-signaling network. *Blood* **121**, 1875-1885 (2013).
3. Sakariassen, K.S., Bolhuis, P.A. & Sixma, J.J. Human blood platelet adhesion to artery subendot helium is mediated by factor VIII-Von Willebrand factor bound to the subendothelium. *Nature* **279**, 636-638 (1979).
4. Savage, B., Saldivar, E. & Ruggeri, Z.M. Initiation of platelet adhesion by arrest onto fibrinogen or translocation on von Willebrand factor. *Cell* **84**, 289-297 (1996).
5. Westein, E., de Witt, S., Lamers, M., Cosemans, J.M. & Heemskerk, J.W. Monitoring in vitro thrombus formation with novel microfluidic devices. *Platelets* **23**, 501-509 (2012).
6. Varga-Szabo, D., *et al.* The calcium sensor STIM1 is an essential mediator of arterial thrombosis and ischemic brain infarction. *J Exp Med* **205**, 1583-1591 (2008).
7. Westein, E., *et al.* Atherosclerotic geometries exacerbate pathological thrombus formation poststenosis in a von Willebrand factor-dependent manner. *Proc Natl Acad Sci U S A* (2013).
8. Grabowski, E.F., Yam, K. & Gerace, M. Evaluation of hemostasis in flowing blood. *Am J Hematol* **87 Suppl 1**, S51-55 (2012).
9. Roest, M., *et al.* Flow chamber-based assays to measure thrombus formation in vitro: requirements for standardization. *Journal of thrombosis and haemostasis : JTH* **9**, 2322-2324 (2011).
10. Heemskerk, J.W.M., *et al.* Collagen surfaces to measure thrombus formation under flow: possibilities for standardization. *Journal of Thrombosis and Haemostasis* **9**, 856-858 (2011).
11. Shrivastava, M. The platelet storage lesion. *Transfus Apher Sci* **41**, 105-113 (2009).
12. Miyaji, R., *et al.* Decreased platelet aggregation of platelet concentrate during storage recovers in the body after transfusion. *Transfusion* **44**, 891-899 (2004).
13. Goodrich, R.P., *et al.* Correlation of in vitro platelet quality measurements with in vivo platelet viability in human subjects. *Vox Sanguinis* **90**, 279-285 (2006).
14. Van Aelst, B., *et al.* Riboflavin and amotosalen photochemical treatments of platelet concentrates reduce thrombus formation kinetics in vitro. *Vox Sanguinis* **108**, 328-339 (2015).
15. Van Aelst, B., Devloo, R., Vandekerckhove, P., Compernolle, V. & Feys, H.B. Ultraviolet c light pathogen inactivation treatment of platelet concentrates preserves integrin activation but affects thrombus formation kinetics on collagen in vitro. Transfusion, n/a-n/a (2015).
16. de Witt, S.M., et al. Identification of platelet function defects by multi-parameter assessment of thrombus formation. *Nat Commun* **5**, 4257 (2014).
17. Cazenave, J.P., *et al.* Preparation of washed platelet suspensions from human and rodent blood. *Methods Mol Biol* **272**, 13-28 (2004).

18. Diedrich, B., Remberger, M., Shanwell, A., Svahn, B.M. & Ringden, O. A prospective randomized trial of a prophylactic platelet transfusion trigger of 10 x 10(9) per L versus 30 x 10(9) per L in allogeneic hematopoietic progenitor cell transplant recipients. *Transfusion* **45**, 1064-1072 (2005).
19. Neeves, K.B., *et al.* Sources of variability in platelet accumulation on type 1 fibrillar collagen in microfluidic flow assays. *PloS one* **8**, e54680 (2013).
20. Born, G.V. Aggregation of blood platelets by adenosine diphosphate and its reversal. *Nature* **194**, 927-929 (1962).
21. Cattaneo, M., *et al.* Recommendations for the Standardization of Light Transmission Aggregometry: A Consensus of the Working Party from the Platelet Physiology Subcommittee of SSC/ISTH. *Journal of thrombosis and haemostasis : JTH* **11**, 1183-1189 (2013).
22. Deckmyn, H. & Feys, H.B. Assays for quality control of platelets for transfusion. *ISBT Science Series* **8**, 221-224 (2013).
23. Andre, P., *et al.* Anticoagulants (thrombin inhibitors) and aspirin synergize with P2Y12 receptor antagonism in thrombosis. *Circulation* **108**, 2697-2703 (2003).
24. Casari, C., *et al.* von Willebrand factor mutation promotes thrombocytopathy by inhibiting integrin alphaIIbbeta3. *J Clin Invest* **123**, 5071-5081 (2013).
25. Gitz, E., *et al.* Improved platelet survival after cold storage by prevention of Glycoprotein Ib clustering in lipid rafts. *Haematologica* (2012).
26. Van Kruchten, R., Cosemans, J.M. & Heemskerk, J.W. Measurement of whole blood thrombus formation using parallel-plate flow chambers – a practical guide. *Platelets* **23**, 229-242 (2012).
27. Zwaginga, J.J., *et al.* Flow-based assays for global assessment of hemostasis. Part 2: current methods and considerations for the future. *Journal of thrombosis and haemostasis : JTH* **4**, 2716-2717 (2006).
28. Zwaginga, J.J., *et al.* Flow-based assays for global assessment of hemostasis. Part 1: Biorheologic considerations. *Journal of thrombosis and haemostasis : JTH* **4**, 2486-2487 (2006).

SUPPLEMENTARY FIGURE

A

B
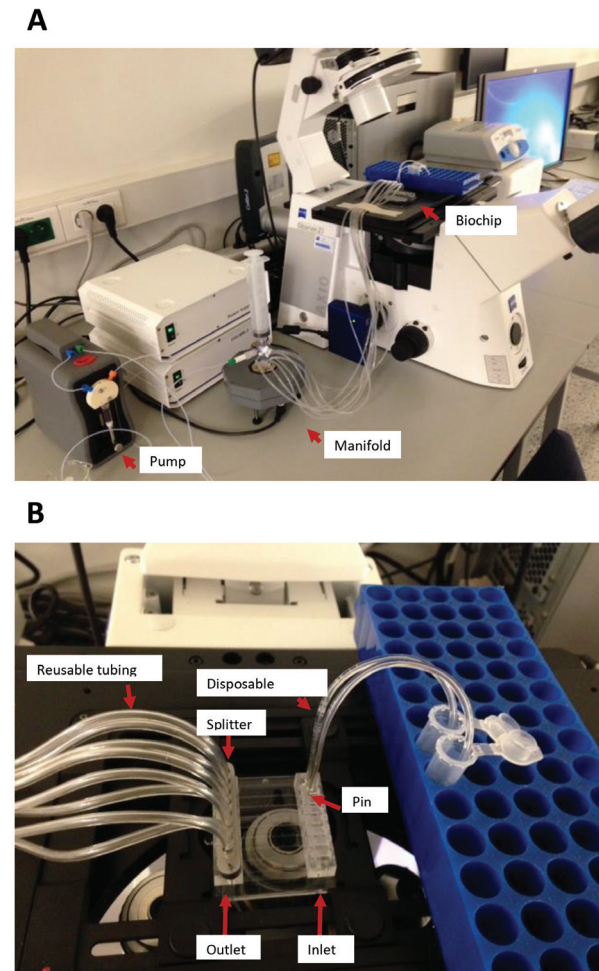
Figure S1: Microfluidic flow chamber hardware setup. *(A) A Vena 8 Fluoro+ biochip is mounted on the automated stage of the microscope and is connected via flexible tubing to a syringe pump with manifold to split the pumping function into eight separate channels. (B) Reconstituted blood flows through the disposable tubing on the right side into the selected channels of the biochip (inlet). The disposable tubing is fixed in the inlet through a stainless steel disposable pin supplied with the setup. Blood flow in (B) is from right to left and is collected in long flexible tubings.*

3. PATHOGEN INACTIVATION OF PLATELETS

3.1 RIBOFLAVIN AND AMOTOSALEN PHOTO-CHEMICAL TREATMENTS OF PLATELET CONCENTRATES REDUCE THROMBUS FORMATION KINETICS *IN VITRO*

Riboflavin and amotosalen photochemical treatments of platelet concentrates reduce thrombus formation kinetics *in vitro*

B. Van Aelst,[1] H. B. Feys,[1] R. Devloo,[1] K. Vanhoorelbeke,[2] P. Vandekerckhove[3,4] & V. Compernolle[1,3,5]

[1]*Transfusion Research Center, Belgian Red Cross-Flanders, Ghent, Belgium*
[2]*Laboratory for Thrombosis Research, KU Leuven Kulak, Kortrijk, Belgium*
[3]*Blood Service of the Belgian Red Cross-Flanders, Mechelen, Belgium*
[4]*Department of Public Health and Primary Care, Catholic University of Leuven, Leuven, Belgium*
[5]*Faculty of Medicine and Health Sciences, University of Ghent, Ghent, Belgium*

INTRODUCTION

Transfusion transmitted infections are a considerable threat to global blood supplies. Because the optimal conditions for safeguarding platelet integrity include storage at room temperature, platelet concentrates are in addition particularly vulnerable to bacterial contamination. Photochemical treatment[1] (PCT) efficiently tackles this problem by chemically damaging bacteria, viruses and protozoans. Three pathogen inactivation methods have been developed for platelet concentrates, one that uses exclusively ultraviolet (UV) C light[2] and two employing an exogenously added photosensitizer with ultraviolet light illumination; ribofla-vin (vitamin B2) pathogen reduction technology (RF-PRT, TerumoBCT, Lakewood, CO) uses broad spectrum UV light[3] and amotosalen (S59) photochemical treatment (AS-PCT, Cerus Corp, Concord, CA) uses UVA[4].

Damage to nucleic acids is a major driver of pathogen kill following photoexcitation of many chemical sensitizers used for blood applications. Psoralens like amotosalen intercalate in helical regions of RNA and DNA and irreversibly form adducts and cross-links with pyrimidines following photoexcitation. For RF-PRT, the pathogen reduction mechanism may be less confined to the sensitizer (dark) binding site[5] but also includes nucleic acid damage[6]. Biostatic methodologies that specifically harm nucleic acids will evidently prevent targeted cells/viruses from replicating but this process by definition cannot be affected in cells without the intrinsic potential to replicate at all, like platelets. Importantly though, this principally theoretical concept drives the notion that both PCTs are highly specific for damaging solely pathogens, which is not necessarily true. For instance, platelets do contain helical nucleic acid in the form of mitochondrial DNA and remnant RNA from their megakaryocytic precursor. Furthermore, all photosensitizers produce reactive oxygen species (ROS) and these are by no means specific in their chemistry with the surrounding milieu. Moreover, photosensitizers not only partition to nucleic acids[7], but also to other biomolecules where reaction can occur.

For both PCTs the past decade has produced extensive *in vitro* data on platelet storage lesion (PSL) markers like pH and glycolytic metabolites, platelet receptor expression and/or hypotonic shock response. However, less attention has gone to functional assays like platelet aggregation[8–11] or (even less) thrombus formation in microfluidic flow chambers under controlled conditions[12]. Notwithstanding this void, the latter is important since it is the most comprehensive functional test with high sensitivity to perturbations in all steps of hemostasis[13].

A recent effort of the Biorheology subgroup of the Scientific and Standardization Committee of the International Society on Thrombosis Haemostasis has demonstrated the importance of comprehensive platelet function testing in systems with well known hydrodynamic shear profiles supplemented with real-time analysis of platelet deposition[14]. The technique is used for screening patients in (pre)clinical settings[15] and has been proven valuable in drug development as well, e.g. to assess platelet functional inhibition[16,17]. We have set up such an *in vitro* model of hemostasis with reconstituted blood perfused through microfluidic chambers combined with real-time measurement of thrombus formation on immobilized collagen and von Willebrand factor (VWF). Our data show that *in vitro* thrombus formation kinetics are affected immediately following both RF-PRT and AS-PCT, but that their main causative biomolecular alterations are different.

MATERIALS AND METHODS

STUDY DESIGN

The two studies for RF-PRT and AS-PCT have been conducted separately, but with comparable design. Within each study the samples were paired, but not between studies. For both RF-PRT and AS-PCT leukocyte-depleted platelet concentrates were prepared by pooling of five and six buffy coats, respectively. In all cases the buffy coats were derived from voluntary non-remunerated whole blood donations after giving written informed consent.

For RF-PRT, three platelet concentrates in additive solution (SSP+, Macopharma, Tourcoing, FR) were pooled, gently mixed and then split in three equivalent products (n=6). One product remained untreated (control), another was RF-PRT treated following a one hour resting period and the last one was treated with 25-50 Gray of gamma irradiation. In this particular study, gamma treated concentrates were included alongside untreated controls to include products that follow the current routine production. For RF-PRT, 35mL of riboflavin (RF) (500µM in saline) was added followed by expelling air bubbles and illumination with a dose of ultraviolet light (265nm-370nm) optimized by the provider for treating products in additive solution[8]. The RF-PRT concentrates were protected from ambient light and all concentrates were kept in the same type of storage container (TerumoBCT).

For AS-PCT, two platelet concentrates in additive solution (SSP+) were pooled, gently mixed and split in two equivalent products (n=6). One product remained untreated (control) and the other was treated with AS-PCT according to the guidelines of the manufacturer. In brief, the product was transferred to an illumination bag while 17.5mL amotosalen (final ~150µM) was added, followed by expelling excess air bubbles and UVA illumination (320-400nm). Following overnight incubation (<16 hours) with the compound adsorption device (CAD), it was transferred to a storage bag. Both concentrates were kept in the same type of storage container (Cerus Corp).

All concentrates were kept under standard blood bank conditions. Low volume samples were aseptically removed through sterile connections under a laminar flow hood to allow experiments before (day 1) and after (day 2, 5 and 7) treatment. The day of phlebotomy is considered day 0.

BLOOD RECONSTITUTION

An ABO-matched blood sample from healthy non-medicated volunteers was collected in heparin vacutainers (REF'368480, BD Diagnostics, Franklin Lakes, NJ) with measures for preserving platelet quiescence[18]. The blood was centrifuged at 250g to prepare platelet rich plasma (PRP) and red blood cells (RBC). The PRP and buffy coat were transferred to a new tube and centrifuged at 4500g to yield platelet-poor plasma. The cell pellet was discarded. To obtain reconstituted blood, packed RBC and plasma from this fresh blood were mixed with platelets from the respective research conditions aiming at 40 percent hematocrit and 250,000 platelets/µL. In the reconstituted blood a mean (±SD) platelet concentration of 236±21 x10³platelets/µL and a hematocrit of 40.4±1.1% was become for RF-PRT and 248±16 x10³platelets/µL and a hematocrit of 40.5±1.3% was become for AS-PCT (both n=6).

PLATELET FUNCTION DURING BLOOD PERFUSION IN MICROFLUIDIC CONDITIONS

Perfusion experiments were performed using Vena8 Fluoro+™ biochips (Cellix Ltd, Dublin, Ireland). The microfluidic channels were incubated with 50µg/mL type I collagen (Takeda, Osaka, Japan) or 5IU/mL VWF (Wilfactin, CAF-DCF, Brussels, Belgium) at 4°C overnight and next blocked with 10mM 4-(2-hydroxyethyl)-1-piperazineethanesulfonic acid (HEPES) buffer, pH 7.4 with 0.9% NaCl (HBS) containing 1.0% (w/v) bovine albumin and 0.1% (w/v) D-glucose at room temperature for 30 minutes. Blocking buffer and remainder collagen solution were rinsed with 1mL HBS buffer, pH 7.4 at 200dynes/cm². The reconstituted blood in the RF-PRT study was labeled with 1µM 3,3'-dihexyloxacarbocyanine iodide (DiOC6) (Sigma-Aldrich, Saint Louis, MO) for 10 minutes at 37°C. The reconstituted blood samples in the AS-PCT were labeled with calcein-AM (5µM final) (Life technologies, Carlsbad, CA) or where indicated with DiOC6 as mentioned above.

Paired samples (control vs treated) were perfused simultaneously and in duplicate using an automated microscope stage and a channel splitting manifold. Perfusion was performed at 50dynes/cm² (1,100s⁻¹ flow rate) over collagen and at 135dynes/cm² (3000s⁻¹ flow rate) over VWF using a Mirus Evo microfluidic pump (Cellix). Where indicated 50ng/mL of tirofiban (aggrastat, Sigma-Aldrich) was added to block integrin $\alpha_{IIb}\beta_3$ binding. Every 20 seconds, three side-by-side images were snapped in real-time in each lane during five minutes using an inverted fluorescent microscope at 100X magnification equipped with a Colibri-LED fluorescent light source (488nm) and high resolution CCD camera (all Carl Zeiss, Oberkochen, Germany). One single image per time point was generated by digitally stitching the three side-by-side images (ZEN2012 software (Carl Zeiss)). Surface coverage increased linearly in function of time for at least five minutes **(Figure S1)**. Pixels were positive for platelet deposition using a fixed threshold of 400-4096 arbitrary fluorescence units. Slopes were determined by linear regression (Prism, GraphPad Software Inc, La Jolla, CA) and are a measure for the rate at which thrombi deposit on collagen. Blood reconstituted with RF-PRT platelets maximally contained 12.5µM RF which did not interfere with the readout (data not shown).

BLOOD GASES AND PLATELET COUNT
Glucose, lactic acid and pH were measured immediately after sampling by a point-of-care instrument (Siemens Rapidpoint 500, Munich, Germany). Whole blood counts and mean platelet volume (MPV) were determined using an automated hematology analyzer (pocH-100i™, Sysmex, Kobe, Japan).

FLOW CYTOMETRY
Expression of glycoprotein Ibα (anti-CD42b~fluorescein, Life technologies, Carlsbad, CA), activated integrin $\alpha_{IIb}\beta_3$ (PAC-1~fluorescein, BD Biosciences, Erembodegem, Belgium), P-selectine (anti-CD62P~phycoerythrin, BD Biosciences) and Annexin V (Annexin V~Peridinin chlorophyll-Cy5.5; BD Biosciences) was determined using an acoustic focusing Attune flow cytometer (Life Technologies). Platelets were incubated with labeled antibodies or ligand for 10 minutes at room temperature in HBS, supplemented with 1mM $MgSO_4$, pH 7.4 and diluted thousand fold immediately before readout as described in established methods[19]. For Annexin V measurements, buffers were supplemented with 2mM $CaCl_2$. For measurements of integrin $\alpha_{IIb}\beta_3$ activation on stimulated platelets, the PAR1 agonist thrombin related activating peptide SFLLRN (PAR1AP, Sigma-Aldrich) was added at 30µM. The signals of the isotype antibody controls were used to set threshold gates including 0.5% of 10,000 negative events. Mean or median fluorescence intensities and percentage positive events were determined of 10,000 cells staining positive for the platelet marker CD61 (anti-CD61~allophycocyanin, Life Technologies).

AGGREGATION
Platelet aggregation was determined by light transmission in a dual-channel lumiaggregometer (Chrono-log, Helena Laboratories, Haverton, PA) using three different platelet agonists, each at two concentrations. A saturating concentration to boost aggregation and a threshold (i.e. halfmaximal or EC50) concentration to investigate platelet sensitivity. Both concentrations were determined in separate serial dilution experiments (data not shown) using the same assay conditions as below. For collagen (American Biochemical & Pharmaceuticals, Epsom, United Kingdom) 25µg/mL and 10µg/mL was used, PAR1AP at 10µM and 6µM and ristocetin (American Biochemical & Pharmaceuticals) at 1.5mg/mL and 0.6mg/mL. Aggregation cuvettes contained platelets diluted to 250,000 platelets/µL with the corresponding autologous platelet free plasma with additive solution. The latter was prepared by centrifugation at 4500g for 20 minutes to pellet the platelet fraction. The readout comprises maximal aggregation (amplitude (%)), rate (slope), and total aggregation potential (area under curve). In all cases maximal aggregation is shown, but the corresponding auxiliary parameters were comparable.

VWF BINDING TO GLYCOCALICIN
Binding of VWF to GPIb was determined with the VWF:RCo enzyme-linked immunosorbant assay (ELISA) as previously published[20]. In brief, the anti-GPIbα monoclonal antibody 24B3 is coated and following a blocking step, the binding sites are saturated with glycocalicin derived from a normal human plasma pool (n=38). Next, the suspending media of the platelet concentrates are incubated in the presence of 1mg/mL ristocetin to allow binding of VWF to the immobilized glycocalicin. After washing excess medium, bound VWF is detected by horse radish peroxidase labeled anti-VWF polyclonal antibody (Dako, Glostrup, Denmark).

STATISTICAL ANALYSIS
Comparison of mean values of the study arms in function of time was with repeated measures two-way ANOVA with Tukey's or Sidak's correction for multiple comparisons testing and a 0.05 significance level. Analyses were performed with Prism software version 6.01 (GraphPad Software Inc).

RESULTS

PHOTOCHEMICAL TREATMENT DECREASES THE RATE OF THROMBUS FORMATION IN MICROFLUIDIC FLOW CHAMBERS
The supplementary video files show that thrombus growth was faster from day two onwards for control conditions compaired to photochemical treated arms in both the RF-PRT and AS-PCT study. **Figure 1** shows platelet deposition (surface coverage) in function of perfusion time and confirms significant decreases for both inactivation methods. This result was independent of the fluorescent label used to visualize growing thrombi **(Figure S2)**. Platelet concentrates treated with gamma irradiation in the context of the RF-PRT study were not significantly different from controls. We conclude that in reconstituted heterologous blood, *in vitro* hemostatic function of photochemically treated platelets is affected from the day after treatment with no signs of functional recovery during storage for both methods.

RF-PRT AFFECTS PLATELET AGGREGATION
An important step in hemostasis is interplatelet cross-linking which was measured by light transmission aggregometry using different agonists. The thrombin-mimetic PAR1 activating peptide SFLLRN (PAR1AP) acts through the G protein-coupled receptor PAR1 while collagen activates platelets via GPVI-FcγRIIa and ristocetin modulates VWF to initiate agglutination through GPIbα. **Figure 2** shows that RF-PRT affects platelet aggregation when compared to control and gamma irradiation at both agonist concentrations. However, the decrement is smaller at high **(Figure 2B, D and F)** than at low-dose agonist concentrations **(Figure 2A, C and E)**, which may indicate decreased amplification[21]. Gamma irradiation had no measurable effect compared to controls.
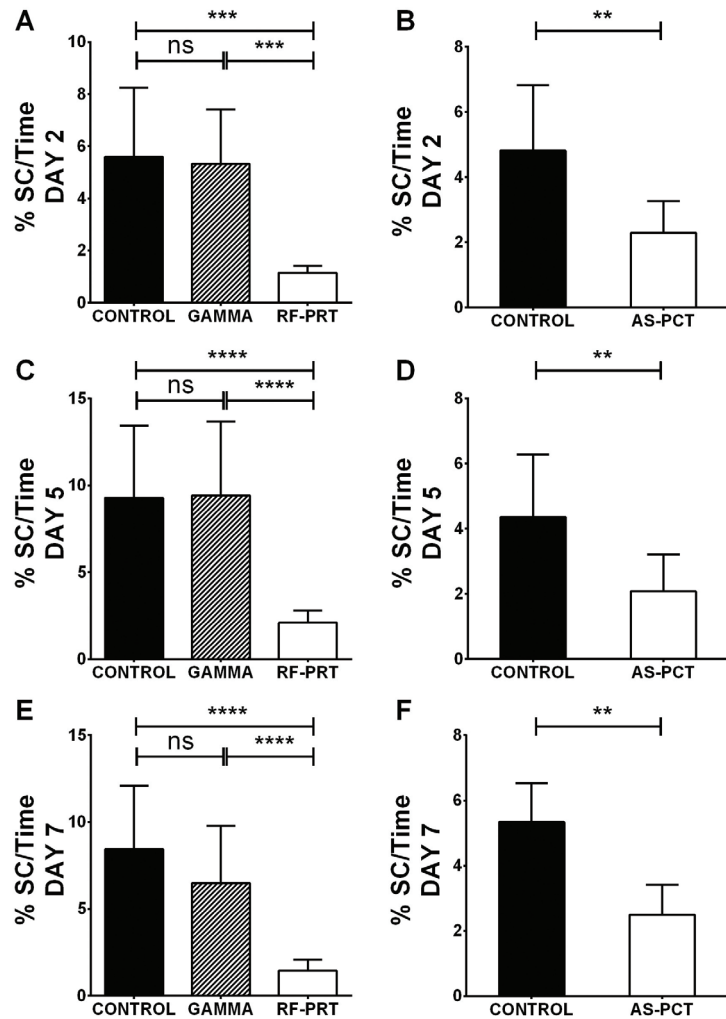
Figure 1: Photochemical treatment decreases the rate of thrombus formation, in vitro. *Blood was reconstituted with platelets from control (closed bars), gamma (shaded bars) and photochemically treated (open bars) concentrates and perfused in microfluidic flow chambers at a shear stress of 50dyne/cm². Data are shown for RF-PRT (A,C and E) and AS-PCT (B,D and F) studies. Real-time video microscopy measured surface coverage in function of time (%SC/Time). Results are shown for days 2 (A-B), 5 (C-D) and 7 (E-F) post phlebotomy as indicated. The statistical results of two-way ANOVA is shown on top of the panels (ns=not significant;**P<.01;***P<.001;****P<.0001).*
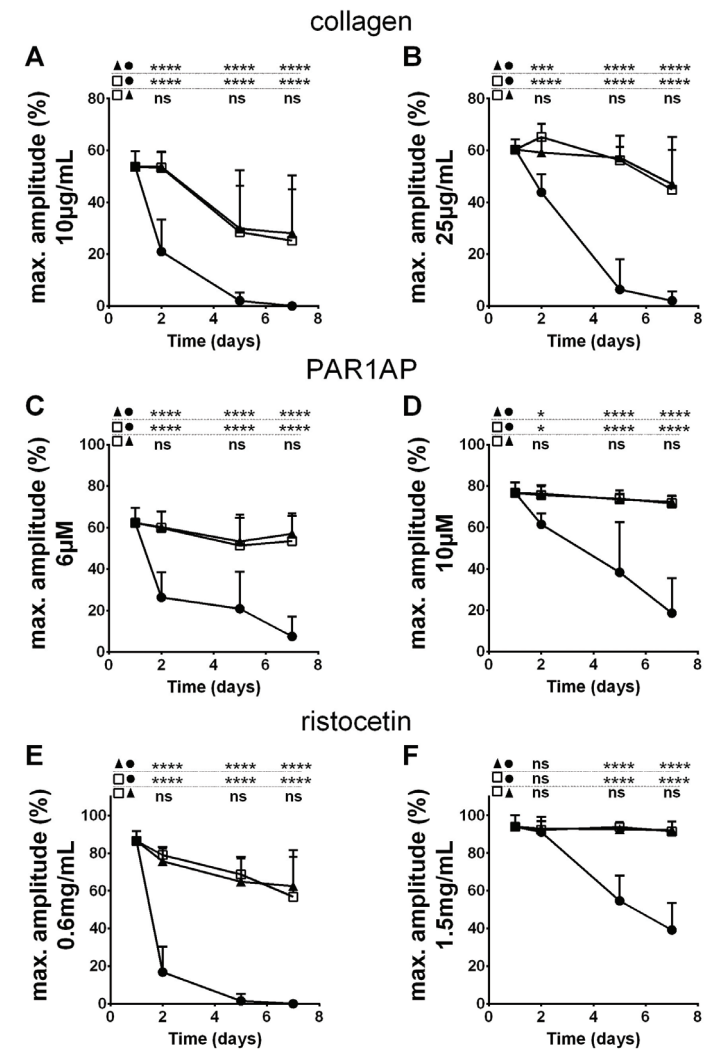
Figure 2: RF-PRT affects platelet aggregation. *Light transmission aggregometry was performed with three agonists, each in a low (A,C and E) and high (B,D and F) concentration. Maximal aggregation is depicted as means with standard deviation (n=6). Control (□), gamma (▲) and RF-PRT (●) platelets were analyzed before (day 1) and after (day 2, 5 and 7) treatment. The statistical results of two-way ANOVA is shown on top of the panels (ns=not significant;*P<.05;***P<.001;****P<.0001).*
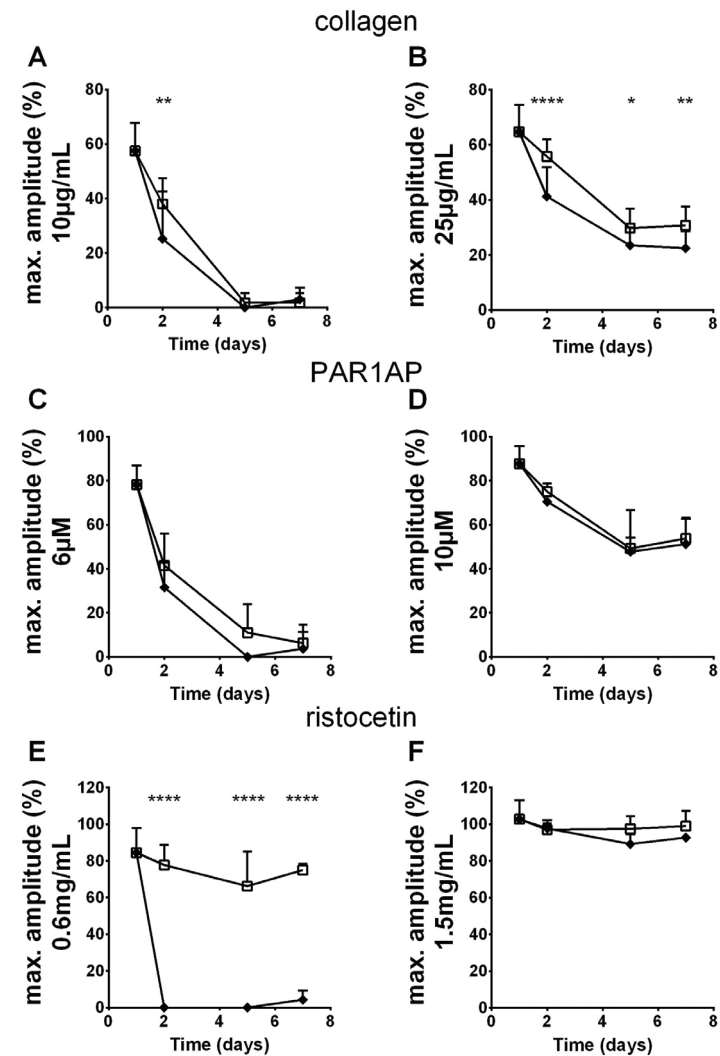
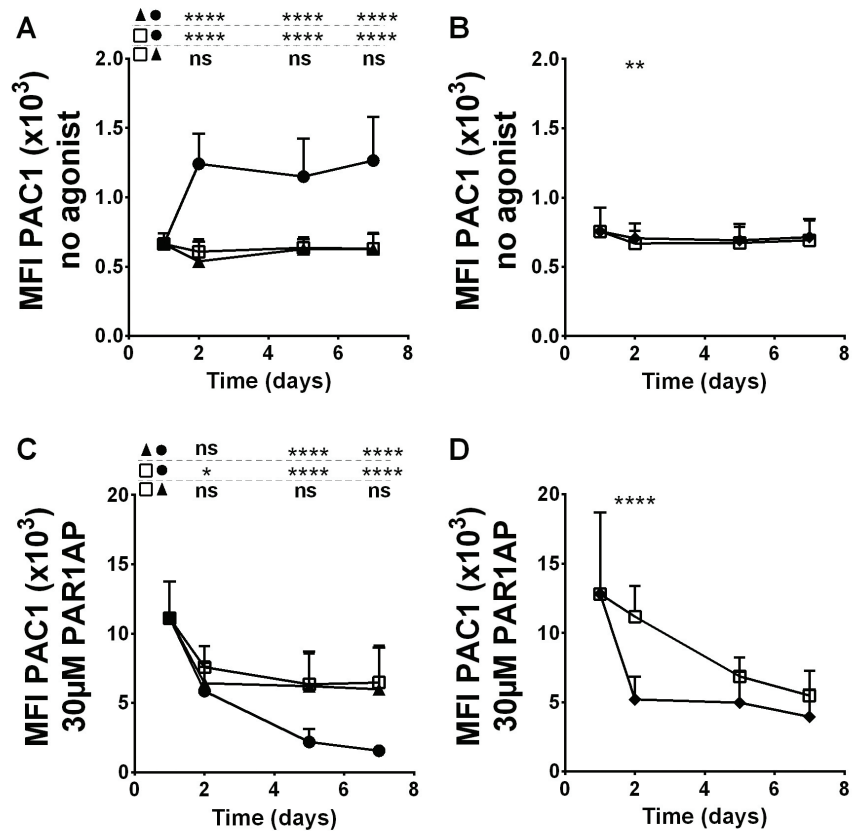## AS-PCT SPECIFICALLY TARGETS RISTOCETIN INDUCED AGGLUTINATION

Differences in aggregometry between untreated control and AS-PCT treated platelets **(Figure 3)** were noticeably smaller or non appearant compared to results for RF-PRT **(Figure 2)**. Of note, platelet storage profoundly decreased the aggregation response of both untreated control and AS-PCT platelets unlike the RF-PRT study. This may be caused by differences in storage container or in the number of composing buffy coats between AS-PCT and RF-PRT studies. Anyway, this phenomenon reduced the dynamic range of the assay thereby masking potential differences in aggregometry between AS-PCT and control platelets after storage. Nonetheless, AS-PCT induced decreased aggregation in response to collagen on day two **(Figure 3A and B)** and aggregation responses to PAR1AP were not different throughout the study period **(Figure 3C and D)**. However, complete abolition of ristocetin induced agglutination was found but only at low-dose agonist concentrations **(Figure 3E)**. High concentrations of ristocetin elicited normal agglutination of AS-PCT, together indicating altered affinity or avidity of the interacting biomolecules **(Figure 3F)**.

RF-PRT AND AS-PCT AFFECT INTEGRIN $\alpha_{IIb}\beta_3$ ACTIVATION IN A DIFFERENT WAY

The monoclonal antibody PAC1 binds to the activated conformation of the fibrinogen receptor integrin $\alpha_{IIb}\beta_3$ and is a surrogate marker for platelet activation which can be measured in flow cytometry. RF-PRT induced spontaneous and irreversible activation of this integrin **(Figure 4A)** which may be caused by the UVB spectrum during illumination[22]. In a subsequent experiment, PAR1AP was added prior to PAC1 flow cytometry to investigate the platelet activation response. RF-PRT platelets did not react very different than untreated or gamma treated platelets on day two, but were less sensitive to this stimulation following storage **(Figure 4C)**. AS-PCT platelets reacted differently because no spontaneous integrin $\alpha_{IIb}\beta_3$ activation **(Figure 4B)** could be observed in 'resting' platelets while PAR1AP induced platelet activation was significantly and irreversibly affected on day two **(Figure 4D)**. No differences for gamma irradiated platelets were noted.

Figure 3: AS-PCT affects low-dose ristocetin agglutination. *Light transmission aggregometry was performed with three agonists, each in a low (A,C and E) and high (B,D and F) concentration. Maximal aggregation is shown as means with standard deviation (n=6). Control (□) and AS-PCT (◆) platelets were analyzed before (day 1) and after (day 2, 5 and 7) treatment. The statistical results of two-way ANOVA is shown on top of the panels (ns=not significant;*P<.05;**P<.01;****P<.0001).*

A

B

C

D

RF-PRT MAINLY ACCELERATES PLATELET STORAGE LESION

Next, markers of the storage lesion were measured in flow cytometry with slight but significant decreases in GPIbα expression **(Figure 5A and B)** for both AS-PCT and RF-PRT following storage. The fraction of platelets that had degranulated in response to RF-PRT significantly increased **(Figure 5C)** from day two onwards until the end of the study as measured by expression of the α-granule marker P-selectin. Storage of RF-PRT platelets moreover increased the PSL apoptosis marker for phosphatidylserine/-ethanolamine exposure, annexin V **(Figure 5E)**. Furthermore, there was an increased rate of lactic acid production and glucose consumption in RF-PRT platelets **(Figure S3)**. This caused a decreasing trend in pH **(Figure S4)** which nonetheless remained above 6.4 in all RF-PRT units at the end of storage. P-selectin also increased over controls during storage of AS-PCT treated platelets **(Figure 5D)**, but the difference with controls was much smaller than for RF-PRT. Furthermore, there was no marked annexin V binding **(Figure 5F)** nor anaerobic glycolytic increase **(Figure S3-S4)**.

AS-PCT MAINLY AFFECTS PLATELET ACTIVATION

Because low-dose ristocetin agglutination was defective in AS-PCT **(Figure 3E)**, flow chamber experiments were performed onto immobilized VWF and total platelet deposition was measured at two minutes perfusion **(Figure 6 and supplementary video file)**. Like on collagen, AS-PCT platelets formed fewer thrombi on VWF under these conditions of high shear stress **(Figure 6A)**. To discriminate between GPIb binding to VWF and integrin $\alpha_{IIb}\beta_3$ interactions with fibrinogen and VWF, the experiment was repeated in the presence of 50ng/mL tirofiban, a potent integrin $\alpha_{IIb}\beta_3$ inhibitor. In this case, platelets do not form thrombi on the matrix but instead individually bind. In the presence of tirofiban, no difference between AS-PCT and untreated platelet binding was seen **(Figure 6B)** indicating no relevant defect in the GPIb-VWF interaction. Endogenous VWF molecules present in the platelet concentrate were not affected by AS-PCT treatment as shown by ristocetin induced binding to immobilized exogenous glycocalicin **(Figure 6C)**. Additionally, activation with the strong platelet activator convulxin via the GPVI-FcγRIIa pathway also resulted in a significant reduction in integrin $\alpha_{IIb}\beta_3$ activation **(Figure 6D)**. Together with the PAR1AP activation data, these findings collectively indicate that activatory signals via PAR1, GPIb/IX/V complex and GPVI-FcγRIIa are not fully translated to integrin $\alpha_{IIb}\beta_3$ in the case of AS-PCT platelets.
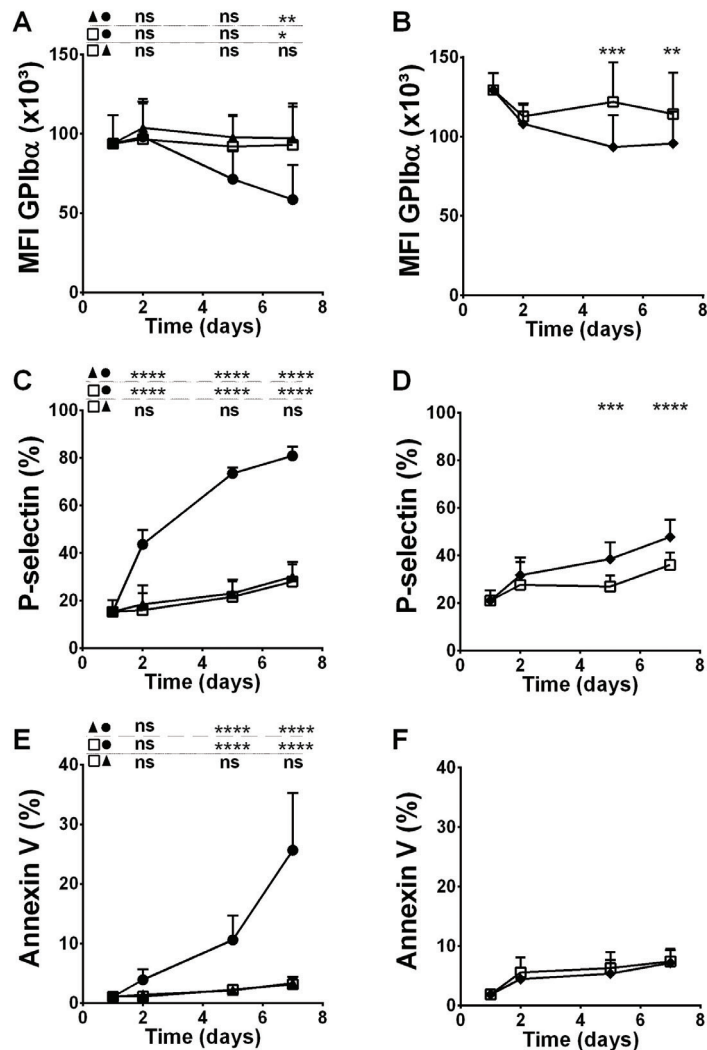
Figure 4: RF-PRT spontaneously activates integrin $\alpha_{IIb}\beta_3$ while AS-PCT inhibits agonist stimulated integrin $\alpha_{IIb}\beta_3$ activation. PAC1 binding is specific for the activated integrin IIb3 and was measured by flow cytometry without agonist (resting conditions; A,B) or following activation (30µM PAR1AP; C,D). The median fluorescence intensity (MFI) is shown for control (□), gamma (▲), RF-PRT (●) and AS-PCT (◆) conditions. The statistical results of two-way ANOVA is shown on top of the panels (ns=not significant;*P<.05;**P <.01;****P<.0001)

Figure 5: RF-PRT increases the rate of storage lesion. *(A,B) The expression level by mean fluorescence intensity (MFI) of GPIbα measured by flow cytometry. (C-F) The percentage of platelets expressing P-selectin and negatively charged phospholipids. In all cases 10,000 platelets were counted for control (□), gamma (▲), RF-PRT (●) and AS-PCT (◆) conditions before (day 1) and after treatment (day 2, 5 and 7). The statistical results of two-way ANOVA is shown on top of the panels (ns=not significant; *P<.05; **P<.01; ***P<.001; ****P<.0001).*

PHOTOSENSITIZATION IS SUFFICIENT TO DECREASE ACTIVATION RESPONSES TO TRAP

In order to find out what manipulation of the three main AS-PCT processing steps has the largest impact on platelet integrin $\alpha_{IIb}\beta_3$ activation, the individual steps or their combinations were analyzed using PAC1 binding following PAR1 stimulation. This experiment showed that there was a minor effect of illumination, amotosalen addition or CAD incubation each by itself **(Figure S5A)**. Combinations of two procedural manipulations on the contrary showed that mere photochemistry (without CAD incubation) had a similar impact as the complete AS-PCT procedure indicating a negligible role of additional CAD incubation. From this follows that CAD incubation is not necessary to study the damage caused by AS-PCT. Indeed, aggregation responses immediately after photosensitization (without CAD incubation) to both collagen and PAR1AP were much more affected than on day two (with CAD) **(Figure S5B-E)**, indicating some recovery. It is currently not clear whether the CAD contributes to this recovery or whether mere overnight storage suffices.

DISCUSSION

The blood storage lesion is the progressive loss of function during storage of live cells isolated from circulation. It is a combination of natural cellular senescence and accumulating artifacts instigated by the procedural steps required for proper isolation and storage. Photochemical treatment of platelet concentrates increases manipulation and procedural steps that attract attention because of conflicting reports[11,12,23,24] on their contribution to PSL as well as decreased transfusion count increments[25].

Our work on RF-PRT is in line with Zeddies *et al*[23] who showed fewer platelet spreading on immobilized collagen following RF-PRT. However, other experiments with RF-PRT platelets recirculating over rabbit aorta[26] or in a viscometer[27] do not corroborate. Different technical approaches probably underlie this, the latter methods continuously recirculate the cell suspension, allowing multiple passages over the activated surface making it more dependent on secondary released paracrine amplificatory mediators while a single unidirectional perfusion is performed in our setup. Furthermore, following recirculation, the cited methods rinse the deposited thrombi with buffer or tap water, chemically fix/stain the sample and then perform a single readout, while our method continuously measures platelet deposition in real-time. Terada *et al*[24] used an affinity chromatography model to demonstrate that RF-PRT platelets are retained twice as well as untreated platelets on collagen coated beads. This model is difficult to compare to because it is independent of platelet aggregation, secretion and integrin interactions with RGD-containing motifs[28] unlike hemostasis *in vivo*[29] and in flow chambers[30]. Importantly, the above mentioned studies all used apheresis derived platelets and illuminated in autologous plasma which may also contribute to the
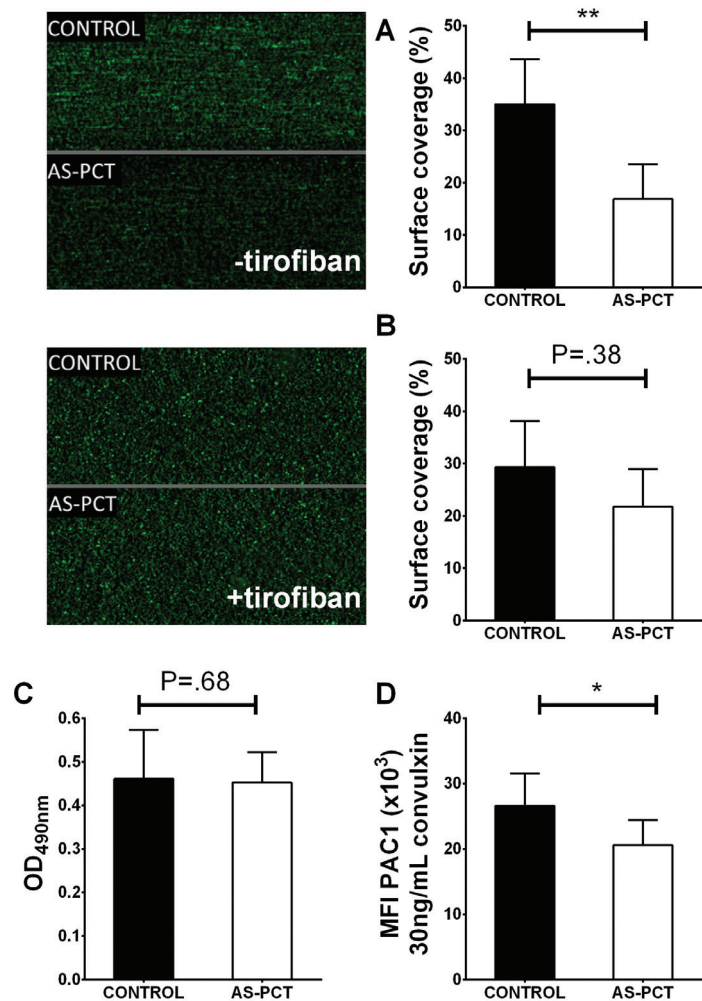
Figure 6: AS-PCT decreases platelet activatability. *Platelet adhesion to immobilized VWF under hydro-dynamic conditions is shown. (A) Adhesion of AS-PCT treated platelet was significantly less than paired untreated controls as shown by representative images (left) taken at two minutes perfusion and by the percentage of platelets covering the surface (right) (n=6,**P<.01). (B) Decreased AS-PCT platelet adhesion was caused by decreased integrin $\alpha_{IIb}\beta_3$ ligand engagement, because the defect was rescued in the presence of the integrin inhibitor tirofiban (50ng/mL). (n=3, not significant). (C) The VWF molecules present in the platelet concentrate bound normally to glycocalicin. (n=10, not significant). (D) Integrin $\alpha_{IIb}\beta_3$ is less activated by 30ng/mL convulxin following treatment with AS-PCT on day two. (n=3, *P<.05). All comparisons of means were with paired t-tests.*

observed differences because plasma proteins may act as scavengers of oxygen radicals[5]. There are few studies using hydrodynamic shear flow with AS-PCT platelets. Hechler et al used a comparable experimental setup to ours measuring accumulation of platelets in real-time but found no major differences between controls and AS-PCT treated platelets. The major difference here was that the platelets were washed with buffer prior to analysis[12]. These authors speculate that washing *reshapes* platelets as would happen upon transfusion. They contemplate that conditioned storage media inhibit platelet function, however in paired samples like ours it seems unlikely that AS-PCT media would inhibit more than control given the relatively low volumes added to fresh blood in our reconstitution experiment and the reported integrity of the remaining plasma fraction[31].

The observed decreased response of RF-PRT platelets to agonists in aggregation and flow chambers may be explained by untimely platelet activation. There are several experimental arguments that support this notion; first, RF-PRT caused premature integrin $\alpha_{IIb}\beta_3$ activation. This has been described by other groups [22,24] and was not seen in paired untreated nor gamma treated controls. Integrin $\alpha_{IIb}\beta_3$ activation may also be responsible for the spontaneous aggregation observed previously[23]. Second, (premature) platelet activation causes degranulation demonstrated by increased P-selectin[8,32]. This receptor normally resides in -granules which are indispensible for normal hemostasis because their deficiency causes the gray platelet syndrome bleeding disorder[33]. Furthermore, dense granules precede secretion of α-granules[34] so this cargo of amplificatory molecules (including ADP) may also be no longer fully available to feed amplification. Third, the gradual increase in annexin V binding indicates phosphatidylserine/-ethanolamine exposure, which is a marker of apoptosis as well as platelet activation[35]. Fourth, there was a clear increase in anaerobic glycolysis following RF-PRT[32,36]. Lactic acid buildup in RF-PRT concentrates has been studied previously[37] to demonstrate that damage to mitochondria underlies the shift to anaerobic glycolysis. However, no immediate effect on the mitochondrial membrane potential could be detected. Therefore, an attractive alternative explanation is increased platelet activation and (subsequent) secretion of granules. These processes increase energy demands[38], and in the specific case of 'low-dose' stimulation primarily anaerobic glycolysis[39]. Whether premature platelet activation indeed underlies the metabolic change in RF-PRT treated platelets will however require further research. Taken together, these observations suggest that RF-PRT 'primes' platelets so that the seminal resources that are required for full platelet activation/participation in hemostasis are partially dissipated and no longer entirely available to accomplish normal thrombus formation or aggregation, *in vitro*. This hypothesis moreover fits with the observation that in the specific context where granule secretion and inter-platelet aggregation are not required, RF-PRT platelets bind better to collagen[24].

Unlike the changes found in platelets treated with RF-PRT, the ones caused by AS-PCT do not involve premature platelet activation. Indeed, platelet anaerobic glycolysis following AS-PCT was either small or unexisting as shown by others[4,10,11,40]. Moreover, premature acti-

vation should increase the exposure of negatively charged phospholipids which was not observed here nor elsewhere[10]. Furthermore, PAC1 bound similarly to resting AS–PCT platelets as to untreated controls. Finally, increased P-selectin expression rates[4,10,11] do not support premature activation since differences with untreated platelets were not significant shortly following treatment.

Nonetheless, our experiments still indicate that thrombus formation on both collagen and VWF were significantly and irreversibly affected by AS–PCT. Because VWF adhesion precedes collagen binding[21], the reduced thrombus formation onto VWF in flow chambers contributes to the decreases seen on collagen. From our flow cytometry data and the flow chamber experiment with tirofiban it is however clear that not GPIbα receptor abundance nor its interaction with VWF underlies this, but rather defective subsequent interactions of integrin $\alpha_{IIb}\beta_3$ posterior to GPIb engagement. From this it seems that signal transduction from GPIb/IX/V to the fibrinogen receptor are decreased. Indeed, our data show that AS–PCT platelets respond less to agonist stimulation, *in vitro*. For instance, integrin $\alpha_{IIb}\beta_3$ activation was decreased by stimulation with convulxin and PAR1AP as reported[11,41]. Despite this observation in flow cytometry, differences in aggregation in response to both collagen and PAR1AP were small or absent. We speculate that amplification signals[21] from secondary messengers including ADP and thromboxane A2, but also outside-in signals from (limited) integrin $\alpha_{IIb}\beta_3$–fibrinogen engegament, are more prominent in bulk experiments like aggregation or recirculating flow, in part compensating for the initial weak response to the agonist. This may also explain why double agonist stimulation with thrombin and convulxin shows normal integrin $\alpha_{IIb}\beta_3$ activation of AS–PCT platelets[12]. Secondary activators and fibrinogen are much more diluted in flow cytometry experiments which may explain the apparent ambiguity between both readouts. Consequently, despite decreased integrin activation, the amplification machinery required for normal *in vitro* aggregation is least affected by AS–PCT. Nevertheless, three other studies with comparable design have included aggregation experiments[10,40,41] and significant decreases by AS–PCT. Taken together, we speculate that decreases in signal transduction from PAR1, GPVI-FcγRIIa and/or GPIb/IX/V underlie the reduced platelet deposition in microfluidic flow chambers on collagen.

Our AS–PCT data furthermore demonstrate that the photochemistry as such, without CAD incubation, is responsible for the decline in activatability. Because the photochemistry by itself had the same impact as full AS–PCT treatment, platelet aggregation immediately following photosensitization could be investigated showing that the responses to collagen, but now also PAR1AP were significantly decreased. This raises the question what biochemical mechanism(s) is/are affected as a consequence of photochemistry alone and what parameters contribute to the (partial) reversibility of aggregation, given that the most comprehensive platelet functional assay (flow chambers) did not indicate any functional recovery during storage.

Finally, it is challenging and beyond this *in vitro* work to speculate on clinical consequences based on our findings. The multifactorial context of the typically severely ill recipients of platelet transfusion adds to this. In a search for analogous platelet behavior in flow chambers, research into (cardio)vascular disease has found similar reduced thrombus formation following treatment with commonly prescribed oral antiplatelet agents[16,17]. These compounds do affect platelet function, but do not overtly tilt the hemostatic balance towards bleeding. Pathogen inactivation methods have been the subject of a number of clinical trials recently summarized in a meta-analytical review concluding that additional studies are required to provide sufficient evidence of non-inferiority to classical products[42]. A number of trials have been completed for AS–PCT and additional ones are on the way for RF–PRT including the PREPAReS (Dutch trial registration NTR2106) and IPTAS (United States NIH trial registration NCT01642563) trials. Currently, these have enrolled around half of patients and no major issues have been identified by the data safety monitoring board (personal communication Terumo BCT).

In conclusion, microfluidic flow chamber experiments show that both photochemical inactivation methods with riboflavin and amotosalen induce a decrease in thrombus formation rate *in vitro* but by different biochemical mechanisms. RF–PRT causes premature platelet activation with subsequent loss of amplificatory potential while AS–PCT platelets are less responsive to several agonists. Deeper research into the origins of certain cellular defects inherently caused by pathogen inactivation and the correlation to clinical outcomes could help to develop and refine methods so as to prevent or attenuate damage whilst retaining pathogen killing potential.

AUTHORSHIP CONTRIBUTION

REFERENCES

1   Pelletier, J. P., Transue, S. & Snyder, E. L. Pathogen inactivation techniques. *Best Pract Res Clin Haematol* **19**, 205–242, doi:10.1016/j.beha.2005.04.001 (2006).

2   Seltsam, A. & Muller, T. H. UVC Irradiation for Pathogen Reduction of Platelet Concentrates and Plasma. *Transfus Med Hemother* **38**, 43–54, doi:10.1159/000323845 (2011).

3   Goodrich, R. P. The use of riboflavin for the inactivation of pathogens in blood products. *Vox Sang* **78** Suppl 2, 211–215 (2000).

4   Lin, L. *et al.* Photochemical inactivation of viruses and bacteria in platelet concentrates by use of a novel psoralen and long-wavelength ultraviolet light. *Transfusion* **37**, 423–435 (1997).

5   Feys, H. B. *et al.* Oxygen removal during pathogen inactivation with riboflavin and UV light preserves protein function in plasma for transfusion. *Vox Sang* **106**, 307–315, doi:10.1111/vox.12106 (2014).

6   Kumar, V. *et al.* Riboflavin and UV-light based pathogen reduction: extent and consequence of DNA damage at the molecular level. *Photochem Photobiol* **80**, 15–21, doi:10.1562/2003-12-23-RA-036.1 (2004).

7   Dardare, N. & Platz, M. S. Binding affinities of commonly employed sensitizers of viral inactivation. *Photochem Photobiol* **75**, 561–564 (2002).

8   Johnson, L. *et al.* The effect of pathogen reduction technology (Mirasol) on platelet quality when treated in additive solution with low plasma carryover. *Vox Sang* **101**, 208–214, doi:10.1111/j.1423-0410.2011.01477.x (2011).

9   Picker, S. M., Tauszig, M. E. & Gathof, B. S. Cell quality of apheresis-derived platelets treated with riboflavin-ultraviolet light after resuspension in platelet additive solution. *Transfusion* **52**, 510–516, doi:10.1111/j.1537-2995.2011.03323.x (2012).

10 Jansen, G. A. *et al.* Functional characteristics of photochemically treated platelets. *Transfusion* **44**, 313–319, doi:10.1111/j.1537-2995.2003.00588.x (2004).

11 Apelseth, T. O. *et al.* In vitro evaluation of metabolic changes and residual platelet responsiveness in photochemical treated and gamma-irradiated single-donor platelet concentrates during long-term storage. *Transfusion* **47**, 653–665, doi:10.1111/j.1537-2995.2007.01167.x (2007).

12 Hechler, B. *et al.* Preserved functional and biochemical characteristics of platelet components prepared with amotosalen and ultraviolet A for pathogen inactivation. *Transfusion* **53**, 1187–1200, doi:10.1111/j.1537-2995.2012.03923.x (2013).

13 Westein, E., de Witt, S., Lamers, M., Cosemans, J. M. & Heemskerk, J. W. Monitoring in vitro thrombus formation with novel microfluidic devices. *Platelets* **23**, 501–509, doi:10.3109/09537104.2012.709653 (2012).

14 Roest, M. *et al.* Flow chamber-based assays to measure thrombus formation *in vitro*: requirements for standardization. *J Thromb Haemost* **9**, 2322–2324, doi:10.1111/j.1538-7836.2011.04492.x (2011).

15 Sakakibara, M. *et al.* Application of ex vivo flow chamber system for assessment of stent thrombosis. *Arterioscler Thromb Vasc Biol* **22**, 1360–1364, doi:10.1161/01.atv.0000027102.53875.47 (2002).

16 Andre, P. *et al.* Anticoagulants (thrombin inhibitors) and aspirin synergize with P2Y12 receptor antagonism in thrombosis. *Circulation* **108**, 2697–2703, doi:10.1161/01.CIR.0000093279.36628.12 (2003).

17 Bossavy, J. P. *et al.* A double-blind randomized comparison of combined aspirin and ticlopidine therapy versus aspirin or ticlopidine alone on experimental arterial thrombogenesis in humans. *Blood* **92**, 1518–1525 (1998).

18 Cattaneo, M. et al. Recommendations for the Standardization of Light Transmission Aggregometry: A Consensus of the Working Party from the Platelet Physiology Subcommittee of SSC/ISTH. *J Thromb Haemost* **11**, 1183–1189, doi:10.1111/jth.12231 (2013).

19 Goodall, A. H. & Appleby, J. Flow-cytometric analysis of platelet-membrane glycoprotein expression and platelet activation. *Methods Mol Biol* **272**, 225–253, doi:10.1385/1-59259-782-3:225 (2004).

20 Vanhoorelbeke, K. *et al.* Plasma glycocalicin as a source of GPIb in the von Willebrand factor ristocetin cofactor ELISA. *Thrombosis and Haemostasis* **93**, 165–171, doi:10.1160/th04-04-0402 (2004).

21 Broos, K., Feys, H. B., De Meyer, S. F., Vanhoorelbeke, K. & Deckmyn, H. Platelets at work in primary hemostasis. *Blood Rev* **25**, 155–167, doi:10.1016/j.blre.2011.03.002 (2011).

22 van Marwijk Kooy, M., Akkerman, J. W., van Asbeck, S., Borghuis, L. & van Prooijen, H. C. UVB radiation exposes fibrinogen binding sites on platelets by activating protein kinase C via reactive oxygen species. *Br J Haematol* **83**, 253–258 (1993).

23 Zeddies, S. *et al.* Pathogen reduction treatment using riboflavin and ultraviolet light impairs platelet reactivity toward specific agonists in vitro. *Transfusion* **54**, 2292–2300, doi:10.1111/trf.12636 (2014).

24 Terada, C., Mori, J., Okazaki, H., Satake, M. & Tadokoro, K. Effects of riboflavin and ultraviolet light treatment on platelet thrombus formation on collagen via integrin alphaIIbbeta3 activation. *Transfusion* **54**, 1808–1816, doi:10.1111/trf.12566 (2014).

25 Cid, J., Escolar, G. & Lozano, M. Therapeutic efficacy of platelet components treated with amotosalen and ultraviolet A pathogen inactivation method: results of a meta-analysis of randomized controlled trials. *Vox Sang* **103**, 322–330, doi:10.1111/j.1423-0410.2012.01614.x (2012).

26 Perez-Pujol, S. *et al.* Effects of a new pathogen-reduction technology (Mirasol PRT) on functional aspects of platelet concentrates. *Transfusion* **45**, 911–919, doi:10.1111/j.1537-2995.2005.04350.x (2005).

27 Picker, S. M., Schneider, V. & Gathof, B. S. Platelet function assessed by shear-induced deposition of split triple-dose apheresis concentrates treated with pathogen reduction technologies. *Transfusion* **49**, 1224–1232, doi:10.1111/j.1537-2995.2009.02092.x (2009).

28 Polanowska-Grabowska, R. & Gear, A. R. High-speed platelet adhesion under conditions of

rapid flow. *Proc Natl Acad Sci U S A* **89**, 5754-5758 (1992).

29   Topol, E. J., Byzova, T. V. & Plow, E. F. Platelet GPIIb-IIIa blockers. Lancet 353, 227-231, doi:10.1016/S0140-6736(98)11086-3 (1999).

30   Fressinaud, E., Girma, J. P., Sadler, J. E., Baumgartner, H. R. & Meyer, D. Synthetic RGDS-containing peptides of von Willebrand factor inhibit platelet adhesion to collagen. *Thromb Haemost* **64**, 589-593 (1990).

31   Coene, J. *et al.* Paired analysis of plasma proteins and coagulant capacity after treatment with three methods of pathogen reduction. *Transfusion* **54**, 1321-1331, doi:10.1111/trf.12460 (2014).

32   Ostrowski, S. R. *et al.* In vitro cell quality of buffy coat platelets in additive solution treated with pathogen reduction technology. *Transfusion* **50**, 2210-2219, doi:10.1111/j.1537-2995.2010.02681.x (2010).

33   Nurden, A. T. & Nurden, P. The gray platelet syndrome: clinical spectrum of the disease. *Blood Rev* **21**, 21-36, doi:10.1016/j.blre.2005.12.003 (2007).

34   Rendu, F., Marche, P., Maclouf, J., Girard, A. & Levy-Toledano, S. Triphosphoinositide breakdown and dense body release as the earliest events in thrombin-induced activation of human platelets. *Biochem Biophys Res Commun* **116**, 513-519 (1983).

35   Leytin, V. *et al.* Platelet activation and apoptosis are different phenomena: evidence from the sequential dynamics and the magnitude of responses during platelet storage. *Br J Haematol* **142**, 494-497, doi:10.1111/j.1365-2141.2008.07209.x (2008).

36   Picker, S. M., Steisel, A. & Gathof, B. S. Cell integrity and mitochondrial function after Mirasol-PRT treatment for pathogen reduction of apheresis-derived platelets: Results of a three-arm *in vitro* study. *Transfus Apher Sci* **40**, 79-85, doi:10.1016/j.transci.2009.01.013 (2009).

37   Li, J. *et al.* Evaluation of platelet mitochondria integrity after treatment with Mirasol pathogen reduction technology. *Transfusion* **45**, 920-926, doi:10.1111/j.1537-2995.2005.04381.x (2005).

38   Zharikov, S. & Shiva, S. Platelet mitochondrial function: from regulation of thrombosis to biomarker of disease. *Biochem Soc Trans* **41**, 118-123, doi:10.1042/BST20120327 (2013).

39   Akkerman, J. W. & Holmsen, H. Interrelationships among platelet responses: studies on the burst in proton liberation, lactate production, and oxygen uptake during platelet aggregation and Ca2+ secretion. *Blood* **57**, 956-966 (1981).

40   Johnson, L., Loh, Y. S., Kwok, M. & Marks, D. C. In vitro assessment of buffy-coat derived platelet components suspended in SSP+ treated with the INTERCEPT Blood system. *Transfus Med* **23**, 121-129, doi:10.1111/tme.12020 (2013).

41   Prudent, M. et al. Aggregation and Proteomic Analyses of Intercept-Treated Platelets. *Transfusion* **52**, 63A-63A (2012).

42   Butler, C. *et al.* Pathogen-reduced platelets for the prevention of bleeding. *Cochrane Database Syst Rev* **3**, Cd009072, doi:10.1002/14651858.CD009072.pub2 (2013).

SUPPLEMENTARY FIGURES
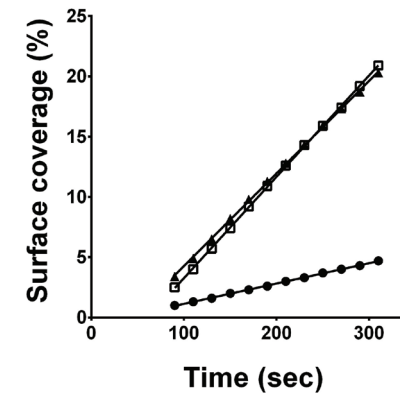
Figure S1: Platelet deposition in function of time as measured by surface coverage (%) in a single representative microfluidic flow experiment. *Platelet deposition in microfluidic flow chamber experiments is determined by real-time video microscopy and subsequent image analysis of the platelet surface coverage (%) in function of time. This relationship is linear for at least five minutes and regression analysis allows for determination of the slope to deduce kinetics of hemostasis. Conditions in this case were untreated control (□), gamma treated (▲) and photochemically RF-PRT treated platelets (●).*
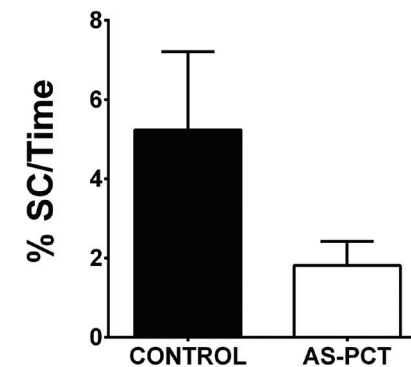
Figure S2: Thrombus formation differences on immobilized collagen are independent of the fluorescent label used. *Analogous to the data in Figure 1 biologically paired reconstituted blood samples, containing either control (closed bar) or AS-PCT (open bar) platelets were perfused at 50dynes/cm² over immobilized collagen on day two. Thrombus formation kinetics were determined from the linear relationship of surface coverage (%SC) in function of perfusion time by regression analysis (Figure S1). In this case however, the cell suspension was labeled with DiOC6 instead of calcein that was used to generate the data for AS-PCT in Figure 1. Data are depicted as mean with standard deviation as whiskers (n=3).*

Figure S4: The pH of RF-PRT platelet concentrates gradually declines. The pH at ambient temperature of control (□), gamma treated (▲), RF-PRT treated (●) and AS-PCT treated (◆) platelet concentrates (n=6) was determined in function of storage time. The means were statistically analyzed by two-way ANOVA and Tukey's or Sidak's multiple comparisons algorithm and the results are shown on top of each panel (ns = not significant; ****$P<.0001$).

Figure S3: Glucose consumption and lactic acid production rates are significantly increased by RF-PRT but not AS-PCT. (A and B) Glucose consumption and (C and D) lactic acid production in function of storage time (in hours) is depicted for untreated control (□), gamma treated (▲), RF-PRT (●) and AS-PCT (◆) treated concentrates. (E and F) The glucose consumption (filled bars) and lactic acid production rates (open bars) are derived from the data in A and B by linear regression analysis. Data are shown as means with standard deviation (n=6).

Figure S5: Photochemistry on itself has the largest impact on platelet activation. *(A) Integrin $\alpha_{IIb}\beta_3$ activation to 30µM PAR1AP was measured by labeled PAC1 binding in flow cytometry. Platelet concentrates were treated with all possible combinations of the three principal AS-PCT steps (addition of photosensitizer (AS), illumination (UV) and adsorption (CAD)). Negative controls (closed bar) were not treated and positive controls (open bars) were treated according to the standard AS-PCT protocol. The other conditions (shaded bars) were either treated by UV, AS and CAD alone or by a combination of UV+CAD, AS+CAD and AS+UV. The median fluorescent PAC1 signal (MFI) of a minimum of two (AS, UV, AS+CAD, UV+CAD) or three (both control conditions, CAD and AS+UV) repeat experiments is shown. (B-E) Aggregation by light transmission was performed with collagen (B and C) and PAR1AP (D and E) each in a threshold (B and D) and high (C and E) concentration (n=4). The maximal amplitude is depicted relative to the result of untreated control platelets on day one. Data of paired samples were collected immediately following photosensitization without incubation on CAD on day 1 (D1) and following overnight (16h) incubation on CAD (D2). Two-way ANOVA with SIDAK's multiple comparisons test was used to detect significant differences (*P<.05; **P<.01; ***P<.001). All data are shown as mean values with standard deviations*

SUPPLEMENTARY VIDEOS

http://onlinelibrary.wiley.com/doi/10.1111/vox.12231/suppinfo

3.2 ULTRAVIOLET C LIGHT PATHOGEN INACTIVATION TREATMENT OF PLATELET CONCENTRATES PRESERVES INTEGRIN ACTIVATION BUT AFFECTS THROMBUS FORMATION KINETICS ON COLLAGEN IN VITRO

ORIGINAL RESEARCH

Ultraviolet C light pathogen inactivation treatment of platelet concentrates preserves integrin activation but affects thrombus formation kinetics on collagen in vitro

Britt Van Aelst,[1] Rosalie Devloo,[1] Philippe Vandekerckhove,[2,3,4] Veerle Compernolle,[1,2,4] and Hendrik B. Feys[1]

INTRODUCTION

The increased risk for bacterial growth caused by room temperature storage of platelet concentrates and for (emerging) transfusion transmissible diseases including virus strains with long window periods are genuine reasons for introducing broad spectrum pathogen inactivation[1]. There are currently three different standardized methods to inactivate pathogens in platelet concentrates. Two marketed systems use ultraviolet (UV) light combined with an exogenously added photoactive reagent, either the psoralen derivative amotosalen with 320-400nm UV-A light[2] (AS-PCT) called the Intercept Blood System (Cerus Corporation, Concord, CA) or riboflavin with 265-370nm broad spectrum UV-light[3] (RF-PRT) called Mirasol Pathogen Reduction Technology System (TerumoBCT, Lakewood, CO). More recently, a third inactivation method has been developed that uses the microbiocidal and virucidal characteristics inherent to short wavelength (254nm) UV-C light[4] without exogenously added photosensitizer (UV-C) called THERAFLEX UV-Platelets (Macopharma, Tourcoing, France). This particular technology mitigates concerns about toxicological effects of added photochemicals and/or photoproducts generated during illumination.

The biochemical mechanism involved in UV-C treatment has not been demonstrated as such but is claimed[5] to be similar to the general chemistry[6] underlying UV-C induced damage of nucleic acids. If true, then photochemical formation of cyclobutane pyrimidine dimers, pyrimidine 6-4 pyrimidone dimers as well as abasic sites, strand breaks and oxidative products prevent elongation of nucleic acid transcripts[7] if not repaired by cellular machinery. A major practical hurdle is to obtain sufficient penetrance of the incident light because proteins as well as particles (including platelets) will respectively absorb and scatter incoming photons thereby dissipating the energy required for inactivation. Therefore conditions have been optimized to assure efficient delivery of UV-C light including reducing the plasma content to 30-40% with additive solution, exposing both sides of the bag to the light sources, increasing the surface area, and agitating vigorously during illumination[5,8,9]. This way, *in vitro* pathogen inactivation of several transfusion transmitted pathogens has been demonstrated[8,9].

Functional and biochemical studies of UV-C pathogen inactivated platelets showed an acceleration of the storage lesion with decreased pH and hypotonic shock response, increased glucose consumption and lactic acid production. In addition, increased values for degranulation (P-selectin expression), phosphatidylserine expression (annexin V binding) and integrin $\alpha_{IIb}\beta_3$ activation (PAC1 binding) indicate moderate activation of platelets following UV-C treatment[8-12]. There is a low impact on the platelet proteome[9] and neoantigen formation could not be detected in a dog model[13]. Furthermore, the results of a phase I study with autologous transfusions in healthy volunteers met the primary safety and tolerance criteria[14] and Bashir *et al* demonstrated platelet recovery and survival rates within acceptance criteria following autologous transfusions in healthy volunteers[12].

There are few studies that investigate the influence of pathogen inactivation on integrated platelet function, for example in aggregometry or microcapillary flow chambers. The latter is a comprehensive functional *in vitro* test with high sensitivity to perturbations in all steps of hemostasis; adhesion, activation and aggregation[15]. Furthermore, *in vivo* studies of thrombus formation in mice have demonstrated that many of the regulatory processes determining arterial thrombosis can well be assessed with these *in vitro* flow experiments[16].

In the current study we have compared UV-C treated and untreated paired platelet concentrates using quality markers like pH, metabolic rate and receptor expression as well as the more comprehensive platelet function assays of light transmission aggregation and microfluidic flow chamber experiments.

MATERIALS AND METHODS

STUDY DESIGN

Whole blood donations from voluntary non-remunerated donors fulfilling Belgian eligibility criteria were used to prepare leukocyte depleted platelet concentrates from five buffy coats with a plasma content of approximately 35% and the remainder platelet additive solution (SSP+, Macopharma) following standard operating procedures of the blood service of the Belgian Red Cross Flanders. Three blood group matched platelet concentrates were pooled and split again to deliver three equivalent platelet concentrates of which one was left untreated to serve as control, one was treated with 25-50 Gray gamma irradiation and one was UV-C treated. UV-C treatment was according to the THERAFLEX UV-platelets standard operation protocol only with products fulfilling the inclusion criteria as set by the provider. In brief, the bag content was transferred to an UV-C-permeable ethyl vinyl acetate illumination container which was placed in the Macotronic UV illuminator (Macopharma). A total dose of $0.2J/cm^2$ of 254nm UV light was delivered under continual agitation in a timespan not exceeding one minute. Next, the treated platelet concentrate was transferred to the n-butyryl tri n-hexyl citrate plasticised polyvinyl chloride storage bag included in the THERAFLEX UV-C bag combination. The paired control and gamma irradiated products were stored in the same bag type to ascertain similar storage conditions for all study arms. All products were kept under standard blood bank conditions at 20-24°C on a flatbed agitator. The experiments described below were performed on small volumes taken aseptically from the concentrates before (day 1) and after (day 2, 5 and 7) treatment. The design included a total of six independent repeat experiments (n=6) unless where indicated differently.

BLOOD GASES AND PLATELET COUNT

Lactic acid, glucose and pH were determined immediately after sampling using a point-of-care blood gas analyzer (Siemens Rapidpoint 500, Munich, Germany). Whole blood counts were performed with an automated hematology analyzer (PocH-100i, Sysmex, Kobe, Japan).

BLOOD RECONSTITUTION

Whole blood was taken from healthy non-medicated donors in heparin vacutainers (REF 368480, BD Diagnostics, Franklin Lakes, NJ) taking measures for preserving platelet quiescence[17]. A first soft centrifugation (12 minutes at 250g) divided the whole blood samples in platelet rich plasma (PRP) and concentrated red blood cells. Platelets of the PRP were then spun down by hard centrifugation (20 minutes at 4500g) to yield platelet poor plasma (PPP). Reconstitution was by mixing appropriate volumes of these packed red blood cells, PPP and either of the three subject platelet concentrates (control, gamma or UV-C) achieving 40 percent hematocrit and 250,000 platelets/μL on average.

MICROFLUIDIC FLOW CHAMBER EXPERIMENTS

Reconstituted blood samples were perfused through microfluidic channels of dimensions 400μmx100μmx28mm (Vena8 Fluoro+ Biochips) at a shear stress of $50dynes/cm^2$ (flow rate of 1,100s-1) using a Mirus Evo microfluidic pump (All Cellix Ltd, Dublin, Ireland). The channels were coated overnight at 4°C with 50μg/mL Horm collagen type I (Takeda, Osaka, Japan). Next, the channels were blocked with 1.0% (w/v) bovine serum albumin and 0.1% (w/v) glucose in 10mM 4-(2-hydroxyethyl)-1-piperazineethanesulfonic acid (HEPES) buffered saline (HBS; 0.9% (w/v) NaCl, pH 7.4) at room temperature for 30 minutes. The channels were then rinsed with 1mL plain HBS to remove remainder blocking buffer and unbound collagen. Platelets in the reconstituted blood samples were labeled with 1μM (final) of the fluorescent dyes 3,3'-di-hexyloxacarbocyanine iodide (DiOC6) (Sigma-Aldrich, Saint Louis, MO) or 5μM calcein-AM (Life technologies, Carlsbad, CA) where indicated.

Samples were perfused in duplicate at the same time using a channel splitting manifold and an automated x-y stage allowing up to eight simultaneous runs in one experiments. The biochip is mounted on a Z.1 Observer fluorescent microscope equipped with a Colibri-LED fluorescent light source (488nm) and high resolution CCD camera (all Carl Zeiss, Oberkochen, Germany). A simultaneous recording of three side-by-side images per microcapillary channel was performed in real-time during five minutes at 100X magnification. The three side-by-side images were digitally stitched to deliver one single compound image per time point. A fixed threshold of 400-4096 arbitrary fluorescence units was used to define platelet adherence allowing to determine the percentage of pixels covered by platelets in the measurement field (i.e. surface coverage) in function of time (ZEN2012 software, Carl Zeiss). The slopes of these relationships were determined by linear regression (Prism, GraphPad Software Inc, La Jolla, CA) and are a measure for thrombi growth kinetics.

FLOW CYTOMETRY

Expression of glycoprotein Ibα (fluorescein labeled anti-CD42b, Life technologies), activated integrin $\alpha_{IIb}\beta_3$ (fluorescein labeled PAC1, BD Biosciences, Erembodegem, Belgium), P-selectin (phycoerythrin anti-CD62P, BD Biosciences) and Annexin V (Peridinin chlorophyll-Cy5.5 labeled Annexin V, BD Biosciences) of either platelet concentrate was analyzed with an acoustic focusing Attune flow cytometer (Life Technologies). Platelets were incubated with labeled antibodies or ligand for 10 minutes at room temperature in HBS, supplemented with 1mM $MgSO_4$ and diluted thousand fold immediately before readout according to previous published work[18]. For Annexin V measurements, buffers were supplemented with 2mM CaCl2. For measurements of integrin $\alpha_{IIb}\beta_3$ activation on stimulated platelets, the PAR-1 agonist thrombin related activating hexapeptide SFLLRN (PAR1AP; Sigma-Aldrich) at 30μM or the

GPVI-FcγRIIa agonist convulxin (Santa Cruz Biotechnology Inc, Dallas, TX) at 6ng/mL were used. The signals of the respective isotype antibody controls were used to set threshold gates including 0.5% of 10,000 negative events. Mean or median fluorescence intensities and percentage positive events were determined for 10,000 cells staining positive for the platelet marker CD61 (allophycocyanin labeled anti-CD61, Life Technologies).

PLATELET AGGREGATION

Platelet aggregation was with a light transmission aggregometer (Chrono-Log, Helena Laboratories, Haverton, PA). Three different platelet agonists were used, each at two concentrations. A high agonist concentration to saturate signal transduction and a low concentration to investigate platelet sensitivity. For collagen (American Biochemical & Pharmaceuticals, Epsom, United Kingdom) 10μg/mL and 4.5μg/mL was used, PAR1AP at 10μM and 5μM and ristocetin (American Biochemical & Pharmaceuticals) at 1.5mg/mL and 0.6mg/mL. These agonist concentrations were determined in separate serial dilution experiments (data not shown). Aggregation cuvettes contained platelets diluted to 250,000 platelets/μL with the corresponding autologous platelet free plasma with additive solution prepared by centrifugation. Maximal aggregation (amplitude (%)) is reported here, the other parameters (slope and area under the curve) were comparable.

PARTIAL PRESSURE REDUCTION OF MOLECULAR OXYGEN BY DEGASIFICATION

An independent series (n=5) of pool and split was performed for this experiment. Again, three blood group matched platelet concentrates were pooled and split; one platelet concentrate was left untreated to serve as a control, one was immediately processed with UV-C and one was treated to reduce the dissolved molecular oxygen partial pressure as described elsewhere[19] before processing with UV-C pathogen inactivation. To reduce molecular oxygen partial pressures inert nitrogen gas (Air Liquide, Paris, France) was blown into the illumination bag (not bubbled) under continuous gentle agitation to allow reequilibration of dissolved gases following Henry's law. After seven minutes the residual molecular oxygen partial pressure in the platelet concentrate suspension was 1.8±0.5kPa compared to 7.5±1.4kPa in controls as measured by a submerged Clark electrode in real time. Flow cytometric analysis and microfluidic flow chamber experiments of these concentrates were performed as described above.

STATISTICAL ANALYSIS

Results are reported as mean values with standard deviation and analyzed with two-way ANOVA with Tukey's multiple comparisons algorithm with Prism software version 6.01 (GraphPad Software Inc.) to determine significance (P≤0.05) between the three subject groups.

RESULTS

UV-C TREATED PLATELETS SHOW IMPAIRED THROMBUS FORMATION KINETICS FOLLOWING STORAGE

UV-C treated platelets were compared with gamma irradiated and untreated controls by measuring thrombus formation kinetics onto collagen coated microcapillaries. **Figure 1** and the supplementary video files show a mean decreased surface coverage in function of time onto collagen coated microcapillary. This was found from day two on, but only statistically significant following storage on day five and seven.
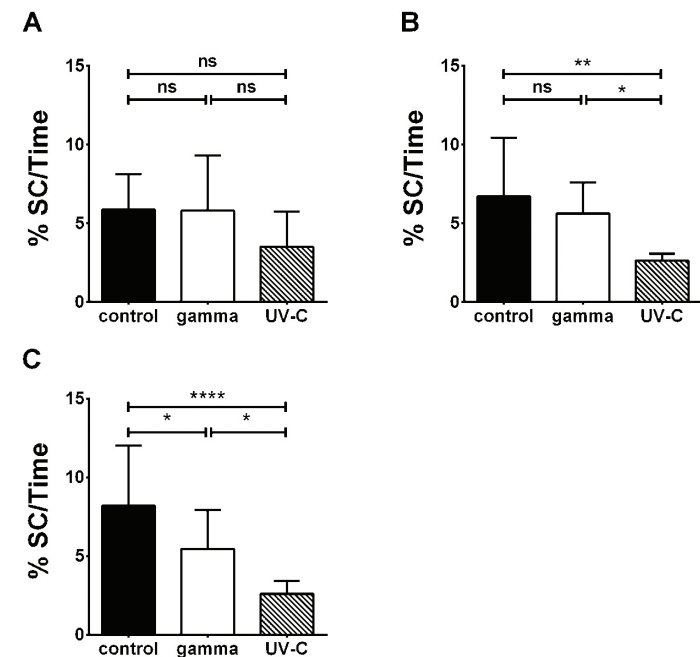
Figure 1: Platelet thrombus formation kinetics are affected by UV-C treatment following storage. Microfluidic flow chamber experiments with collagen coated microcapillaries were performed in duplicate on day two (A), five (B) and seven (C). Thrombus formation kinetics was followed in real-time using video microscopy and software measuring platelet surface coverage. The results are depicted as surface coverage in function of perfusion time (%SC/Time) for control (closed bars), gamma irradiated (open bars) and UV-C treated (shaded bars) platelets in reconstituted blood. The data are shown as means with standard deviation (n=8). Results from the statistical analysis are depicted on top of each panel. (ns=not significant; *P<.05; **P<.01; ****P<.0001).

INTEGRIN α_{IIB}β₃ CONFORMATIONAL CHANGES AFTER UV-C TREATMENT

During thrombus formation, platelet integrin $\alpha_{IIb}\beta_3$ becomes activated in a calcium-dependent manner to expose the fibrinogen binding site and promote platelet cross linking. The PAC1 monoclonal antibody binds a neo-epitope on this receptor and so is a surrogate marker for integrin activation. **Figure 2A** shows that UV-C treatment caused increased PAC1 binding compared to both control and gamma irradiated platelets in the absence of any additional agonist. This "activated" receptor state persisted during subsequent seven day storage. We hypothesized that this premature receptor activation would compromise further activation of platelets by exogenous agonists. However, this was not the case as integrin $\alpha_{IIb}\beta_3$ activation by both PAR1AP and convulxin was not significantly decreased for UV-C treated platelets **(Figure 2B-C)**. Instead, a distinct increase was seen in the UV-C treated group following PAR1AP stimulation which may be attributed to the subpopulation of receptors that got 'pre-activated' by UV-C treatment. The overall potency of convulxin to induce and sustain inside-out integrin activation is larger than for PAR1AP and therefore this particular 'additive' effect may be masked in this case.

PLATELET AGGREGATION IS MOSTLY UNAFFECTED

Unlike PAC1 measurements in highly diluted flow cytometry conditions, aggregation is more inclusive taking into account effects of platelet shape change and amplification by vesicle release. The above mentioned 'additive' effect of integrin $\alpha_{IIb}\beta_3$ activation was also noticed during low-dose collagen aggregations, where UV-C treated platelet displayed a slightly increased response on day two **(Figure 3A)**. However, this observation could not be generalized to the other conditions **(Figure 3B-F)**, in particular to low dose PAR1AP and low dose ristocetin stimulation where a slightly decreased response was found on day two and following storage, respectively. Overall however, few differences with gamma irradiated or untreated control platelets were found.
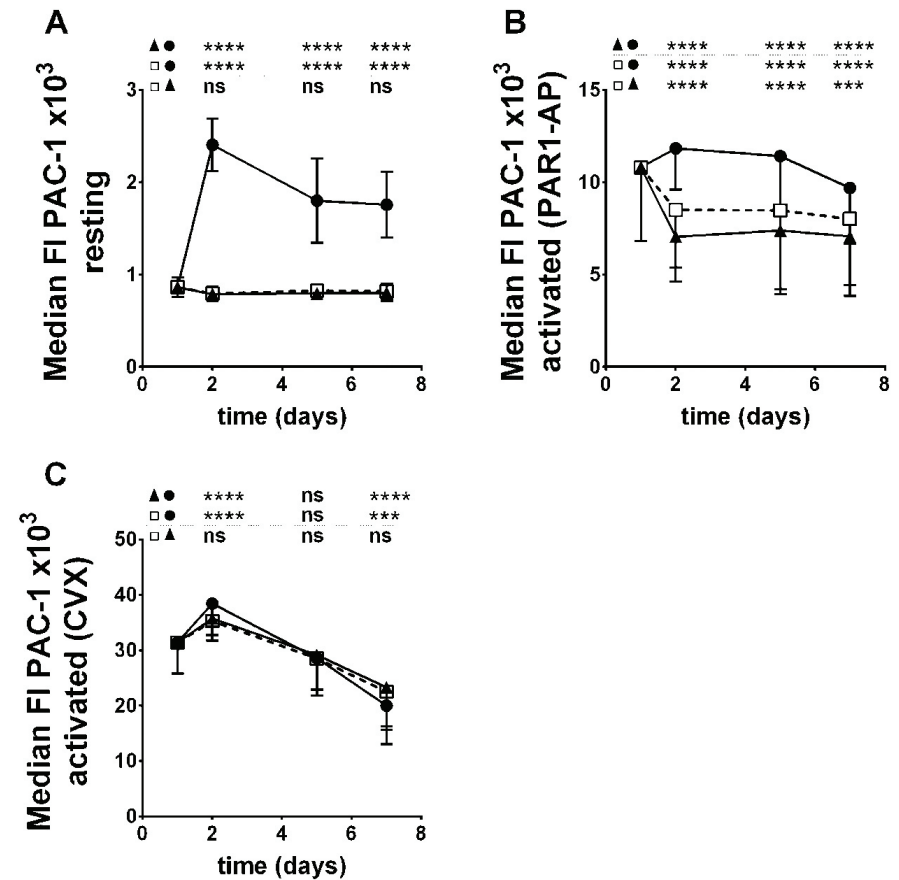
Figure 2: UV-C treatment induces integrin $\alpha_{IIb}\beta_3$ conformational changes that does not affect further activation through PAR1 or GPVI. *Integrin $\alpha_{IIb}\beta_3$ activation was measured by binding of fluorescein labeled PAC1 to 10,000 CD61 positive events in flow cytometry. Samples were analyzed in resting conditions (A) or following stimulation with 30μM PAR1AP (B) or 6ng/mL convulxin (CVX) (C) before (day 1) and after treatment (day 2, 5 and 7). Data of UV-C (●), gamma irradiated (▲) and untreated control (□; dotted line) are shown as mean values with standard deviation. Results from the statistical analysis are depicted on top of each panel. (ns=not significant; ***P<.001; ****P<.0001).*
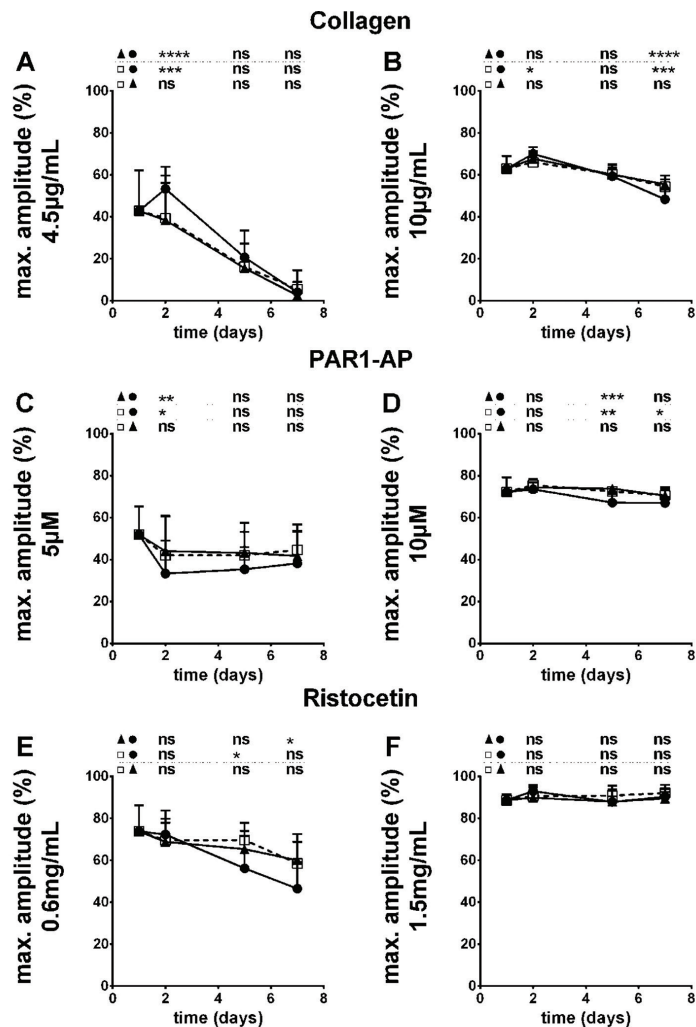
Figure 3: Light transmission aggregation is not substantially different. Plate-let light transmission ag-gregometry was performed at 250,000 platelet per μL. Three different agonists were used each in a low (A, C and E) and high (B, D and F) concentration as indi-cated on the y-axis. Maximal aggregation (or amplitude %) is shown as means with standard deviation. Untreated control (□ ; dotted line), gamma irradiated (▲) and UV-C (●) are shown before (day 1) and after treatment (day 2, 5 and 7) . Results from the statistical analysis are depicted on top of each panel. (ns=not significant; *P<.05; ****P<.0001).

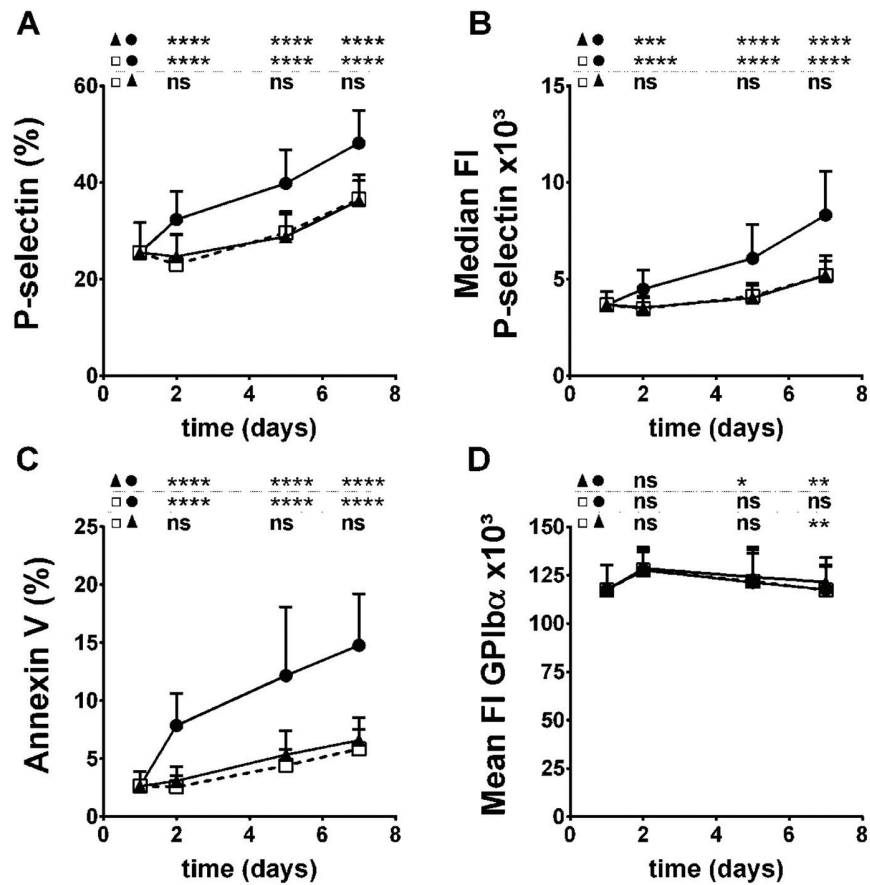## UV-C TREATMENT CAUSED α-DEGRANULATION AND PHOSPHATIDYLSERINE EXPOSURE

Platelets contain a number of distinguishable storage α-granules including granules, lyso-somes and dense granules. During activation, platelet degranulation occurs thereby releasing proteins and small molecules that act as modulators of hemostasis by para- and autocrine signaling. P-selectin is a marker of α-granule secretion and showed a significant increase following UV-C treatment indicating increased spontaneous degranulation **(Figure 4A-B)**. Furthermore, the expression of phosphatidylserine/-ethanolamine is measured by annexin V binding. Just like P-selectin there was an increased exposure after UV-C treatment **(Figure 4C)**. GPIbα expression was only marginally affected by UV-C treatment **(Figure 4D)**.

UV-C TREATMENT SLIGHTLY INCREASES PLATELET METABOLISM

A significantly higher glucose consumption and lactic acid production was seen for UV-C treated platelets **(Figure 5A-C)** resulting in a different pH trend **(Figure 5D)** with respect to the control conditions. These data indicate a slightly higher metabolic activity, but pH never dropped below 7.2.

DECREASED MOLECULAR OXYGEN LEVEL CANNOT RESCUE PLATELET THROMBUS FORMATION KINETICS

Previous work from our group showed that experimentally decreased partial pressures of molecular oxygen rescues coagulation factor decreases in RF-PRT treated plasma by preventing oxidative damage[20]. We hypothesized that the variability in thrombus formation kinetics observed on day two **(Figure 1A)** was caused by variable molecular oxygen partial pressures in the primary product thus resulting in variable oxidative damage. In order to reduce oxidative damage during UV-C treatment, the partial pressure of molecular oxygen was lowered in the platelet concentrate before UV-C treatment by nitrogen gas equilibration. However, **figure 6** shows that such treatment did not alter the decreased thrombus formation kinetics onto collagen on day two. Of note, this experiment independently replicated the results from **figure 1** confirming no statistically significant difference on day two for an additional five repeats. As a matter of control for the impact of nitrogen gas equilibration, glycoprotein Ibα, P-selectin, annexin V and activated integrin $\alpha_{IIb}\beta_3$ expression were measured but found not to be different between these conditions **(Figure S1)**.

Figure 4: Platelet degranulation and expression of negatively charged phospholipids is increased following UV-C treatment. Degranulation was measured by binding of a labeled P-selectin antibody and the percentage above isotype control (A) and median fluorescence intensities (B) are depicted. Externalization of phosphatidylserine/-ethanolamine was measured by binding of labeled annexin V (C) and percentage above control is shown. GPIb receptor expression is shown as mean fluorescence intensities (D). Untreated control (□ ; dotted line), gamma irradiated (▲) and UV-C (●) are shown before (day 1) and after treatment (day 2, 5 and 7). Results from the statistical analysis are depicted on top of each panel. (ns=not significant; *P<.05; **P<.01; ***P<.001; ****P<.0001).
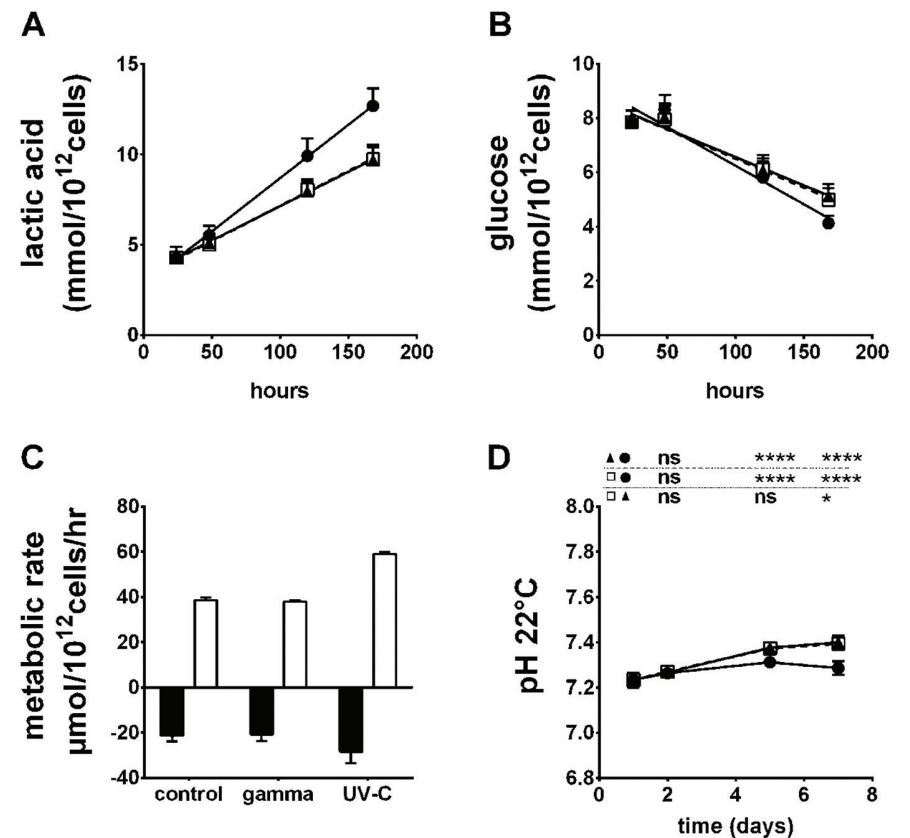
Figure 5: Increased metabolic rate following UV-C treatment. The lactic acid production (A) and glucose consumption (B) per 10^12 platelets of untreated control (□ ; dotted line), gamma irradiated (▲) and UV-C treated (●) platelet concentrates was measured using a point-of-care blood gas analyzer. Linear regression was performed on the lactic acid production and glucose consumption in function of time to model the kinetics of respectively lactic acid (open bars) and glucose metabolism (shaded bars) (C). One-way ANOVA of the mean values indicated a significant difference between the lactic acid production (P<.0001) and glucose consumption (P<.003) of UV-C and both control and gamma irradiated platelet concentrates. Platelet concentrate pH (D) was determined before (day 1) and after treatment (day 2, 5 and 7). Untreated control (□ ; dotted line), gamma irradiated (▲) and UV-C (●) are shown before (day 1) and after treatment (day 2, 5 and 7). (ns=not significant; *P<.05; ****P<.0001).

DISCUSSION

Three pathogen inactivation methods for platelet concentrates have been developed aiming to minimize chances of bacterial growth and/or transmission of virus. The UV-C procedure under study here is operationally straightforward and takes approximately eight minutes per product. There is no additional work load compared with methods that involve supplementation with a photoactive compound and especially to AS-PCT where an additional photosensitizer removal step is required. On the other hand, criticisms on the UV-C method include its limited inactivation of certain viruses[11] including HIV1 and its restrictive inclusion criteria[5].
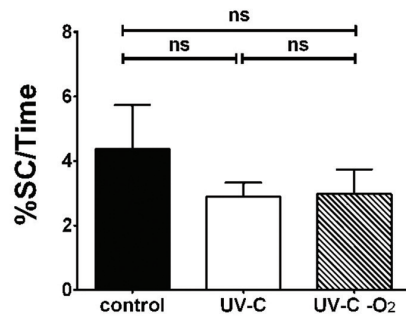
Figure 6: Lowering the partial pressure of dissolved molecular oxygen does not alter reduced thrombus formation kinetics. *Platelet surface coverage in function of perfusion time (%SC/Time) is measured in microfluidic flow chambers coated with collagen on day 2 according to figure 1. Paired reconstituted blood samples containing untreated control (closed bar), UV-C treated normoxic (open bar) and UV-C treated hypoxic (UV-C-O$_2$) (shaded bar) platelets analyzed in duplicate at a shear stress of 50dynes/cm^2. Mean values with standard deviation as whiskers (n=5) are shown. Results from the statistical analysis are depicted on top of each panel. (ns = not significant).*

There are substantial data on the *in vitro* quality of platelet concentrates generated by AS-PCT and RF-PRT, generally indicating increased rates of storage lesion with a variable range of magnitude[21-25]. Published data on residual quality of platelets treated with UV-C are less abundant but also indicate a slightly increased anaerobic metabolic rate causing significant differences in lactic acid concentrations and pH. However, this is mostly near or beyond expiration dates[8-10,12] which is in line with our findings. Small but significant increases in degranulation (P-selectin)[9,10] and phosphatidylserine/-ethanolamine exposure[12] also support our

data and may collectively indicate basal platelet activation or increased apoptosis. Of note, in terms of lesion kinetics our data indicate a small but sudden increase in both degranulation and annexin V binding **(Figure 4)** with a subsequent normal rate of additional storage lesion when compared to gamma irradiated or untreated controls.

Platelet functional assays have been used less frequently to evaluate residual platelet quality following pathogen inactivation, also for the other two commercial photochemical methods. We recently published data indicating that both AS-PCT and RF-PRT significantly and irreversibly affected thrombus formation kinetics onto immobilized collagen[25]. The same experimental setup was applied to UV-C here and also showed an irreversible decrease although the impact on day two was variable but not statistically significant. We hypothesized that this is caused by the inherent variability in the partial pressures of dissolved molecular oxygen in the primary products based on our experience with RF-PRT where secondary superoxide anion formation causes biomolecular damage[20]. Therefore, we experimentally lowered the molecular oxygen partial pressures but this could not reverse variability nor the impact on thrombus formation kinetics **(Figure 6)**.

The increased binding of PAC1 to integrin $\alpha_{IIb}\beta_3$ following UV-C treatment confirms the findings published in the landmark study by Verhaar *et al*[26]. They showed that short wavelength light reduces disulfide bonds to free thiols in the fibrinogen receptor core structure. It is plausible that this disulfide reshuffling which is a fundamental biochemical aspect of integrin activation[27,28] alters the conformation promoting untimely fibrinogen binding. Even though the overall physical conditions of the Verhaar study differ (they used a lower UVC dose of 0.15J/cm^2, delivered to a different primary product with lower plasma content and a fixed penetration depth) from the routine procedure of pathogen inactivation by UV-C, it is unlikely that unrelated biochemical mechanisms cause the same observation[5]. In theory, enforced fibrinogen binding should lead to (some) activation of affected platelets through outside-in signal transduction[29] which then subsequently explains the slightly increased metabolic rate[30], phosphatidylserine exposure and degranulation. This is the case for RF-PRT, where the observed premature activation actually desensitizes subsequent platelet activation[25]. The latter was however not observed for UV-C where the platelet's subsequent reaction to external stimuli acting through G-protein coupled receptors (PAR1AP) or receptor tyrosine kinases (CVX) was not abnormal in light transmission aggregation nor in flow cytometry. It is therefore tempting to ascribe this difference between the methods to the well known differential effects of UV-B versus UV-C illumination on platelet function; the former acting through direct activation of signal transduction cascades via protein kinases C[31] and oxidative stress while the latter does not[26]. Furthermore, proteomic analysis has indicated changes in the protein disulfide isomerase ERp72 for UV-C and not UV-B treated platelets[9] which adds to

the data from Verhaar et al[26] a role for redox regulation of integrin $\alpha_{IIb}\beta_3$ in the context of UV-C illumination induced biochemical alterations.

We argue that the hemostatic sequence of platelet adhesion, activation, aggregation and retraction/stability as measured comprehensively in perfusion chambers is affected by all three pathogen inactivation methods albeit not equally in manner and/or magnitude. RF-PRT treatment prematurely activates platelets[22,32] while AS-PCT does not. However, the latter method does specifically affect integrin $\alpha_{IIb}\beta_3$ receptor activation following stimulation with agonists[25]. It is less clear from the current study what aspect of UV-C contributes to its reduced flow chamber thrombus formation, but the redox induced changes in integrin $\alpha_{IIb}\beta_3$ conformation are a likely culprit. We performed two separate but similar experimental series in the flow chambers **(Figure 1 and 6)** and confirmed that despite an average decrease in surface coverage kinetics, statistical difference between UV-C and gamma or untreated control was not reached on day two. Bashir et al[12] previously demonstrated that UV-C pathogen inactivation reduces the post-transfusion recovery of platelets following storage. Whether the effect of storage of UV-C treated platelets on both post-transfusion recovery and on *in vitro* flow chambers reflect a related phenomenon is worth addressing.

In our hands, all pathogen inactivation techniques have more or less of an impact on platelet thrombus formation rates under hydrodynamic flow. Despite the absence of serious adverse (bleeding) events in the published clinical studies[33] for RF-PRT and AS-PCT, our findings do raise questions about the exact contribution of pathogen inactivated transfusion platelets in arterial hemostasis.

AUTHORSHIP CONTRIBUTIONS

HBF, BVA, and VC designed research; VC and PV contributed critical analytical tools, reagents, or samples and facilitated research; BVA, RD, and HBF performed research and collected data; BVA, RD, VC, and HBF analyzed and interpreted data; BVA, RD, and HBF performed statistical analyses; HBF and BVA wrote the manuscript; and all authors critically reviewed and amended the manuscript.

REFERENCES

1   Dodd, R. Y. Current risk for transfusion transmitted infections. *Curr Opin Hematol* **14,** 671-676, doi:10.1097/MOH.0b013e3282e38e8a (2007).

2   Irsch, J. & Lin, L. Pathogen Inactivation of Platelet and Plasma Blood Components for Transfusion Using the INTERCEPT Blood System. *Transfus Med Hemother* **38**, 19-31, doi:10.1159/000323937 (2011).

3   Marschner, S. & Goodrich, R. Pathogen Reduction Technology Treatment of Platelets, Plasma and Whole Blood Using Riboflavin and UV Light. *Transfus Med Hemother* **38**, 8-18, doi:10.1159/000324160 (2011).

4   Kallenbach, N. R., Cornelius, P. A., Negus, D., Montgomerie, D. & Englander, S. Inactivation of viruses by ultraviolet light. *Curr Stud Hematol Blood Transfus* **56**, 70-82 (1989).

5   Seltsam, A. & Muller, T. H. UVC Irradiation for Pathogen Reduction of Platelet Concentrates and Plasma. *Transfus Med Hemother* **38**, 43-54, doi:10.1159/000323845 (2011).

6   Douki, T. Inter-strand photoproducts are produced in high yield within A-DNA exposed to UVC radiation. *Nucleic Acids Res* **31**, 3134-3142, doi:10.1093/nar/gkg408 (2003).

7   Rastogi, R. P., Richa, Kumar, A., Tyagi, M. B. & Sinha, R. P. Molecular Mechanisms of Ultraviolet Radiation-Induced DNA Damage and Repair. *Journal of Nucleic Acids* **2010**, 1-32, doi:10.4061/2010/592980 (2010).

8   Mohr, H., Gravemann, U., Bayer, A. & Muller, T. H. Sterilization of platelet concentrates at production scale by irradiation with short-wave ultraviolet light. *Transfusion* **49**, 1956-1963, doi:10.1111/j.1537-2995.2009.02228.x (2009).

9   Mohr, H. *et al.* A novel approach to pathogen reduction in platelet concentrates using short-wave ultraviolet light. *Transfusion* **49**, 2612-2624, doi:10.1111/j.1537-2995.2009.02334.x (2009).

10   Sandgren, P., Tolksdorf, F., Struff, W. G. & Gulliksson, H. In vitro effects on platelets irradiated with short-wave ultraviolet light without any additional photoactive reagent using the THERAFLEX UV-Platelets method. *Vox Sang* **101**, 35-43, doi:10.1111/j.1423-0410.2010.01454.x (2011).

11   Terpstra, F. G. *et al.* Potential and limitation of UVC irradiation for the inactivation of pathogens in platelet concentrates. *Transfusion* **48**, 304-313, doi:10.1111/j.1537-2995.2007.01524.x (2008).

12   Bashir, S. *et al.* Pathogen inactivation of platelets using ultraviolet C light: effect on *in vitro* function and recovery and survival of platelets. *Transfusion* **53**, 990-1000, doi:10.1111/j.1537-2995.2012.03854.x (2013).

13   Pohler, P. *et al.* Evaluation of the tolerability and immunogenicity of ultraviolet C-irradiated autologous platelets in a dog model. *Transfusion* **52**, 2414-2426, doi:10.1111/j.1537-2995.2012.03583.x (2012).

14   Thiele, T. *et al*. Open phase I clinical trial on safety and tolerance of autologous UVC-treated single donor platelet concentrates in healthy volunteers – dose escalation study. *Transfus Med Hemother* **40**, 50 (2013).

15   de Witt, S. M. *et al*. Identification of platelet function defects by multi-parameter assessment of thrombus formation. *Nat Commun* **5**, 4257, doi:10.1038/ncomms5257 (2014).

16   Roest, M. *et al*. Flow chamber-based assays to measure thrombus formation in vitro: requirements for standardization. *J Thromb Haemost* **9**, 2322-2324, doi:10.1111/j.1538-7836.2011.04492.x (2011).

17   Cattaneo, M. *et al*. Recommendations for the Standardization of Light Transmission Aggregometry: A Consensus of the Working Party from the Platelet Physiology Subcommittee of SSC/ISTH. *J Thromb Haemost* **11**, 1183-1189, doi:10.1111/jth.12231 (2013).

18   Goodall, A. H. & Appleby, J. Flow-cytometric analysis of platelet-membrane glycoprotein expression and platelet activation. *Methods Mol Biol* **272**, 225-253, doi:10.1385/1-59259-782-3:225 (2004).

19   Dodd, R. Y. *et al*. Inactivation of viruses in platelet suspensions that retain their in vitro characteristics: comparison of psoralen-ultraviolet A and merocyanine 540-visible light methods. *Transfusion* **31**, 483-490, doi:10.1046/j.1537-2995.1991.31691306242.x (1991).

20   Feys, H. B. *et al*. Oxygen removal during pathogen inactivation with riboflavin and UV light preserves protein function in plasma for transfusion. *Vox Sang* **106**, 307-315, doi:10.1111/vox.12106 (2014).

21   Johnson, L. *et al*. The effect of pathogen reduction technology (Mirasol) on platelet quality when treated in additive solution with low plasma carryover. *Vox Sang* **101**, 208-214, doi:10.1111/j.1423-0410.2011.01477.x (2011).

22   Zeddies, S. *et al*. Pathogen reduction treatment using riboflavin and ultraviolet light impairs platelet reactivity toward specific agonists in vitro. *Transfusion* **54**, 2292-2300, doi:10.1111/trf.12636 (2014).

23   Apelseth, T. O. *et al*. In vitro evaluation of metabolic changes and residual platelet responsiveness in photochemical treated and gamma-irradiated single-donor platelet concentrates during long-term storage. *Transfusion* **47**, 653-665, doi:10.1111/j.1537-2995.2007.01167.x (2007).

24   Jansen, G. A. *et al*. Functional characteristics of photochemically treated platelets. *Transfusion* **44**, 313-319 (2004).

25   Van Aelst B *et al*. Riboflavin and amotosalen photochemical treatments of platelet concentrates reduced thrombus formation kinetics *in vitro. Vox Sang in press* **(2014)**.

26   Verhaar, R. *et al*. UV-C irradiation disrupts platelet surface disulfide bonds and activates the platelet integrin alphaIIbbeta3. *Blood* **112**, 4935-4939, doi:10.1182/blood-2008-04-151043 (2008).

27   Sun, Q. H., Liu, C. Y., Wang, R., Paddock, C. & Newman, P. J. Disruption of the long-range GPIIIa Cys(5)-Cys(435) disulfide bond results in the production of constitutively active GPIIb-IIIa (alpha(IIb)beta(3)) integrin complexes. *Blood* **100**, 2094-2101, doi:10.1182/blood-2002-02-0418 (2002).

28   Butta, N. *et al*. Disruption of the beta3 663-687 disulfide bridge confers constitutive activity to beta3 integrins. *Blood* **102**, 2491-2497, doi:10.1182/blood-2003-01-0213 (2003).

29   Shattil, S. J. Signaling through platelet integrin alpha IIb beta 3: inside-out, outside-in, and sideways. *Thromb Haemost* **82**, 318-325 (1999).

30   Akkerman, J. W. & Holmsen, H. Interrelationships among platelet responses: studies on the burst in proton liberation, lactate production, and oxygen uptake during platelet aggregation and Ca2+ secretion. *Blood* **57**, 956-966 (1981).

31   van Marwijk Kooy, M., Akkerman, J. W., van Asbeck, S., Borghuis, L. & van Prooijen, H. C. UVB radiation exposes fibrinogen binding sites on platelets by activating protein kinase C via reactive oxygen species. *Br J Haematol* **83**, 253-258 (1993).

32   Terada, C., Mori, J., Okazaki, H., Satake, M. & Tadokoro, K. Effects of riboflavin and ultraviolet light treatment on platelet thrombus formation on collagen via integrin alphaIIbbeta3 activation. *Transfusion* **54**, 1808-1816, doi:10.1111/trf.12566 (2014).

33   Estcourt, L. *et al*. Prophylactic platelet transfusion for prevention of bleeding in patients with haematological disorders after chemotherapy and stem cell transplantation. *Cochrane Database Syst Rev* **5**, CD004269, doi:10.1002/14651858.CD004269.pub3 (2012).

SUPPLEMENTARY FIGURE

SUPPLEMENTARY VIDEOS

http://onlinelibrary.wiley.com/doi/10.1111/trf.13137/suppinfo
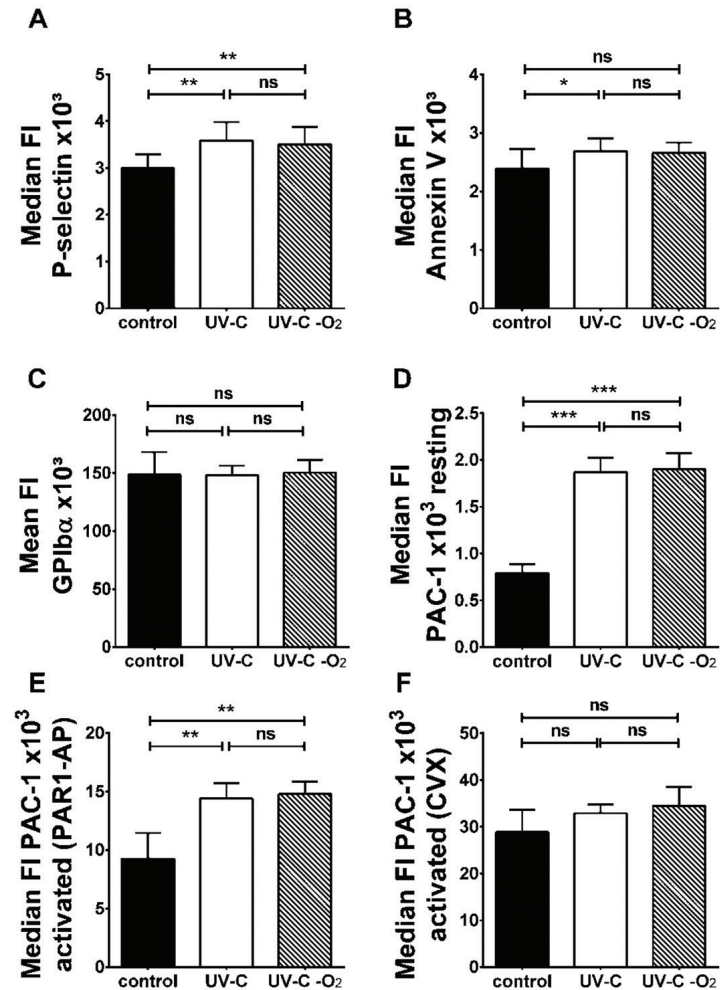
Figure S1: Lowering molecular oxygen partial pressures has no effect on platelets. (A) P-selectin, (B) phosphatidylserine/-ethanolamine by annexin V binding, (C) GPIbα and (D) integrin $\alpha_{IIb}\beta_3$ activation was not different in normoxic (open bars) versus hypoxic (shaded bars) conditions. (E) Integrin activation in response to 30μM PAR1AP or (F) 6ng/mL convulxin was also not different. The differences with untreated controls (closed bars) were consequently comparable. The results from statistical analyses are indicated on top of each panel (n=5). ns=not significant; *P<.05; **P<.01; ***P<.001.

3.3 SPECIFIC INHIBITION OF EFFECTOR KINASE RECRUITMENT TO PI(3,4,5)P3 BY PSORALEN AND UVA LIGHT TREATMENT IN PLATELETS AND T LYMPHOCYTES

B. Van Aelst[1], R. Devloo[1], P. Zachée[2], R. t'Kindt[3], K. Sandra[3], P. Vandekerckhove[4,5,6], V. Compernolle[1,4,6] and H. B. Feys[1]

[1]Transfusion Research Center, Belgian Red Cross-Flanders, Ghent, Belgium; [2]Department of Hematology, Hospital Network Antwerp, Antwerp, Belgium; [3]Research Institute for Chromatography, Kortrijk, Belgium; [4]Blood Service of the Belgian Red Cross-Flanders, Mechelen, Belgium; [5]Department of Public Health and Primary Care, KULeuven, Leuven, Belgium; [6]Faculty of Medicine and Health Sciences, University of Ghent, Ghent, Belgium

Manuscript submitted

INTRODUCTION

Psoralens are linear furanocoumarins. The heterocyclic aromatic core reversibly intercalates nucleic acids in cells and cell nuclei[1]. Absorption of ultraviolet A (UVA) light excites psoralens, supplying energy for covalent bond formation. When binding to nucleic acids, the reaction is primarily with pyrimidine moieties[2]. This chemical addition is irreversible and prevents normal replication of DNA[3], explaining why severe phytophotodermatitis occurs in sun exposed skin that has been in contact with psoralen producing plants. This biostatic photochemistry is utilized in a pathogen inactivation technology (Intercept Blood System, Cerus Corp, Concord, CA) for plasma and platelet concentrates in transfusion medicine[4] where it is intended to prevent replication of potentially infectious pathogens transmitted from the donor to the blood product. In the field of dermatology, PUVA technology is used to treat psoriasis, certain dermatoses and cutaneous T-cell lymphoma (CTCL)[5]. In these cases the psoralen is administered topically or systemically, followed by local or whole body UVA illumination. Treatment modalities are diverse and may differ by psoralen derivative and/or by doses of UVA light[6].

Furthermore, PUVA is under clinical investigation for the treatment of multiple other diseases, mostly involving uncontrolled cell proliferation[7]. But although broadly applied in medicine, the biochemical mechanism of PUVA is poorly understood.

Of note, psoralens are not therapeutic without UVA illumination and despite its well documented photoreaction with DNA, PUVA photochemistry is not specific for this particular biologic target alone. In theory, photoexcited psoralens can react with many other common biomolecules. Consequently, the net effect of PUVA in a cellular milieu is unlikely to be restricted to consequences of its chemistry with solely DNA as was acknowledged already in the late seventies[8]. This seemingly random reaction with multiple biomolecules explains why the quest for insights into PUVA and optimized therapies has been exceptionally challenging. For example, the systemic PUVA treatment modality called extracorporeal photopheresis (ECP) is used to treat CTCL and although clinically succesful[9], the mechanism of action has remained elusive ever since its first application. Researchers speculate that induction of apoptosis through DNA damage causes priming of the immune system. However, apoptosis induction alone is insufficient for the typical immomodulation caused by PUVA[10,11]. Despite this indistinctness, ECP is used "off-label" for (auto)immune diseases including graft-versus-host disease (GvhD), bronchiolitis after stem cell transplantation and Crohn's disease[12,13]. But without understanding of definite biochemical mechanisms, both protocol uniformity and outcome variability remain problematic.

Adduct formation of photoexcited psoralens with targets other than DNA[11,14] is primarily with membrane components[15,16]. Psoralens efficiently partition into lipid bilayers[17,18] where reaction chemistry occurs with double bonds in unsaturated acyl chains[19,20]. As a consequence, rational hypotheses on the cell biological consequences of these modifications have been postulated[21,22], but mechanisms explaining how membrane modifications exactly impact downstream cell signal transduction are underinvestigated.

We chose platelets as a model cell to study these DNA-unrelated effects of PUVA because platelets have no nucleus, are easily isolated from whole blood and contain a complex signal transduction machinery exemplary of key signaling processes in eukaryotic cells. Furthermore, recent work has shown that PUVA significantly affects platelet function in an *in vitro* model of hemostasis[23]. Our data now show that PUVA can inhibit signal transduction of the PI 3-kinase pathway by preventing efficient plasma membrane binding of important small effector kinases such as Akt (alternative name protein kinase B) and Bruton's tyrosine kinase (Btk). Our findings are not restricted to platelets, because T lymphocytes in patient samples treated with ECP displayed attenuation of Akt phosphorylation as well.

MATERIAL AND METHODS

MATERIALS

Ticagrelor dissolved at 30mM in DMSO (Cayman Chemical, Ann Arbor, MI); D-phenylala-nyl-L-prolyl-L-arginine chloromethyl ketone (PPACK) dissolved at 40mM in distilled water (Enzo Life Sciences, Farmingdale, NY); wortmannin dissolved at 2mM in DMSO, anti-P-Akt (clone D25E6), anti-total (pan) Akt (40D4), anti-phospho-PKC Substrate Motif [(R/KXpSX-(R/K)] MultiMab corresponding secondary peroxidase labeled antibodies, anti-total-Btk (C82B8) (Cell Signaling Technologies, Danvers, MA); apyrase dissolved at 200U/mL in distilled water, SFLLRN hexapeptide dissolved at 1mg/mL in distilled water with 0.1% trifluoroacetic acid, indomethacin dissolved at 35mM in ethanol, pluronic F-127, calcium ionophore A23187 dissolved at 5mM in DMSO, 4-chloro-7-nitrobenzofurazan (NBD) chloride, *tris*(2-carboxyeth-yl)phosphine (TCEP), RPMI-1640 medium without phenol red, L-glutamine, 8-methoxyp-soralen (8-MOP) dissolved at 15mM in DMSO, Interleukin-2 (IL2) (Sigma-Aldrich, St Louis, MO); thrombopoietin dissolved at 200µg/mL in distilled water with 4mM hydrogen chloride and 0,1% human serum albumin, anti-P-Btk (clone 797837) (R&D systems, Minneapolis, MN); AYPGKF hexapeptide (Anaspec, Waddinxveen, The Netherlands) dissolved at 5mM in distilled water; CRP-XL (University of Cambridge, Cambridge, United Kingdom) dissolved at 5mg/mL in 0.01M acetic acid; Halt Protease & Phosphatase inhibitor cocktail (Thermo Scientific, Waltham, MA); 2-(Methylthio)adenosine 5-diphosphate (Santa Cruz Biotechnology, Dallas, TX) dissolved at 37mM in distilled water; anti-pleckstrin antibody (ab17020), human wild type -synuclein (ab51188) (Abcam, Cambridge, UK). Oregon Green 488nm 1,2-bis(o-aminofenoxy) ethane-N,N,N',N'-tetra acetic acid-(acetoxymethyl) ester (BAPTA-AM), NBD iodoacetamide (IANBD), Dynabeads Human T-activator CD3/C28 (Life Technologies, Carlsbad, CA); All phospholipids were purchased dissolved in chloroform (Avanti Polar Lipids, Alabaster, AL); ALPS peptide was custom made (Proteogenix, Schiltigheim, France) and based on the first 38 amino acids of the GMAP210 protein[24] except for the N-terminal methionine which was changed to cysteine to allow targeted labeling; Ficoll-Paque Premium (d=1.077g/mL at 20°C) (GE Healthcare, Little Chalfont, United Kingdom). Anticoagulated AB RhD- serum was provided by the blood bank.

PUVA TREATMENT

PUVA treatment of platelets was with the Intercept pathogen inactivation method developed by Cerus Corporation (Concord, CA) using amotosalen (AS) as the active photosen-sitizing psoralen and ultraviolet A light (320-400nm) in a calibrated illumination device[25]. Platelet concentrates for transfusion (PC) which each fulfill the acceptance criteria set by Cerus Corporation were used in accordance to the instructions of the manufacturer[26]. PC were prepared by the buffy coat method[27] which is by pooling of six buffy coats and resus-pension in additive solution (SSP+, Macopharma, Tourcoing, France) as described[23]. To generate paired samples, two PCs were pooled, mixed and split again in two equivalent volumes. One volume remained untreated (control) and the other was PUVA treated. The latter PC was thereto transferred to an illumination bag while 17.5mL amotosalen (final ~150µM) was added, followed by expelling excess air bubbles and UVA illumination at a dose of 3.9J/cm². Following overnight incubation on an orbital shaker at room temperature with a compound adsorption device to remove amotosalen and its photoproducts, treated PCs were transferred to a storage bag. Storage was under standard blood bank conditions. Experiments on platelets were performed 16-24 hours after PUVA by sampling low volumes through sterile connections under a laminar flow hood.

SIGNAL TRANSDUCTION ANALYSIS

Platelet samples from PC were washed in Tyrode's buffer (5mM 4-(2-hydroxyethyl)-1-piper-azineethanesulfonic acid (HEPES) pH 7.4 with 136.5mM NaCl, 2.7mM KCl, 11.9mM NaHCO$_3$, 0.4mM NaH$_2$PO$_4$, 1mM MgCl$_2$ and 0.1% (m/v) D-glucose), as previously described[28]. Washed platelets were rested for maximally half an hour at 37°C prior to activation with the indicated agonists and incubation times. Activated platelets were lysed in ice-cold buffer (50mM Tris(hydroxymethyl)aminomethane (Tris) pH 8.0 with 100mM NaCl, 1.0% (v/v) octyl-phe-noxypolyethoxyethanol (Igepal-CA630), 0.1% (m/v) sodium dodecyldisulphate (SDS), 10mM activated Na$_3$VO$_4$, and Halt protease cocktail) and mixed. Platelet lysates were loaded on 4-15% polyacrylamine Tris-Glycine TGX gels (Bio-Rad, Hercules, CA) in reducing Laemmli sample buffer for SDS PAGE western blotting. Primary and secondary antibodies to blotted targets were prepared in tris buffered saline (TBS pH7.4, 25mM Tris with 150mM NaCl and 2mM KCl) with 5% (m/v) skimmed milk. Where required, membranes were reprobed following incubation for 30min at 60°C submerged in western reprobe buffer (50mM Tris pH 7.0, 2.0% (m/v) SDS and 100mM β-mercaptoethanol). Images of bound antibody were developed with enhanced chemiluminescence and an imaging system (ChemiDoc MP) equipped with a CCD camera and analysis software (ImageLab v4.0.1) for densitometry (Bio-Rad).

LIPID EXTRACTION AND LIPID SAMPLE PREPARATION

The solvents used for the lipid extraction and LC-MS separation were HPLC-grade chloroform, ULC-MS grade water and ULC-MS grade methanol (Biosolve, Valkenswaard, The Netherlands). HPLC grade ammonium formate, HCl and HPLC grade methyl-*tert*-butyl-ether were purchased from Sigma-Aldrich. Phosphoinositides from platelet lipid extracts were derivatized and analyzed as described[29] with minor modifications. In brief, three

volumes of chloroform/methanol (1:2, v/v) were added to one volume of platelet suspension for extraction of neutral lipids. The samples were vortex-mixed, followed by centrifugation at 13,000g for two minutes. The supernatant was transferred to an LC-MS vial and used as such for analysis of phospholipids and phospholipids in complex with amotosalen. Internal standards PI(4,5)P$_2$(17:0/20:4) and PI(3,4,5)P$_3$(17:0/20:4) were added at 5µg/mL to the remaining pellet. A volume of 1365µL methyl-*tert*-butyl-ether/methanol/2M HCl (200:60:13; v/v/v) was used to re-suspend the fraction followed by incubation for 15 minutes at room temperature with intermittent mixing. Next, 250µL of 0.1M HCl was added, vortexed and centrifuged at 6,500g for 2 minutes. The upper organic phase was transferred to a new tube and 500µL of pre-derivatization wash solution (lower phase of methyl-tert-butyl-ether/methanol/0.01M HCl 100:30:25 (v/v/v)) was added. The samples were again centrifuged at 6,500g for 2 minutes and the upper phase was transferred for derivatization. Hereto, 50µL of 2M trimethylsilyl-diazomethane in hexane was added and mixed for 10 min at room temperature followed by addition of 6µL of glacial acetic acid (all Sigma-Aldrich) to stop the methylation reaction. Next, 500µL of post-derivatization wash solution (upper phase of chloroform/methanol/water 120:60:45 (v/v/v)) was added, vortex-mixed and centrifuged for 5 minutes at 1,500g. The upper phase was transferred to a high recovery glass vial and dried down in a centrifugal vacuum evaporator (MiVac duoconcentrator, Genevac, Ipswich, United Kingdom) at 37°C. The dried sample was reconstituted in 50µL of chloroform/methanol (1:2, (v/v)) before injection.

ANALYSIS OF (PHOSPHO)LIPIDS

The lipid analysis is based on high-resolution liquid chromatography coupled to high-resolution quadruple time-of-flight mass spectrometry[30,31]. For lipidomics analyses, a 1290 Infinity LC system (Agilent Technologies, Waldbronn, Germany) was used. Lipid extracts were analyzed on an Acquity UPLC BEH Shield RP18 column (2.1 x 100mm; 1.7µm; Waters, Milford, MA, USA) placed in a Polaratherm 9000 series oven (Selerity Technologies, Salt Lake City, UT, USA) at 80°C. Elution was carried out with a multistep gradient of (A) 20mM ammonium formate pH 5 and (B) methanol, starting from 50% B to 70% B in 5 minutes, followed by a slow gradient of 70–90% B in 30 minutes. Mobile phase B subsequently reached 100% in 0.1 minutes where it was maintained for an additional 5 minutes. The flow rate was 0.5mL/minute and the injection volume 10µL for both positive and negative electron spray ionization (ESI) measurements. The whole system was allowed to re-equilibrate under starting conditions for 15 minutes. For measurement of derivatized phosphoinositides, elution was optimized using the same mobile phases at a flow rate of 1.0mL/minutes: starting from 50% B to 85% B in 5 min, followed by a very slow gradient of 85–90% B in 15 min. At the end of the analysis, mobile phase B reached 100% in 2 minutes where it was maintained for an additional 3 minutes. High-resolution accurate mass measurements were obtained on an Agilent 6550 Q-TOF mass spectrometer (Agilent Technologies) equipped with a dual Jetstream

ESI source. The instrument was operated in both positive and negative ESI mode. Needle voltage was optimized to +/- 3.5kV, the drying and sheath gas temperatures were set to 290°C and 400°C, and the drying and sheath gas flow rates were set to 13 and 12L/minute, respectively. Data were collected in centroid mode from m/z 100–3,200 at an acquisition rate of 2 spectra/second in the extended dynamic range mode (2GHz), offering an in-spectrum dynamic range of 10^5 and a resolution of ± 20,000 FWHM in the lipid m/z range. MS/MS experiments were performed in targeted MS/MS mode. The quadrupole was operated at medium resolution and the collision energy was fixed at either 20eV or 35eV. Study samples were analyzed in randomized order. Samples were kept at 4°C in the autosampler tray while waiting for injection.

Abundances (area under the curve or AUC) of lipid species were extracted by the Find by Ion extraction algorithm in MassHunter Qualitative Analysis 7.0 software package (Agilent Technologies) using predefined mass (10ppm) and retention time extraction windows (15 seconds). The Agile integrator was used, with an absolute peak height cut-off of 1000 counts.

Molecular formulas, based on accurate mass, isotopic abundance, and spacing both in positive and negative ionization modes, are complemented with accurate mass database searching in an in-house build database (populated with LIPID MAPS and HMDB entries and theoretical lipid structures) and MS/MS measurement in both modes. Lipid fragmentation mechanisms and spectra in both positive and negative ionization modes were equal to those reported in literature[31]. Each lipid class displays characteristic fragment ions in positive and/or negative ESI mode. Other parameters such as lipid elution behavior and adduct formation interpretation further assisted in the identification. Regarding phosphoinositides, LC-MS cannot discriminate between bisphosphorylated phosphatidylinositol (PIP2) isomers differing in the position of phosphates on the inositol ring. For trisphosphorylated PIP3, the only known isomer is PI(3,4,5)P3.

FLOW CYTOMETRY

Expression of activated integrin $\alpha_{IIb}\beta_3$ (fluorescein labeled PAC1, BD Biosciences, Erembodegem, Belgium) was analyzed with an acoustic focusing Attune flow cytometer (Life Technologies, Carlsbad, CA). Platelets were incubated with labeled antibodies with agonists or the respective vehicle buffer for 10min at room temperature in HEPES buffered saline pH 7.4 with 1.0mM MgSO$_4$ and diluted thousand fold immediately before readout according to previously published work[32]. Signals of the isotype antibody controls were used to set threshold gates including 0.5% of 10,000 negative events. Median fluorescence intensities and percentage positive events were determined for 10,000 cells staining positive for the platelet marker CD61 (allophycocyanin labeled anti-CD61, Life Technologies).

CALCIUM SIGNALING

Kinetics of calcium release from internal stores was measured by fluorescence of Oregon Green BAPTA-AM loaded platelets. Washed platelets were incubated for 45min with 5mM Oregon Green BAPTA-AM in the presence of 0.05% pluronic F-127. The platelet suspension was centrifuged and redissolved in Tyrode's buffer with 3.5mg/mL human serum albumin and 250µM ethylene glycol tetraacetic acid (EGTA) to chelate trace extracellular calcium. A microplate reader equipped with a pipetting robot and thermostat (Tecan, Männedorf, Switzerland) was used to deliver Oregon Green loaded platelets in all white 96-well plates (100µL per second) containing agonists and/or antagonists followed by immediate readout at 550nm (excitation 488nm) in function of time for 4min. Cytosolic calcium concentrations were determined by extrapolation of signals using maximal fluorescence as determined by short incubation of loaded platelets with 5µM of calcium-ionophore A23187 in the presence of 2mM $CaCl_2$ and minimal fluorescence as determined by addition of 0.5% (v/v) Triton-X-100 and 8mM EGTA.

LIPID PACKING ANALYSIS IN LIPOSOMES

Binding experiments of lipid packing sensors were based on pioneering work by Vanni *et al*[33] and Pranke *et al*[34]. First, the lipid packing sensing peptide ALPS was covalently labeled with NBD to their N-termini. The ALPS peptide contained just one cysteine (at the N-terminus) and was kept in a reducing environment (10-fold molar excess of TCEP). Labeling was to that free N-terminal thiol using IANBD at a molar ratio of IANBD to ALPS of 10:1 in HK buffer (50mM HEPES pH7.2 with 120mM potassium acetate) for 2 hours at room temperature in the dark. The reaction mixture was dialyzed (membrane molecular weight cut-off 2,000) to 4L of HK buffer during 24 hours at 4°C. The degree of labeling for both peptides was determined by optical absorbance at wavelengths for peptides, bound and free label.

Surface partition constants for ALPS-NBD binding to PUVA treated or control liposomes were determined by serial dilution of the phospholipid fraction as liposomes. Liposome preparation was with sonication as described above. Liposome composition is given in **Figure 4.** PUVA treatment was with amotosalen at 150µM. A serial dilution of liposomes (PUVA treated or not) was prepared in HKAc buffer (50mM HEPES pH7.2 with 120mM potassium acetate, 1mM $MgCl_2$, 1mM dithiothreitol) and supplemented with 0.17µM ALPS-NBD or unlabeled ALPS (for background correction). Fluorescence (emission 535nm) was measured at 37°C (excitation 485nm). The Surface partition constant (K_p) was calculated as described for NBD labeled peptides to lipid bilayers[35]. In brief, data were modeled by linear regression (Prism 6 v6.01, GraphPad Software, San Diego, CA) to equation (1), where X_b^* is the corrected molar ratio of bound peptide to lipid. The correction factor is a constant and finds its origin in the fact that only the outer leaflet of the bilayer is accessible for the binding partner. Cf is the equilibrium concentration of free peptide in solution.

$$X_b^* = K_p x C_f \qquad\qquad eq. 1$$

T-CELL ACTIVATION

PBMC were prepared by Ficoll gradient centrifugation of buffy coats prepared by centrifugation of whole blood donations from healthy non-renumerated donors. Isolated PBMC preparations were washed three times in sterile phosphate buffered saline (PBS, pH 7.4) by soft centrifugation to remove contaminating platelets. Finally, the cells were resuspended in phenol red-free RPMI-1640 medium with 2mM L-glutamine, 10mM HEPES and 10% (v/v) AB (RhD-) human serum and rested for 2 hours at room temperature. The rested cells were resuspended to 40,000 leukocytes per µL in Tyrode's buffer and mixed with 8MOP or amotosalen in a final amount of 60X106 leukocytes. Illumination of the suspension with UVA light was in a quartz cuvette. Following PUVA, T-cells were activated in Tyrode's buffer with $2.5X10^6$ CD3/CD28 human T-activator Dynabeads per 10^6 leukocytes in the presence of 10ng/mL of IL2 for 30min at 37°C on a rotator. Cells were lysed with ice-cold buffer and centrifuged at 20,000g for 3min. Supernatant was analyzed by SDS PAGE western blotting in reducing sample buffer.

EXTRACORPOREAL PHOTOPHERESIS SAMPLES

A patient enrolled in a clinical trial not related to this study at the Hospital Network Antwerp (Belgium) for the treatment of chronic GvhD with off-line ECP gave informed consent for sampling of cells from the buffy coat suspension before and after PUVA. The study was approved by the hospital's ethical committee (approval number 4591). The ECP procedure involved a leukapheresis (Spectra Optia, Terumo BCT, Lakewood, CO) yielding a buffy coat cell suspension that was diluted with saline in an illumination bag to a final 300g by mass. The psoralen 8MOP was added to a final 0.9µM followed by illumination in a Macogenic G2 UVA illumination device (Macopharma) which delivered $2J/cm^2$ or $2.5J/cm^2$ depending on the suspension's hematocrit of <2% or ≥2%, respectively. Before and after illumination, 2mL samples were taken aseptically from the bag. PBMC were prepared from these samples followed by activation of T-cells as described above. A total of three ECP procedures were performed on the patient. For each procedure PBMC isolation and T-cell activation were performed in triplicate to control for variation in SDS PAGE western blotting and densitometry.

RESULTS

PLATELET INTEGRIN ACTIVATION IS DECREASED BY PUVA

Platelet activation involves a series of complex signaling cascades culminating in a number of pivotal functions that drive hemostasis. One of these is platelet aggregation which is mediated by crosslinking of soluble trimeric fibrinogen to multiple platelet integrin $\alpha_{IIb}\beta_3$ receptors. This abundant but platelet specific integrin adopts a non-binding "closed" conformation during circulation in healthy vessels. A dramatic conformational change "opens" up the receptor caused by inside-out activatory signals initiated by extracellular agonists released at sites of vessel injury. The molecular change in integrin $\alpha_{IIb}\beta_3$ can be measured by a monoclonal antibody (PAC1) that recognizes this activated form only[36]. In flow cytometry this particular readout was used to test how PUVA affects the platelet's response to specific agonists. PUVA decreased platelet integrin activation by half in a dose increasing experiment of the peptide SFLLRN which activates the high affinity thrombin receptor PAR1 **(Figure 1a)**. PAR1 is a G-protein coupled receptor (GPCR), but the defect was not specific for this class of receptors because dose-dependent integrin activation via the unrelated collagen receptor couple GPVI–FcγR using cross-linked collagen related peptides (CRP-XL) was decreased eightfold **(Figure 1b)**. Moreover, the respons of low affinity thrombin receptor PAR4, another GPCR that is closely related to PAR1, to the AYPGKF peptide was normal **(Figure 1c)**. The latter experiment indicates that the conformational change of the integrin $\alpha_{IIb}\beta_3$ itself was not affected as such by PUVA. Besides, membrane expression levels of key platelet receptors GPVI, PAR1, FcγR and α_{IIb} on the platelet surface were normal in PUVA treated platelets, both in resting and activated conditions (Data not shown).
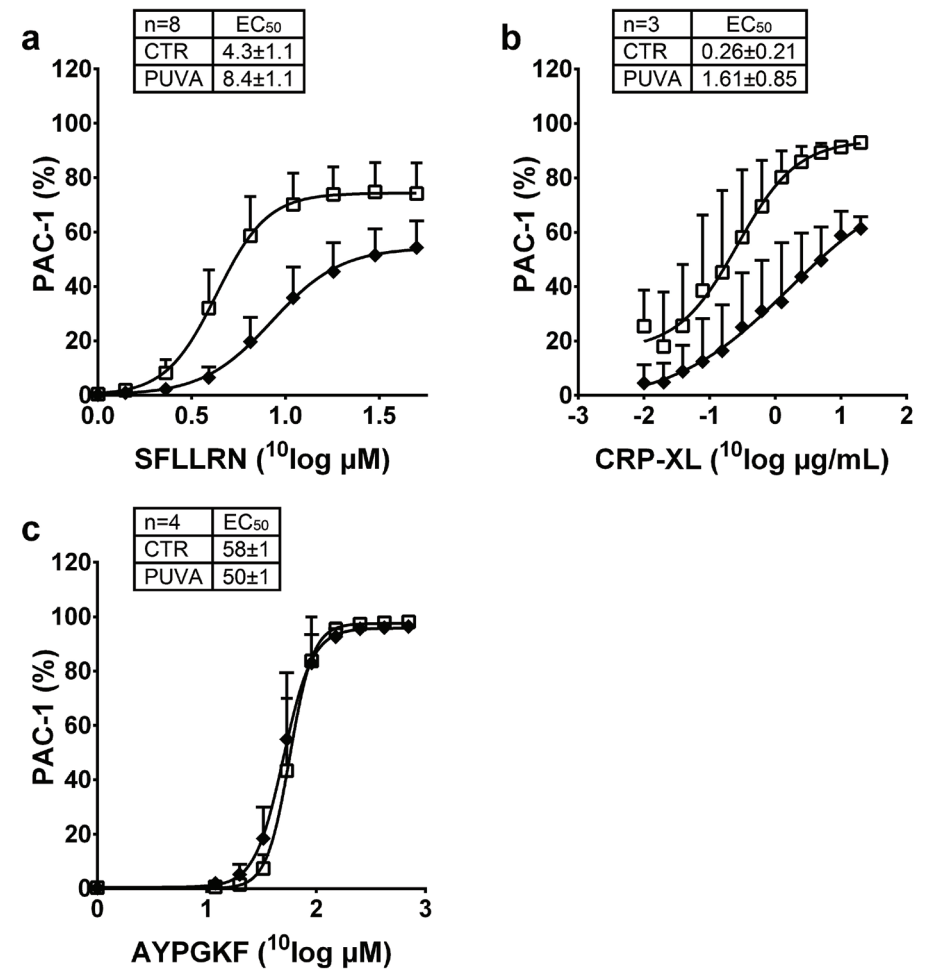
*Figure 1 : Effect of PUVA on inside-out signaling of integrin $\alpha_{IIb}\beta_3$. Paired platelet samples were treated with PUVA (◆) or not (CTR, □) and then incubated with the indicated agonists and labeled with PAC1 for flow cytometry. The percentage of platelets exposing the PAC1 epitope following dose-response activation by (**a**) SFLLRN, (**b**) CRP-XL and (**c**) AYPGKF peptides are shown. The data were fitted by non-linear regression. Effective half-maximal concentrations (EC_{50}) were calculated from these fits and are depicted in the inset tables. Data are shown as means with standard deviations, the number of repeats is indicated in the inset tables.*

PUVA SELECTIVELY INHIBITS AKT AND BTK PHOSPHORYLATION

The normal integrin activation in response to specific PAR4 stimulation indicated that the PUVA dependent defects were restricted to selected signal transduction pathways. Therefore, key effector phosphorylations upstream of integrin $\alpha_{IIb}\beta_3$ activation were interrogated. Following GPCR and RTK signal transduction $PI(4,5)P_2$ can be phosphorylated by PI 3-kinase to yield $PI(3,4,5)P_3$ which in his turn regulates the phosphorylation of Akt and Btk. Furthermore, $PI(4,5)P_2$ can also be hydrolyzed by PLC enzymes into IP_3 and DAG.

While investigating the PI 3-kinase pathway, we found a significanty decreased phosphorylation of Akt and Btk in response to both CRP-XL and SFLLRN **(Figure 2)**. The experiment with SFLLRN included methyl-thio-adenosine diphosphate (MeSADP) to stimulate the purinergic P2Y12 GPCR because phosphorylation of Akt is not efficient without co-stimulation[37]. Specificity of the PI 3-kinase-Akt pathway was confirmed by use of Wortmannin (Wm) which inhibits all PI 3-kinase isoforms. Because GPVI-FcγR activation by CRP-XL causes amplificatory feedforward signals through remote GPCRs by thrombin, thromboxane A2 generation and adenosinediphosphate (ADP) release, the experiment was repeated in the presence of respective secondary signaling inhibitors D-phenylalanyl-L-prolyl-L-arginyl chloromethyl ketone, indomethacine and ticagrelor, yielding similar results (data not shown). In addition, phosphorylation of Akt via the differential JAK signaling pathway in response to thrombopoietin (TPO) was also decreased **(Figure 3a, c)**. The TPO receptor (alternative name, CD110) does not cause platelet activation[38], confirming that the signal transduction defect is not a consequence of simultaneously activated remote pathways. Akt phosphorylation through combined activation of PAR4 and P2Y12 by AYPGKF and MeSADP respectively was normal **(Figure 3b, c)**.

To investigate if the other pivotal signaling pathway was affected by PUVA, phospholipase C (PLC) activation was measured. Platelets use PLCβ and PLCγ2 in response to GPCRs and GPVI-FcγR, respectively. The PLC activation causes archetypical inositol-tris-phosphate and diacylglycerol second messenger responses. The former was measured by calcium release from internal stores in function of time and the latter by phosphorylation of the major phosphokinase C reporter pleckstrin. Both processes **(Figure 4)** were however normal, demonstrating that PLC pathways were unaffected by PUVA.
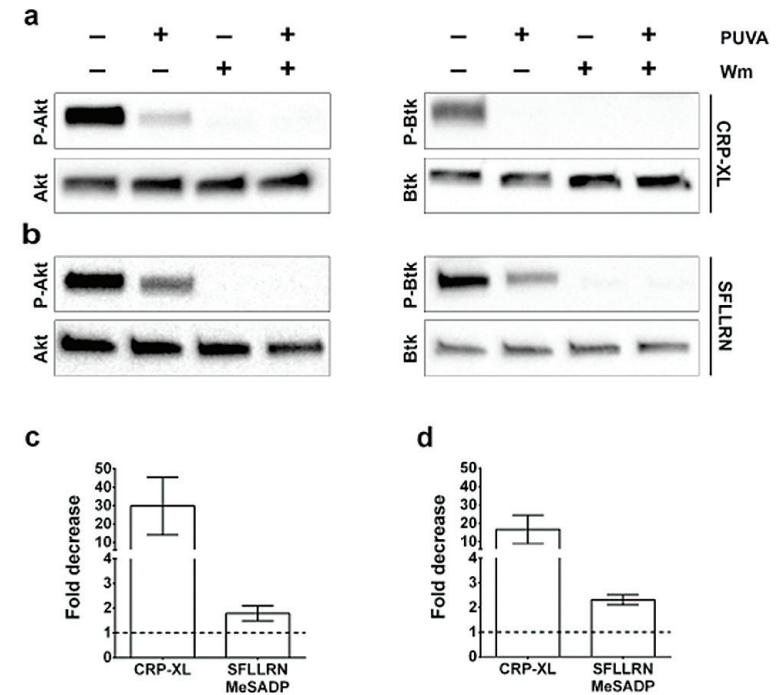
Figure 2: PUVA inhibits Akt and Btk phosphorylation. Platelet lysates were analyzed by western blotting and subsequent densitometry. Antibodies to T308 phosphorylated Akt (P-Akt) or Y551 phosphorylated Btk (P-Btk) were used. For control of gel loading, the membranes were reprobed for total Akt (Akt) or total Btk (Btk). PUVA treatment in the presence or absence of 0.5µM Wm is indicated on top of the panels. (a) Platelets were activated with 1µg/mL CRP-XL for 2 minutes or (b) with 30µM SFLLRN in combination with 10µM MeSADP for 3 minutes. (c, d) The decrease in mean protein band density of the ratio phosphorylated kinase to total kinase (n=6) in PUVA treated platelets relative to untreated control counterparts is given. No change is emphasized by the horizontal dashed line.
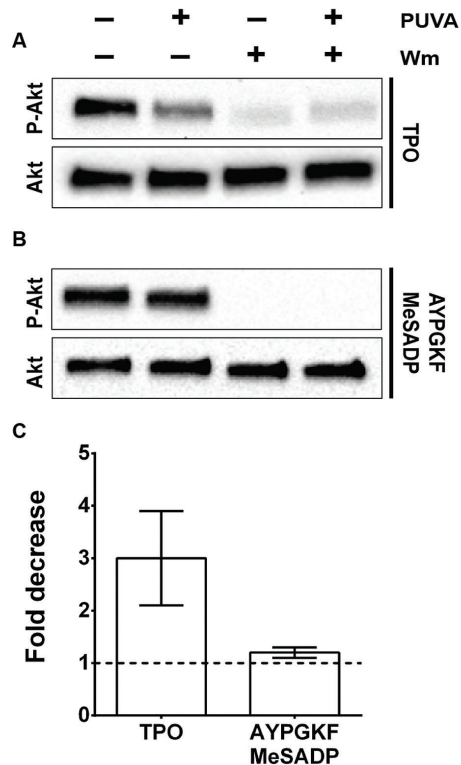
Figure 3: PUVA affects phosphorylation of Akt following signal transduction through the TPO receptor, but not through PAR4. (a) Platelets were activated with 100ng/mL TPO for 10 minutes or (b) with 250μM AY-PGKF and 10μM MeSADP for 5 minutes. Platelets were lysed and the samples analyzed by western blotting. Antibodies to T308 phosphorylated Akt (P-Akt) were used. Membranes were reprobed for total Akt (Akt) as a control for loading. Wortmannin (0.5μM) was used to confirm that Akt phosphorylation was PI 3-kinase dependent. (c) The mean decrease in Akt signal (n=6) of PUVA treated platelets relative to untreated control counterparts is depicted. No change is emphasized by the horizontal dashed line.

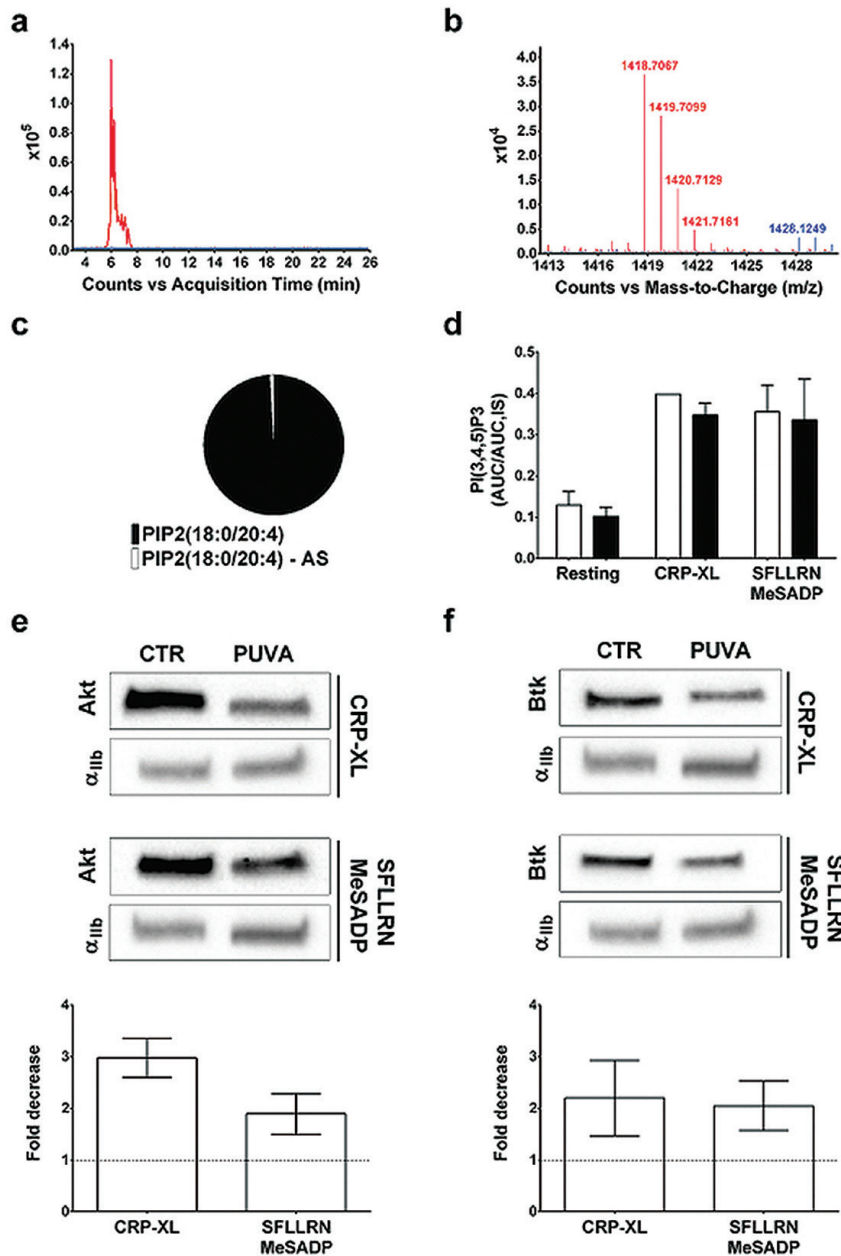## PUVA IMPEDES NORMAL RECRUITMENT OF AKT AND BTK TO THE PLASMA MEMBRANE

The signaling pathways of PAR1 and GPVI-FcγR are dissimilar, yet both result in defective Akt and Btk phosphorylation in PUVA treated platelets. Although these effector kinases exert diverse functions in the cell, both rely on a pleckstrin homology domain (PH) to interact with the inner membrane leaflet. This interaction is facilitated by PI(3,4,5)P3 which is produced from PI(4,5)P2 by activated PI 3-kinase. Therefore, we hypothesized that PI(3,4,5)P3 formation was defective in PUVA treated cells. Lipid extracts of PUVA treated platelets were analyzed by reversed phase liquid chromatography (RP-LC) coupled to high-resolution quadrupole time-of-flight (Q-TOF) mass spectrometry (MS) which primarily showed covalent adduct formation between the psoralen amotosalen and PIP2 in UVA illuminated platelet samples **(Figure 5a, b)**. In control cells incubated with amotosalen in the dark, no covalent adduct formation was detected. Adduct formation with amotosalen was however not restricted to PI because also phosphatidylserine (PS), phosphatidylcholine (PC) and phosphatidylethanolamine (PE) adducts were found (data not shown). Notably, the relative amount of PIP2 in complex with amotosalen was at most 1.2% of total **(Figure 5c)** and therefore unlikely to interfere with PI 3-kinase activity. Indeed, PI(3,4,5)P3(18:0/20:4) levels were normal following stimulation with CRP-XL or SFLLRN/MeSADP in PUVA treated platelets **(Figure 5d)**. These data indicate that defective PI(3,4,5)P3 formation is not the cause of attenuated Akt and Btk phosphorylation. Therefore and because the primary role of PI(3,4,5)P3 is to support recruitment of peripheral effector proteins to the plasma membrane compartment, recruitment of Akt and Btk was investigated. Hereto, the membrane fraction of lysed platelets was isolated by differential (ultra)centrifugation. Western blotting indicated significantly defective localization to this subcellular compartment of both Akt and Btk in response to both CRP-XL and SFLLRN/MeSADP **(Figure 5e, f)**. Together, the data indicate that in the presence of normal PI(3,4,5)P3, PUVA treatment interferes with adequate plasma membrane recruitment of Akt and Btk in response to selected agonists.

PUVA INHIBITS MEMBRANE BINDING OF MODEL PEPTIDES

Because the photochemical reaction between psoralens and phospholipids is uniquely through unsaturated carbon bonds[19,20], we hypothesized that alterations in the membrane bulk properties were underlying the PUVA related signal transduction defects. Half of platelet phospholipids is unsaturated[39] and Akt phosphorylation decreases in cells that contain few monounsaturated phospholipids[40]. One of the biophysical roles of unsaturated acyl chains is to fine-tune lipid packing. Their "hinged" geometry renders the phospholipid conical rather than cylindrical (**Figure 6a, b**) creating imperfections in lipid packing. These lipid packing defects[33] (LPD) facilitate protein-membrane binding[41,42] by creating dynamic gaps in the hydrophilic sheet that tops each bilayer leaflet. To investigate if PUVA affects this biophysical property, we used fluorescently labeled ALPS peptide. This sequence is derived from the GMAP210 protein's N-terminus and specifically partitions to curved liposomes of high but not low LPD content[33]. As expected, the ALPS probe efficiently bound to liposomes enriched in conical phospholipids, which is 15 mol% 1-2-dioleoyl-*sn*-glycerol and 85 mol% 1,2-dioleoyl-*sn*-glycero-3-PC **(Figure 6c)**. When treated with PUVA, binding to these liposomes was completely abolished, down to background levels similar of ALPS binding to purely cylindrical 1-palmitoyl-2-oleoyl-*sn*-glycero-3-PC liposomes. Surface partition constants were estimated by regression analysis confirming hampered partitioning of the ALPS peptide to the LPD enriched liposomes. Because curvature is another significant determinant of ALPS partitioning to liposomes, size distributions were analyzed prior to binding studies but were not different between controls and PUVA treated preparations (data not shown). Hence, differences in binding are not related to changes in curvature. To confirm this observation with another unrelated lipid binding protein, fluorescently labeled α-synuclein was used. This particular peptide recognizes LPD containing liposomes in a different way than ALPS and it requires the presence of PS[34]. However, binding to its preferred liposomes was similarly affected (data not shown) indicating that PUVA prevents efficient insertion of membrane binding proteins in model bilayers.
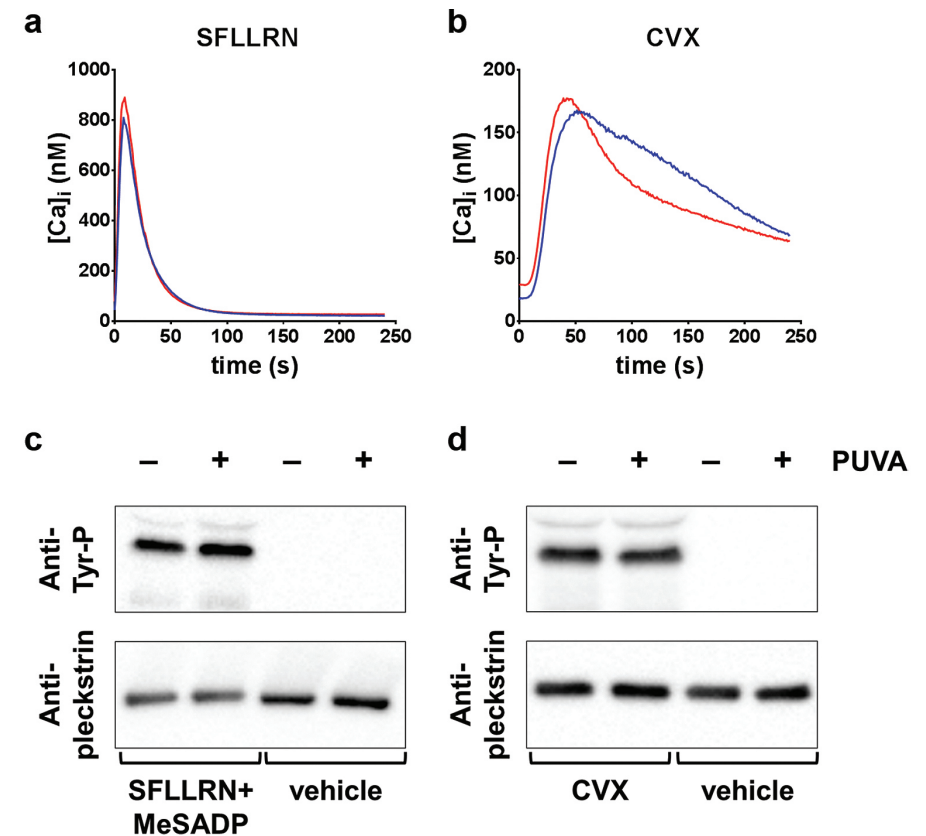
Figure 4: Calcium release and PKC phosphorylation in response to platelet agonists. (a and b) BAPTA-Oregon Green 488 loaded platelets were used to monitor kinetics of intracellular calcium release in response to selected agonists, indicated on top of the panels. The PAR1 activating SFLLRN peptide (30μM) and the GPVI-FcγR agonist convulxin (CVX, 22ng/mL) were used. Platelets treated with PUVA (red) were compared to paired untreated control cells (blue) in simultaneous runs. The calcium dependent fluorescent signal (excitation 488nm, emission 550nm) was recorded. Values were corrected for background. The concentration of ionized calcium [Ca]i was estimated by extrapolation using maximal and minimal signals of known calcium concentrations in separate control wells. Tracings are representative of three repeats. (c and d) Platelet activation through PAR1 was with 30μM SFLLRN and 10μM MeSADP or through GPVI-FcγR with 22ng/mL CVX. Paired control samples for resting platelets were incubated with the respective vehicle buffers. Following activation for 3 and 5 minutes, respectively platelets were lysed and the lysates were analyzed by western blotting. anti-phospho-tyrosine antibodies (Anti-Tyr-P) and anti-pleckstrin antibodies (Anti-pleckstrin)

a

b

c

d

e

f

Figure 5: PUVA inhibits recruitment of Akt and Btk to the PI(3,4,5)P3 activated plasma membrane. (a) Overlaid extracted ion LC-MS chromatograms (m/z 1418.7073±10 ppm) of PUVA treated platelets (red tracing) indicate de novo formation of PIP2(18:0/20:4)-amotosalen covalent adducts which are absent in control extracts (blue tracing) that were not UVA treated. (b) Overlaid accurate mass spectra indicating covalent complexes of amotosalen and PIP2(18:0/20:4) in the PUVA treated (red) spectrum and its absence in not UVA illuminated control (blue) spectrum. (c) This pie chart indicates the amount of PIP2(18:0/20:4) forming adducts with amotosalen (AS) relative to total PIP2(18:0/20:4) in PUVA treated extracts. (d) The amount of PI(3,4,5)P3(18:0/20:4) in platelet lipid extracts depicted as the ratio of the peak integral (AUC) relative to the internal standard peak integral (AUC, IS). Platelets were activated with 1µg/mL CRP-XL or 10µM SFLLRN+10µM MeSADP. Untreated controls (open bars) and PUVA treated samples (closed bars) are shown. Activation times were 2 and 3 minutes, respectively. Resting platelets were incubated with vehicle. Mean with SD is shown (n=4). (e, f) The platelet membrane fraction was analyzed by western blotting and subsequent densitometry. Antibodies to total Akt (Akt) or total Btk (Btk) were used. Loading was controlled by reprobing the membrane with an antibody to the membrane specific integrin a_{IIb}. PUVA treatment or not (CTR) is indicated on top of the panels. The decrease in mean protein band density of the ratio kinase to a_{IIb} (n=3) in PUVA treated platelets relative to untreated control counterparts is given.

PUVA DECREASES PHOSPHORYLATION OF AKT IN T LYMPHOCYTES FROM ECP TREATED GVHD PATIENTS

As a model for PUVA treatment of nucleated human cells, peripheral blood mononuclear cells (PBMCs) were isolated from fresh blood donations of healthy consenting volunteers. To activate PI 3-kinase-Akt axis in this cell mixture, stimulation of T-cells was performed by incubation with T-cell receptor activating CD3/CD28 beads in the presence of co-stimulating interleukin-2 (IL2). The effect of two psoralens 8–methoxypsoralen (8MOP) and amotosalen was compared in paired experiments even though only 8MOP is currently used as an active component for ECP. The data show that both psoralens dose-dependently inhibited T cell receptor mediated phosphorylation of Akt following a fixed UVA dose **(Figure 7a, b)**. Because DNA may coincidently be affected by PUVA in nucleated cells, immediate cell death was investigated by Sytox staining in flow cytometry. But for the course of the T-cell activating experiment and in the psoralen concentration ranges used, no increase in Sytox staining was observed (data not shown). These data confirm a direct link between the presence of photoexcited psoralens and inhibition of Akt phosphorylation independent of cell death. Furthermore, it shows that amotosalen is more efficient than 8MOP achieving half maximal inhibition at lower concentrations. To confirm if Akt activation is affected in clinically relevant tissue, buffy coat cells from GvhD patients enrolled in a clinical efficacy study were collected before and after ECP. In these samples, Akt activation in T lymphocytes was also significantly decreased **(Figure 7c, d)**. Together, these data show that PI(3,4,5) P3 dependent signaling is affected by PUVA in cells other than platelets and in the exact clinical setting of ECP treatment.

DISCUSSION

Despite its widespread clinical use, many aspects of PUVA's mode of action have remained uncertain. Our data show for the first time that PUVA treatment specifically but selectively inhibits the PI 3-kinase-Akt pathway. This inhibition is not on the PI 3-kinase enzyme itself. In contrast, the binding of crucial PI(3,4,5)P3 dependent effector kinases to the activated cytosolic membrane compartment is prevented in response to specific stimuli. Our model **(Figure 8)** suggests that covalent modification of phospholipids by photoexcited psoralen in the plasma membrane prevents efficient interactions with membrane binding proteins. Covalent binding of photoexcited psoralen to unsaturated fatty acids has indeed been described both in cell-free test tubes and in cell extracts[19,20,43]. Our mass spectra of PUVA treated platelet extracts have confirmed covalent reaction with unsaturated acyl side chains which complies with the preferred partitioning of psoralens to the inner apolar phase of lipid bilayers[17]. Of note, all investigated phospholipid classes were more or less affected, indicating no obvious dependence on the hydrophilic head group. Despite this unspecific chemistry, signal transduction inhibition was remarkably specific for the PI 3-kinase pathway because Akt and Btk phosphorylation was decreased but the concurrent PLC axis showed no defect, even though both PI 3-kinase and PLC utilize the same PI(4,5)P2 substrate. Therefore it seemed unlikely that PUVA caused substantial decreases in the functional pool of substrate. Indeed, even the levels of PI(3,4,5)P3 in response to agonist activation were normal meaning that the defect causing decreased Akt and Btk activation was downstream of PI 3-kinase. Besides, very little PI(4,5)P2 was in complex with amotosalen after PUVA. Collectively, these data suggest that psoralen modifications of PI(4,5)P2 are not directly inhibiting activation of Akt and Btk. Elevated PI(3,4,5)P3 levels should normally recruit cytosolic Akt and/or Btk to the plasma membrane where locally restricted enzymes catalyze their phosphorylation[44,45]. Activated Akt and Btk next dissociate from the confined plasma membrane environment to execute central tasks in the cell cytoplasm (or nucleus). Plasma membrane recruitment thus is a crucial step preceding successful Akt and Btk activation[46,47]. Our data show that this plasma membrane recruitment is significantly decreased following activation of certain receptors in PUVA treated platelets. Because of normal PI(3,4,5)P3 levels however, this suggests that efficient plasma membrane sublocalization of Akt and Btk is depending on auxiliary facilitators. Since unsaturated fatty acids are the prime target of PUVA chemistry, such additional factors must require normal (levels of) fatty acyl unsaturations to fulfill their role. Even though primary binding is assumed to be between the PH domain sequence K-X$_n$(K/R)XR[48] and PI(3,4,5)P3, these additional factors (in)directly support Akt and Btk plasma membrane recruitment. In that regard, some amino acids in the PH domains of PLCδ1 and GRP1 are known to penetrate the inner hydrophobic core of the membrane[49,50]. Such membrane insertion may require that the targeted membrane compartment contains a certain degree of LPD[33,51].

154
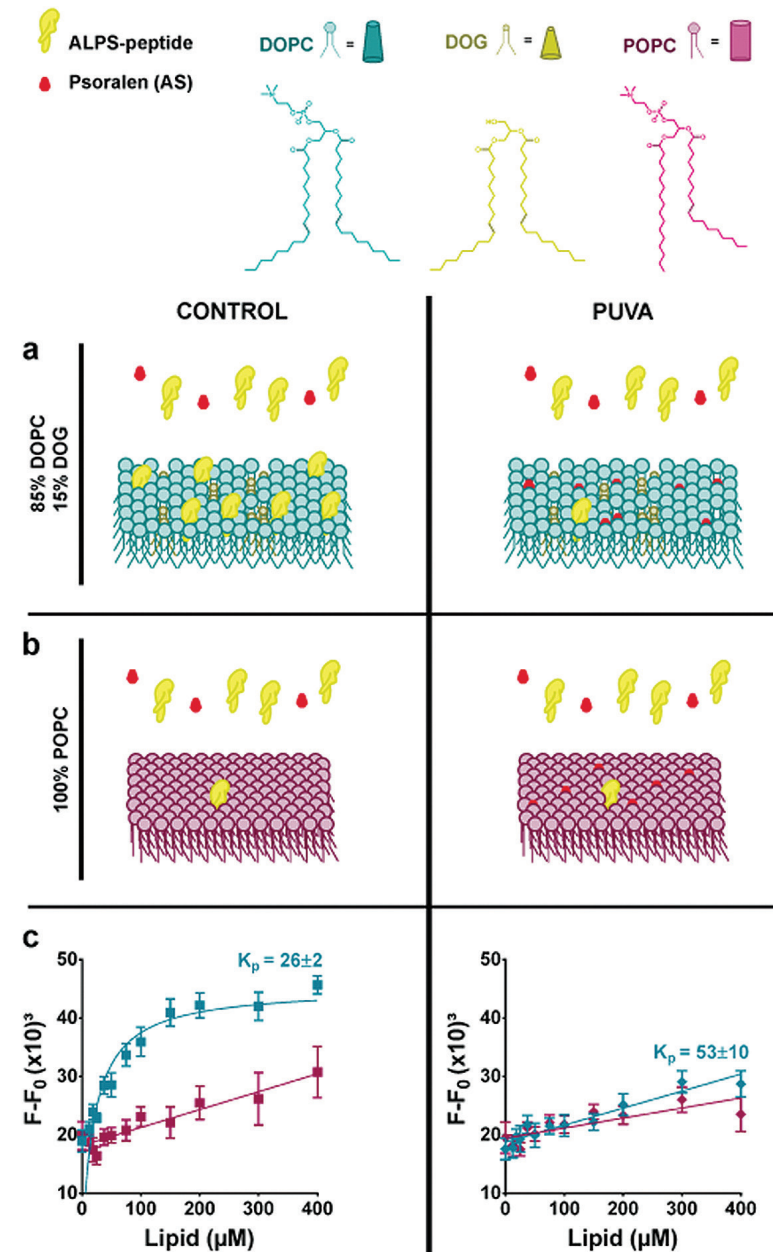
Figure 6: PUVA interferes with ALPS-NBD binding to LPD-rich liposomes. Binding of the NBD labeled ALPS peptide to (a) LPD-rich liposomes (cyan) composed of conical 1,2-dioleoyl-sn-glycero-3-phosphocholine (85mol% DOPC) and 1-2-dioleoyl-sn-glycerol (15mol% DOG) was compared with (b) LPD-poor liposomes (magenta) entirely composed of cylindrical 1-palmitoyl-2-oleoyl-sn-glycero-3-phosphocholine. Liposome preparations containing 150μM amotosalen were treated with UVA light (PUVA, right panel series, ◆) or not (CONTROL, left panel series, ■) (c) The corrected peak fluorescence signal (F-F$_o$) of NBD at 535nm (emission wavelength) is plotted in function of increasing concentrations of lipid. Data for LPD-rich liposomes were analyzed by regression to generate surface partition constants (K$_p$) as indicated. Data are shown as means with standard deviations (n=6).

Our data show that binding of LPD probes to model bilayers is hampered by PUVA, indicating that membrane insertion as promoted by conical phospholipids is inhibited. We thus hypothesize that lipid packing is the additional factor that cooperatively strengthens binding to accomplish successful coincidence detection[52] between PH domains and the cytosolic membrane leaflet. The data provide the first proof in live cells that the acyl side chain milieu of phospholipids determines binding success of major PH-domain containing effector kinases in the presence of normal PI(3,4,5)P3 levels.

The extent of Akt and Btk inhibition following PUVA treatment depends on the nature of the stimulus, i.e. the ligand-receptor couple. Inside-out communication to activate integrin $\alpha_{IIb}\beta_3$ was most affected starting from GPVI-FcγR, less when PAR1 was activated and not at all through PAR4. This means that the integrin $\alpha_{IIb}\beta_3$ activation machinery at least is able to respond normally if the required signals come in correctly from the upstream cue. How this variability then is established remains uncertain. Maybe the separate ligand-receptor circuits reside in plasma membrane microdomains of specific phospholipid composition[53] that is more or less susceptible to modifications by PUVA. This would follow the spatiotemporal dogma of PI 3-kinase dependent signaling stating that PI(3,4,5)P3 are temporary scaffolding molecules for locally restricted signalosomes to build upon[54]. Such spatiotemporal restriction assigns distinct signal identity, but in a physiologic environment containing multiple extracellular chemicals each of these will integrate to a single compound output per cell that thus is variably modified by PUVA **(Figure 6)**.
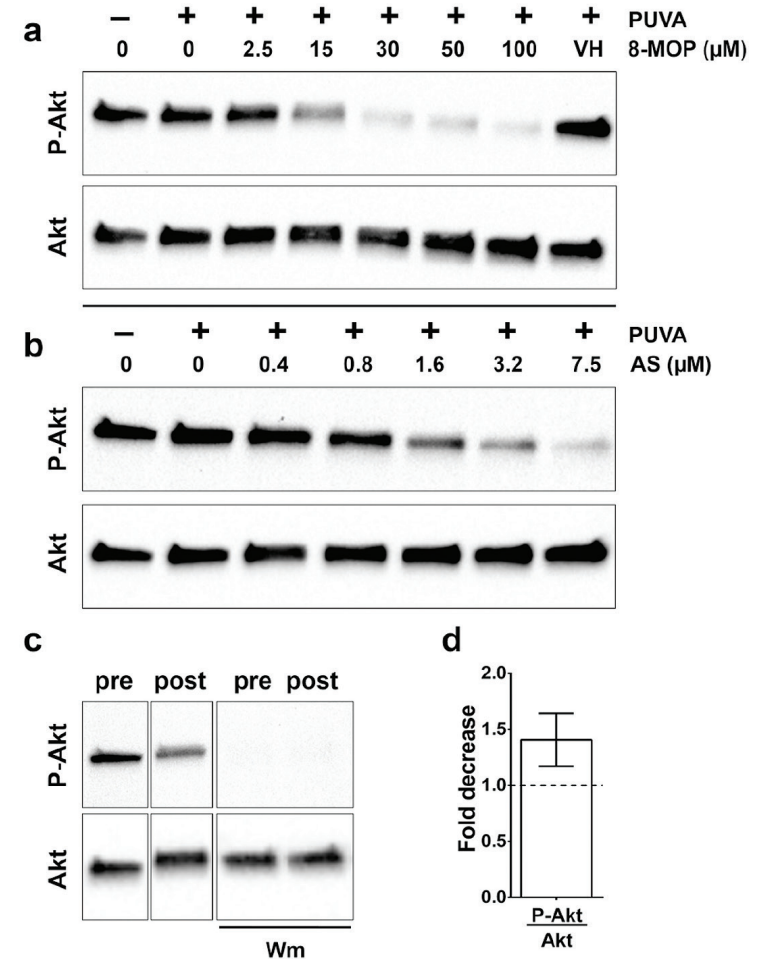
Figure 7: PUVA causes decreased Akt phosphorylation in T lymphocytes. (a) Dose escalations of (a) 8MOP or (b) amotosalen (AS) were added to isolated PBMC from healthy donors and subsequently illuminated with UVA light or not, as indicated on top of each panel. Vehicle (VH) contained no psoralen and was used as a negative control. (c) PBMC were isolated from clinical buffy coat samples before (pre) and after (post) ECP treatment for GvhD. T lymphocyte activation in the presence of 0.5μM Wm was used to control for specificity of the PI 3-kinase axis. (a–c) T lymphocytes were activated by receptor ligation in the presence of IL2 followed by western blotting of whole cell lysates. Antibodies to T308 phosphorylated Akt (P-Akt) were used and membranes were reprobed for total Akt (Akt) to control for loading. (d) The mean decrease in the P-Akt over Akt signal ratio in samples post ECP relative to pre ECP is depicted (n=3). No change is emphasized by the horizontal dashed line.

In platelets, this altered output presents as delayed thrombus formation on immobilized collagen *in vitro*[23]. Other experimental means of PI(3,4,5)P3 dependent signaling inhibition in platelets confirm significant function defects in mouse models of Akt isoform deficiency[55], PDK1 deficiency[56] or PI 3-kinase isoform deficiency[57]. Of note, also Btk inhibition using ibrutinib significantly increases the risk of bleeding in patients suffering from B cell malignancies[58]. PUVA is currently used in blood banks to treat platelet concentrates for transfusion. It efficiently reduces pathogen and white blood cell viability by damaging its DNA. Originally platelets were believed to be unsusceptible to PUVA because they do not contain a nucleus. Our findings now reveal mechanisms of functionality decreases caused by DNA unrelated side-effects of PUVA treatment. Of note, side-effects following transfusion of psoralen-modified phospholipids represent an additional major clinical unknown.

Our findings also have consequences for other fields that commonly apply PUVA. The exact drivers of clinical success in skin pathologies or GvhD for instance remain not fully understood. We propose a substantial role for selective PI 3-kinase axis inhibition, given the results of the buffy coat samples from our GvhD patient which clearly demonstrate reduced Akt phosphorylation. Yet, this single readout merely demonstrates attenuation of just one effector kinase (Akt), in one cell type and to one ligand-receptor combination. The exact cellular composition of PUVA treated tissue by type and number as well as their individual susceptibility to PUVA will eventually determine the response in a relevant physiological environment. Further study will thus require a systems approach[59] to unravel the dependence of relevant ligand-receptor couples to PUVA and combine the findings in an integrated view, taking into account effects on DNA replication and transcription as well.

In conclusion, our research shows that PUVA selectively inhibits recruitment of Akt and Btk kinases to activated plasma membranes. This suggests that unsaturations in the plasma membrane co-determine kinase-lipid binding. We furthermore propose that the variable susceptibility of ligand-receptor couples to PUVA contributes to complex rewiring of cell and tissue fate, explaining the complexity in output and thus clinical success.
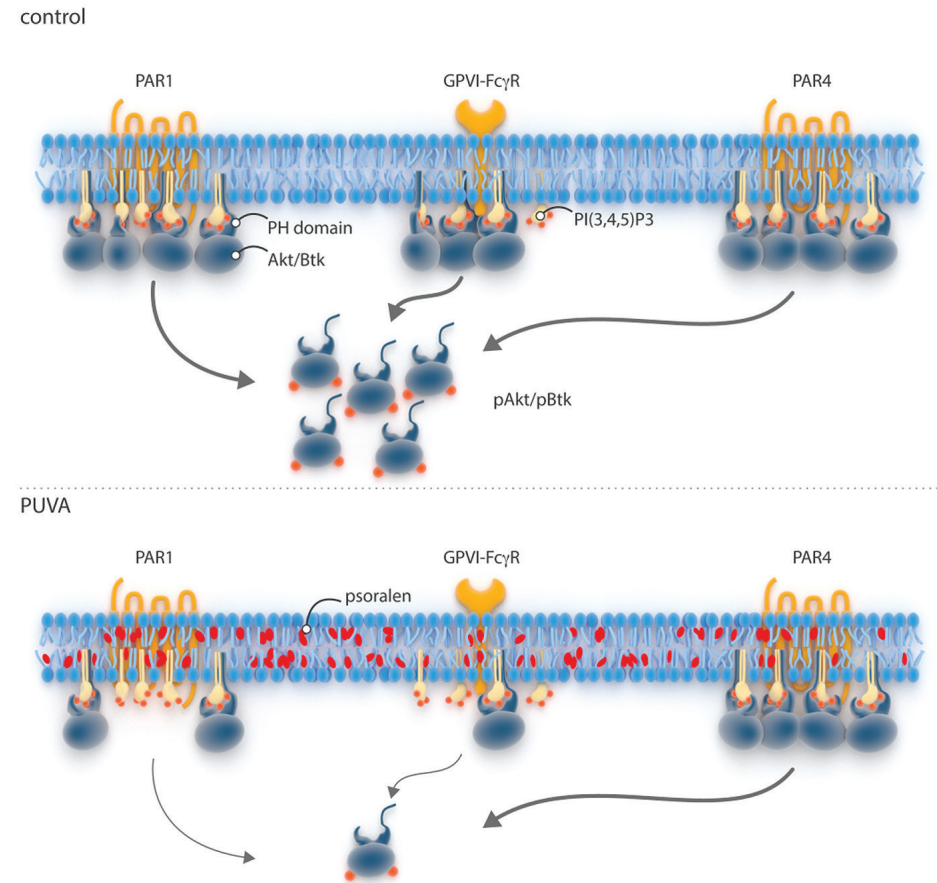
Figure 8: PI(3,4,5)P3 dependent processes are selectively downregulated by PUVA. Stimulation of membrane receptors including GPCRs (PAR1 & PAR4) or immune receptors (like the collagen receptor complex GPVI-FcR) in platelets results in recruitment of PH domain containing effector molecules like Akt and Btk to the spatiotemporally restricted scavenger phospholipids PI(3,4,5)P3 in the cytosolic leaflet of the membrane. This causes phosphorylation of such targets (pAkt/pBtk), their release from the confined plasma membrane space and execution of several cellular functions downstream. Following PUVA however, covalent modification of several unsaturated acyl side chains attenuates efficient recruitment to PI(3,4,5)P3 in response to certain (like PAR1 and GPVI-FcγR) but not all (PAR4) ligand-receptor couples.

AUTHORSHIP CONTRIBUTION

BVA designed research, executed experiments, interpreted data and wrote the paper; RD executed experiments and interpreted data; RTK and KS were responsible for mass spectrometry experiments, its data analysis and its figure composition; PZ provided patient samples, essential patient data and interpreted data; PV provided essential tools and facilitated research; VC designed research, interpreted data, assisted in writing the paper and managed the research team, HBF designed research, interpreted data, wrote the paper and managed the research.

REFERENCES

1   Cimino, G. D., Gamper, H. B., Isaacs, S. T. & Hearst, J. E. Psoralens as photoactive probes of nucleic acid structure and function: organic chemistry, photochemistry, and biochemistry. *Annu Rev Biochem* **54**, 1151–1193, doi:10.1146/annurev.bi.54.070185.005443 (1985).

2   Lai, C. *et al.* Quantitative analysis of DNA interstrand cross-links and monoadducts formed in human cells induced by psoralens and UVA irradiation. *Anal Chem* **80**, 8790–8798, doi:10.1021/ac801520m (2008).

3   Pathak, M. A. & Fitzpatrick, T. B. The evolution of photochemotherapy with psoralens and UVA (PUVA): 2000 BC to 1992 AD. *J Photochem Photobiol B* **14**, 3–22 (1992).

4   Lin, L. *et al.* Photochemical inactivation of viruses and bacteria in platelet concentrates by use of a novel psoralen and long-wavelength ultraviolet light. *Transfusion* **37**, 423–435 (1997).

5   Wolf, P. Psoralen-ultraviolet A endures as one of the most powerful treatments in dermatology: reinforcement of this 'triple-product therapy' by the 2016 British guidelines. *Br J Dermatol* **174**, 11–14, doi:10.1111/bjd.14341 (2016).

6   Ling, T. C. *et al.* British Association of Dermatologists and British Photodermatology Group guidelines for the safe and effective use of psoralen–ultraviolet A therapy 2015. *Br J Dermatol* **174**, 24–55, doi:10.1111/bjd.14317 (2016).

7   Greinix, H. T. & Knobler, R. *Extracorporeal Photopheresis*. Vol. 1 (De Gruyter, 2012).

8   Waksvik, H., Brogger, A. & Stene, J. Psoralen/UVA treatment and chromosomes. I. Aberrations and sister chromatid exchange in human lymphocytes in vitro and synergism with caffeine. *Hum Genet* **38**, 195–207 (1977).

9   Edelson, R. *et al.* Treatment of cutaneous T-cell lymphoma by extracorporeal photochemotherapy. Preliminary results. *N Engl J Med* **316**, 297–303, doi:10.1056/NEJM198702053160603 (1987).

10 van Iperen, H. P. *et al.* The lack of efficacy of 4,6,6'-trimethylangelicin to induce immune suppression in an animal model for photopheresis: a comparison with 8-MOP. *Photochem Photobiol* **63**, 577–582 (1996).

11 Böhm, F., Meffert, H. & Bauer, E. PUVA therapy damages psoriatic and normal lymphoid cells within milliseconds. *Arch Dermatol Res* **279**, 16–19, doi:10.1007/bf00404352 (1986).

12 Sanford, K. W. & Balogun, R. A. Extracorporeal photopheresis: clinical use so far. *J Clin Apher* **27**, 126–131, doi:10.1002/jca.21217 (2012).

13 Del Fante, C. *et al.* Extracorporeal photopheresis as a new supportive therapy for bronchiolitis obliterans syndrome after allogeneic stem cell transplantation. *Bone Marrow Transplant*, doi:10.1038/bmt.2015.324 (2016, in press).

14 Laskin, J. D., Lee, E., Yurkow, E. J., Laskin, D. L. & Gallo, M. A. A possible mechanism of psoralen phototoxicity not involving direct interaction with DNA. *Proc Natl Acad Sci U S A* **82**, 6158–6162 (1985).

15 Zarebska, Z. Cell membrane, a target for PUVA therapy. *J Photochem Photobiol B* **23**, 101–109 (1994).

16 Beijersbergen van Henegouwen, G. M., Wijn, E. T., Schoonderwoerd, S. A. & Dall'Acqua, F. A method for the determination of PUVA-induced in vivo irreversible binding of 8-methoxypsoralen (8-MOP) to epidermal lipids, proteins and DNA/RNA. *J Photochem Photobiol B* **3**, 631–635 (1989).

17 dos Santos, D. J., Saenz-Mendez, P., Eriksson, L. A. & Guedes, R. C. Properties and behaviour of tetracyclic allopsoralen derivatives inside a DPPC lipid bilayer model. *Phys Chem Chem Phys* **13**, 10174–10182, doi:10.1039/c0cp02245d (2011).

18 Dardare, N. & Platz, M. S. Binding affinities of commonly employed sensitizers of viral inactivation. *Photochem Photobiol* **75**, 561–564 (2002).

19 Frank, S., Caffieri, S., Raffaelli, A., Vedaldi, D. & Dall'Acqua, F. Characterization of psoralen-oleic acid cycloadducts and their possible involvement in membrane photodamage. *J Photochem Photobiol B* **44**, 39–44, doi:10.1016/S1011-1344(98)00103-1 (1998).

20 Li, X. Y. & Eriksson, L. A. Photoreaction of skin-sensitizing trimethyl psoralen with lipid membrane models. *Photochem Photobiol* **81**, 1153–1160, doi:10.1562/2005-03-21-RA-467 (2005).

21 Anthony, F. A., Laboda, H. M. & Costlow, M. E. Psoralen-fatty acid adducts activate melanocyte protein kinase C: a proposed mechanism for melanogenesis induced by 8-methoxypsoralen and ultraviolet A light. *Photodermatol Photoimmunol Photomed* **13**, 9–16, doi:10.1111/j.1600-0781.1997.tb00101.x (1997).

22 Wolf, P. *et al.* Platelet-activating factor is crucial in psoralen and ultraviolet A-induced immune suppression, inflammation, and apoptosis. *Am J Pathol* **169**, 795–805, doi:10.2353/ajpath.2006.060079 (2006).

23 Van Aelst, B. *et al.* Riboflavin and amotosalen photochemical treatments of platelet concentrates reduce thrombus formation kinetics in vitro. *Vox Sang* **108**, 328–339, doi:10.1111/vox.12231 (2015).

24 Infante, C., Ramos-Morales, F., Fedriani, C., Bornens, M. & Rios, R. M. GMAP-210, A cis-Golgi network-associated protein, is a minus end microtubule-binding protein. *J Cell Biol* **145**,

83–98 (1999).

25 Knutson, F. *et al.* Photochemical Inactivation of Bacteria and HIV in Buffy-Coat-Derived Platelet Concentrates under Conditions That Preserve in vitro Platelet Function. *Vox Sanguinis* **78**, 209-216, doi:10.1046/j.1423-0410.2000.7840209.x (2000).

26 Irsch, J. & Lin, L. Pathogen Inactivation of Platelet and Plasma Blood Components for Transfusion Using the INTERCEPT Blood System. *Transfus Med Hemother* **38**, 19-31, doi:10.1159/000323937 (2011).

27 Hardwick, J. Blood processing. I*SBT Science Series* **3**, 148-176, doi:10.1111/j.1751-2824.2008.00195.x (2008).

28 Cazenave, J. P. *et al.* Preparation of washed platelet suspensions from human and rodent blood. *Methods Mol Biol* **272**, 13-28, doi:10.1385/1-59259-782-3:013 (2004).

29 Clark, J. *et al.* Quantification of PtdInsP3 molecular species in cells and tissues by mass spectrometry. *Nat Methods* **8**, 267-272, doi:10.1038/nmeth.1564 (2011).

30 Sandra, K., Pereira Ados, S., Vanhoenacker, G., David, F. & Sandra, P. Comprehensive blood plasma lipidomics by liquid chromatography/quadrupole time-of-flight mass spectrometry. *J Chromatogr A* **1217**, 4087-4099, doi:10.1016/j.chroma.2010.02.039 (2010).

31 t'Kindt, R. *et al.* Profiling over 1500 lipids in induced lung sputum and the implications in studying lung diseases. *Anal Chem* **87**, 4957-4964, doi:10.1021/acs.analchem.5b00732 (2015).

32 Goodall, A. H. & Appleby, J. Flow-cytometric analysis of platelet-membrane glycoprotein expression and platelet activation. *Methods Mol Biol* **272**, 225-253, doi:10.1385/1-59259-782-3:225 (2004).

33 Vanni, S., Hirose, H., Barelli, H., Antonny, B. & Gautier, R. A sub-nanometre view of how membrane curvature and composition modulate lipid packing and protein recruitment. *Nat Commun* **5**, 4916, doi:10.1038/ncomms5916 (2014).

34 Pranke, I. M. *et al.* alpha-Synuclein and ALPS motifs ar*e membrane curvature sensors whose contrasting chemistry mediates selective vesicle binding. J Cell Biol* **194**, 89-103, doi:10.1083/jcb.201011118 (2011).

35 Rapaport, D. & Shai, Y. Interaction of fluorescently labeled pardaxin and its analogues with lipid bilayers. *J Biol Chem* **266**, 23769-23775 (1991).

36 Shattil, S. J., Hoxie, J. A., Cunningham, M. & Brass, L. F. Changes in the platelet membrane glycoprotein IIb.IIIa complex during platelet activation. *J Biol Chem* **260**, 11107-11114 (1985).

37 Kim, S., Jin, J. & Kunapuli, S. P. Akt activation in platelets depends on Gi signaling pathways. *J Biol Chem* **279**, 4186-4195, doi:10.1074/jbc.M306162200 (2004).

38 Moore, S. F. *et al.* Dysfunction of the PI3 kinase/Rap1/integrin alpha(IIb)beta(3) pathway underlies ex vivo platelet hypoactivity in essential thrombocythemia. *Blood* **121**, 1209-1219, doi:10.1182/blood-2012-05-431288 (2013).

39 Santos, M. T., Valles, J., Aznar, J., Beltran, M. & Herraiz, M. Effect of smoking on plasma and platelet fatty acid composition in middle-aged men. *Atherosclerosis* **50**, 53-62 (1984).

40 Scaglia, N. & Igal, R. A. Inhibition of Stearoyl-CoA Desaturase 1 expression in human lung adenocarcinoma cells impairs tumorigenesis. *Int J Oncol* **33**, 839-850 (2008).

41 van Meer, G., Voelker, D. R. & Feigenson, G. W. Membrane lipids: where they are and how they behave. *Nat Rev Mol Cell Biol* **9**, 112-124 (2008).

42 Bigay, J. & Antonny, B. Curvature, lipid packing, and electrostatics of membrane organelles: defining cellular territories in determining specificity. *Dev Cell* **23**, 886-895, doi:10.1016/j.devcel.2012.10.009 (2012).

43 Caffieri, S., Zarebska, Z. & Dall'Acqua, F. Psoralen photosensitization: damages to nucleic acid and membrane lipid components. *Acta Biochim Pol* **43**, 241-246 (1996).

44 Alessi, D. R. *et al.* Characterization of a 3-phosphoinositide-dependent protein kinase which phosphorylates and activates protein kinase Balpha. *Curr Biol* **7**, 261-269 (1997).

45 Varnai, P., Rother, K. I. & Balla, T. Phosphatidylinositol 3-kinase-dependent membrane association of the Bruton's tyrosine kinase pleckstrin homology domain visualized in single living cells. *J Biol Chem* **274**, 10983-10989 (1999).

46 Vihinen, M. *et al.* Structural basis for pleckstrin homology domain mutations in X-linked agammaglobulinemia. *Biochemistry* **34**, 1475-1481 (1995).

47 Saito, K., Scharenberg, A. M. & Kinet, J. P. Interaction between the Btk PH domain and phosphatidylinositol-3,4,5-trisphosphate directly regulates Btk. *J Biol Chem* **276**, 16201-16206, doi:10.1074/jbc.M100873200 (2001).

48 Lemmon, M. A. Membrane recognition by phospholipid-binding domains. *Nat Rev Mol Cell Biol* **9**, 99-111, doi:10.1038/nrm2328 (2008).

49 Flesch, F. M., Yu, J. W., Lemmon, M. A. & Burger, K. N. Membrane activity of the phospholipase C-delta1 pleckstrin homology (PH) domain. *Biochem J* **389**, 435-441, doi:10.1042/BJ20041721 (2005).

50 Lumb, C. N. *et al.* Biophysical and computational studies of membrane penetration by the GRP1 pleckstrin homology domain. *Structure* **19**, 1338-1346, doi:10.1016/j.str.2011.04.010 (2011).

51 Bigay, J., Casella, J. F., Drin, G., Mesmin, B. & Antonny, B. ArfGAP1 responds to membrane curvature through the folding of a lipid packing sensor motif. *EMBO J* **24**, 2244-2253, doi:10.1038/sj.emboj.7600714 (2005).

52 Carlton, J. G. & Cullen, P. J. Coincidence detection in phosphoinositide signaling. *Trends Cell Biol* **15**, 540-547, doi:10.1016/j.tcb.2005.08.005 (2005).

53 Locke, D., Chen, H., Liu, Y., Liu, C. & Kahn, M. L. Lipid rafts orchestrate signaling by the platelet receptor glycoprotein VI. *J Biol Chem* **277**, 18801-18809, doi:10.1074/jbc.M111520200 (2002).

54 Riehle, R. D., Cornea, S. & Degterev, A. Role of phosphatidylinositol 3,4,5-trisphosphate in cell signaling. Adv *Exp Med Biol* **991**, 105-139, doi:10.1007/978-94-007-6331-9_7 (2013).

55 Woulfe, D. *et al. Defects in secretion, aggregation, and thrombus formation in platelets from mice lacking Akt2. J Clin Invest* **113**, 441-450, doi:10.1172/JCI20267 (2004).

56 Chen, X. *et al.* PDK1 regulates platelet activation and arterial thrombosis. *Blood* **121**, 3718-3726, doi:10.1182/blood-2012-10-461897 (2013).

57 Gilio, K. *et al.* Non-redundant roles of phosphoinositide 3-kinase isoforms alpha and beta in glycoprotein VI-induced platelet signaling and thrombus formation. *J Biol Chem* **284**, 33750-33762, doi:10.1074/jbc.M109.048439 (2009).

58 Byrd, J. C. *et al.* Ibrutinib versus ofatumumab in previously treated chronic lymphoid leukemia. *N Engl J Med* **371**, 213-223, doi:10.1056/NEJMoa1400376 (2014).

59 Mischnik, M. *et al.* A Boolean view separates platelet activatory and inhibitory signalling as verified by phosphorylation monitoring including threshold behaviour and integrin modulation. *Mol Biosyst* **9**, 1326-1339, doi:10.1039/c3mb25597b (2013).

PART 4

DISCUSSION

1. GENERAL DISCUSSION

REDUCTION OF PARTIAL OXYGEN PRESSURE TO PRESERVE THE QUALITY OF BLOOD COMPONENTS DURING PATHOGEN INACTIVATION

Our work studied the effects of pathogen inactivation on the quality of plasma units and platelet concentrates. For plasma, three bench top pathogen inactivation technologies, using high energy light illumination in combination with chemical photosensitizers, were examined. According to the manufacturers, the main mechanisms of action is crosslinking nucleic acids after photo-activation, thereby preventing replication and (pathogen) proliferation. However, all photo-excited sensitizers can in principle react with multiple electronegative surrounding molecules and therefore not exclusively restrict their chemistry to nucleic acids. Adduct formation of the excited photosensitizer with biomolecules including proteins, carbohydrates or lipids, typically results in biologic modifications potentially harming normal function. Furthermore, in the presence of dissolved molecular oxygen, formation of reactive oxygen species (ROS) is very likely by energy transfer between the ex-

cited photosensitizer and the electronegative oxygen molecule[1]. Typical reaction products are singlet oxygen, superoxide anion and hydrogen peroxide. All three are very oxidative randomly damage (bio)molecules, ranging from proteins to lipids. Our data confirmed that ROS are produced during the RF-PRT illumination process, damaging plasma proteins important for transfusion like fibrinogen, coagulation factor VIII and ADAMTS13. Our data show that by lowering the partial oxygen pressure in the plasma unit prior to RF-PRT, the observed damage to these biomolecules can successfully be mitigated. Similar to our data on plasma, a recent study found increased production of ROS and protein carbonylation in RF-PRT treated platelets confirming our pioneering work[2]. Minimizing the level of dissolved molecular oxygen in a transfusion product to control for off-target effects of pathogen inactivation may seem attractive but has a number of drawbacks. Platelet concentrates are currently stored in specific semipermeable containers to allow exchange of gaseous oxygen and carbon dioxide which is considered crucial for sustained platelet quality. Lowering partial oxygen pressure may thus harm the cells by promoting anaerobic respiration and accumulation of lactic acid. In addition, it is not entirely clear to what extent the factual (RF-PRT) pathogen inactivation depends on the reaction of ROS with pathogens. Even though the suppliers claim that the major or even sole mechanism of inactivation is via direct toxicity on DNA/RNA, scientific evidence is lacking to prove this statement. Especially for RF-PRT which in recent communications the provider has added oxidative stress as a mechanistic explanation for its action on pathogens. In summary, oxygen removal is attractive in theory to mitigate off-target effects (especially in RF-PRT) but the level of pathogen inactivation and the metabolic demands of the platelet should still be met when developing such a technology.

MICROFLUIDIC FLOW CHAMBERS TO EVALUATE PLATELET FUNCTION IN AN *IN VITRO* MODEL OF TRANSFUSION

Platelet function can be investigated with a variety of (indirect) *in vitro* experiments, but the most comprehensive is by using microfluidic flow chambers. This experiment takes into account the biophysical parameter of blood flow and therefore the influence of rheology on participating cells and biomolecules[3]. This challenging technique mimics hemostasis *in vitro* and was implemented and validated at the start of my research project. By reconstituting thrombocytopenic fresh blood we were able to investigate the function of exogenously added platelets from platelet concentrates, treated or not with pathogen inactivation. The clinical translation of this assay has been investigated ever since the first description of "parallel-plate flow chambers"[4]. There are many examples of its utility in clinical investigati-

on as demonstrated in multiple papers of which three are described below.
Casari *et al*[5] uncovered evidence in his study that besides the loss of VWF multimers and thrombocytopenia, a third possible mechanism for bleeding tendency in von Willebrand disease type 2B patients is platelet dysfunction. This impaired platelet function is due to inhibition of integrin $\alpha_{IIb}\beta_3$ and coincides with reduced thrombus growth seen in flow chamber experiments. Nogami *et al*[6] used a microchip flow chamber system succesfully to predict the bleeding score in von Willebrand disease type 1 patients. Finally, Flamm *et al*[7] determined the phenotype of the platelets of individual donors by analyzing the behaviour of these platelets under flow. By using a combination of cell adhesion assays and multiscale computer simulations, they were able to predict patient-specific thrombus formation potential. Moreover, their study revealed a novel thromboxane receptor mutation (TP-V241G) in humans that confers resistance to indomethacin.

HOW DO TRANSFUSED PLATELETS PERFORM IN HEMOSTASIS *IN VIVO*?

Two of three available pathogen inactivation technologies used for the treatment of platelet concentrates utilize a photosensitizer (AS-PCT & RF-PRT) and the other does not (UV-C). In our studies we concluded that all three methods cause decreased platelet function following the results of thrombus growth kinetics in a microfluidic flow chamber experiment. This was confirmed by additional unrelated platelet (function) tests that investigated the metabolic, biochemical, and biologic characteristics of platelets. It is not clear if this observed platelet function decrease *in vitro* sustains *in vivo* or whether platelet function can recover once transfused to the patient. Alternatively, even though the function of treated platelets may be decreased in flow chambers it might still be sufficient to control bleeding because transfused (treated) platelets may indirectly promote coagulation although this needs further research. A platelet plug is a hierarchical structure with a core of densely packed, irreversibly activated platelets overlaid by a shell of loosely packed, less activated platelets[8]. It is currently unclear where transfused allogeneic platelets fit in this revised model of hemostasis. Therefore additional basic research is required to understand the role of transfused platelets in light of this hemostasis model and whether pathogen inactivation alters the behaviour of transfused platelets during hemostasis, *in vivo*.
Clinical trials of transfusion of pathogen inactivated platelets are variable in design and result[9-11]. Platelet recovery is often measured by "corrected count increment" which is a measure for transfusion yield and a questionable surrogate for successful cessation or prevention of bleeding. Clinical trials that directly measure bleeding have been performed, but with conflicting conclusions as discussed in a Cochrane review published in 2013[12]. In addition, bleeding assessment as a clinical outcome is practically difficult and the way this

should be done a matter of debate. Bleeding is a difficult primary endpoint, also because significant bleeding is relatively rare requiring a larger cohort to be included in the trial. Finally, the intrinsic diversity of clinical presentations in the receiving patient population as well as the diversity in primary characteristics of platelet concentrates prepared by a multitude of component preparation methods makes comparison between institutes and hospitals internationally a true challenge. That's why additional clinical studies should focus on standardized outcomes in well-defined research questions. Only this way an evidence based decision for the introduction of a given pathogen inactivation method in a blood bank can be made[13].

THE UNDERLYING MECHANISMS OF PLATELET FUNCTION LOSS AFTER PATHOGEN INACTIVATION

Our data suggest that the underlying biochemical mechanisms of platelet damage significantly differ between the three different pathogen inactivation methods. For instance, RF-PRT treated platelets display increased anaerobic metabolic respiration, continuous degranulation and increased phosphatidylserine exposure rates collectively pointing to an accelerated storage lesion. This has been reported by independent research groups studying RF-PRT[14-16]. Our data for UV-C treated platelets indicate a fixed conformational activation of integrin $\alpha_{IIb}\beta_3$ indistinguishable of physiologic receptor activation. We are unsure what the impact of this is, because even though PAC1 binds to these platelets and fibrinogen is supposed to do so too[17]. However, increased storage lesion like in RF-PRT platelets is not found. Therefore, premature platelet activation via sustained outside-in signal transduction after fibrinogen binding may be possible but is not significantly affecting platelet parameters during further storage. Finally, AS-PCT has a more specific effect on platelet signal transduction. Integrin $\alpha_{IIb}\beta_3$ receptor activation by inside-out signal transduction in response to some but not all platelet agonists is affected. Targeted analysis of signal transduction pathway sections demonstrated an attenuation of PI 3-kinase/Akt/Btk signalling. So each method has different underlying biomolecular effects on platelets which result in decreased thrombus formation rates in microfluidic flow chambers on collagen.

Research to pathogen inactivation has initially focused on achieving maximal log reductions of relevant inoculated pathogens. Potential efforts to minimize the quality loss of treated products received less attention. To successfully develop next generation technologies that take into account the off-target effects, basic understanding is the key: what is causing the loss of platelet or component function? The answer to this question can then be used to optimize and modify the practical process weighting out pathogen inactivation success

and component quality. For this free access to industry manufactured tools is important to openly tackle important questions.

MECHANISTIC INSIGHTS OF DECREASED PLATELET FUNCTION IN AS-PCT, POTENTIAL TO IMPROVE PIT

AS-PCT treated platelets display decreased thrombus formation rates in microfluidic flow chamber experiments. This functional defect was narrowed down to a defect in the signal transduction axis of PI 3-kinase, with diminished Akt and Btk phosphorylation. Next, we found that amotosalen photochemically forms covalent adducts with membrane (phospho) lipids and that the binding of ALPS-NBD to amotosalen treated liposomes (containing packing defects) is impaired. Taking these findings together and knowing that lipid-lipid and lipid-protein interactions play crucial roles in PI 3-kinase-Akt/Btk signalling, we hypothesized that the binding of Akt and Btk to the membrane is compromised. Indeed, following AS-PCT spatiotemporal subcellular localization of PH domain containing proteins is impaired, while sufficient PI(3,4,5)P3 is produced. So we suggest that the membrane acyl chains at least in part cooperate for successful binding[18] of Akt and Btk.

Future research should study how binding of PH domains to membranes is influenced by altered packing. Besides that, pathogen inactivation based on psoralens could be optimized. For example by the use of a psoralen that has sufficient nucleic binding and thus pathogen killing capacities but without any attraction for lipids.

TRANSLATION TO PUVA

Our results help to understand existing PUVA treatments and suggest avenues for improving them. For example, extracorporeal photopheresis (ECP) is a leukapheresis-based PUVA procedure used to treat cutaneous T-cell lymphoma. It is currently under investigation for other disorders like GvhD, transplant rejection, Crohn's disease[19], psoriasis[20] and rheumatoid arthritis[21,22]. The reigning concept of ECP is that treated cells are rendered apoptotic by DNA damage and then opsonized by antigen-presenting (dendritic) cells and/or macrophages. Subsequent T and B lymphocyte presentation then promotes immune tolerance and induces antigen-specific regulatory T cells, IL-10-producing regulatory B cells and regulatory CD8+ T cells, rewiring the immune system[23] in favour disease mitigation. Our data suggest a potential role for PI 3-kinase/Akt signal transduction pathway, since this axis is affected following ECP treatment. The well documented link between PI 3-kinase signal transduction and many of the above mentioned diseases is in favour of this suggestion[24-27]. If proven to be

important in the mechanism of action, PI 3-kinase functional attenuation by ECP could be improved by using a more efficient psoralen or illumination regimen to control the effect on PI 3-kinase signalling.

In conclusion, PUVA treatment specifically decreases the phosphorylation of PH-domain-containing effector molecules, albeit independent of PI(3,4,5)P3 formation. The consequences for treatment of disease and pathogen inactivation are possibly broad but not easily disentangled. PUVA treatment is used for skin diseases as well as systemic T-cell related conditions and PI 3-kinase may thus play a more central role than thus far anticipated in these diseases and its therapies. Thanks to PUVA's membrane changing capacity, biochemical links between the cytoplasmic membrane and the actions of PH-domain containing effector proteins in the cell cytoplasm has been demonstrated.

2. REFERENCES

1   Goodrich, R. P. & Platz, M. S. The design and development of selective, photoactivated drugs for sterilization of blood products. *Drugs Future* **22**, 159-171 (1997).
2   Johnson, L. & Marks, D. Treatment of Platelet Concentrates with the Mirasol Pathogen Inactivation System Modulates Platelet Oxidative Stress and NF-kappaB Activation. *Transfus Med Hemother* **42**, 167-173, doi:10.1159/000403245 (2015).
3   Savage, B., Saldivar, E. & Ruggeri, Z. M. Initiation of platelet adhesion by arrest onto fibrinogen or translocation on von Willebrand factor. *Cell* **84**, 289-297, doi:10.1016/S0092-8674(00)80983-6 (1996).
4   Sakariassen, K. S., Bolhuis, P. A. & Sixma, J. J. Human blood platelet adhesion to artery subendothelium is mediated by factor VIII-Von Willebrand factor bound to the subendothelium. *Nature* **279**, 636-638, doi:10.1038/279636a0 (1979).
5   Casari, C. *et al.* von Willebrand factor mutation promotes thrombocytopathy by inhibiting integrin alphaIIbbeta3. *J Clin Invest* **123**, 5071-5081, doi:10.1172/jci69458 (2013).
6   Nogami, K. *et al.* Assessing the clinical severity of type 1 von Willebrand disease patients with a microchip flow-chamber system. *J Thromb Haemost* **14**, 667-674, doi:10.1111/jth.13273 (2016).
7   Flamm, M. H. *et al.* Multiscale prediction of patient-specific platelet function under flow. *Blood* **120**, 190-198, doi:10.1182/blood-2011-10-388140 (2012).
8   Stalker, T. J. *et al.* Hierarchical organization in the hemostatic response and its relationship to the platelet-signaling network. *Blood* **121**, 1875-1885, doi:10.1182/blood-2012-09-457739
(2013).
9   van Rhenen, D. *et al.* Transfusion of pooled buffy coat platelet components prepared with photochemical pathogen inactivation treatment: the euroSPRITE trial. *Blood* **101**, 2426-2433, doi:10.1182/blood-2002-03-0932 (2003).
10 AuBuchon, J. P. et al. Efficacy of apheresis platelets treated with riboflavin and ultraviolet light for pathogen reduction. *Transfusion* **45**, 1335-1341, doi:10.1111/j.1537-2995.2005.00202.x (2005).
11 Snyder, E. *et al.* Recovery and life span of 111indium-radiolabeled platelets treated with pathogen inactivation with amotosalen HCl (S-59) and ultraviolet A light. *Transfusion* **44**, 1732-1740, doi:10.1111/j.0041-1132.2004.04145.x (2004).
12 Butler, C. *et al.* Pathogen-reduced platelets for the prevention of bleeding. Cochrane Database Syst Rev 3, Cd009072, doi:10.1002/14651858.CD009072.pub2 (2013).
13 Cook, R. J. & Heddle, N. M. Clinical trials evaluating pathogen-reduced platelet products: methodologic issues and recommendations. *Transfusion* **53**, 1843-1855, doi:10.1111/j.1537-2995.2012.03951.x (2013).
14 Picker, S. M., Steisel, A. & Gathof, B. S. Effects of Mirasol PRT treatment on storage lesion development in plasma-stored apheresis-derived platelets compared to untreated and irradiated units. *Transfusion* **48**, 1685-1692, doi:10.1111/j.1537-2995.2008.01778.x (2008).
15 Johnson, L. *et al.* The effect of pathogen reduction technology (Mirasol) on platelet quality when treated in additive solution with low plasma carryover. *Vox Sang* **101**, 208-214, doi:10.1111/j.1423-0410.2011.01477.x (2011).
16 Janetzko, K., Hinz, K., Marschner, S., Goodrich, R. & Kluter, H. Pathogen reduction technology (Mirasol) treated single-donor platelets resuspended in a mixture of autologous plasma and PAS. *Vox Sang* **97**, 234-239 (2009).
17 Verhaar, R. *et al.* UV-C irradiation disrupts platelet surface disulfide bonds and activates the platelet integrin alphaIIbbeta3. *Blood* **112**, 4935-4939, doi:10.1182/blood-2008-04-151043 (2008).
18 Carlton, J. G. & Cullen, P. J. Coincidence detection in phosphoinositide signaling. *Trends Cell Biol* **15**, 540-547, doi:10.1016/j.tcb.2005.08.005 (2005).
19 Knobler, R. et al. Guidelines on the use of extracorporeal photopheresis. *J Eur Acad Dermatol Venereol* **28 Suppl 1**, 1-37, doi:10.1111/jdv.12311 (2014).
20 Wilfert, H., Honigsmann, H., Steiner, G., Smolen, J. & Wolff, K. Treatment of psoriatic arthritis by extracorporeal photochemotherapy. *Br J Dermatol* **122**, 225-232 (1990).
21 Malawista, S. E., Trock, D. H. & Edelson, R. L. Treatment of rheumatoid arthritis by extracorporeal photochemotherapy. A pilot study. *Arthritis Rheum* **34**, 646-654 (1991).
22 Hilliquin, P., Andreu, G., Heshmati, F. & Menkes, C. J. [Treatment of refractory rheumatoid polyarthritis by extracorporeal photochemotherapy]. *Rev Rhum Ed Fr* **60**, 125-130 (1993).
23 Xia, C. Q., Campbell, K. A. & Clare-Salzler, M. J. Extracorporeal photopheresis-induced immune tolerance: a focus on modulation of antigen-presenting cells and induction of regulatory T

cells by apoptotic cells. *Curr Opin Organ Transplant* **14**, 338–343, doi:10.1097/MOT.0b013e32832ce943 (2009).

24   Burger, J. A. & Hoellenriegel, J. Phosphoinositide 3'-kinase delta: turning off BCR signaling in Chronic Lymphocytic Leukemia. *Oncotarget* **2**, 737–738, doi:10.18632/oncotarget.341 (2011).

25   Castor, M. G. *et al.* PI3Kgamma controls leukocyte recruitment, tissue injury, and lethality in a model of graft-versus-host disease in mice. *J Leukoc Biol* **89**, 955–964, doi:10.1189/jlb.0810464 (2011).

26   Pike, M. C., Lee, C. S., Elder, J. T., Voorhees, J. J. & Fisher, G. J. Increased phosphatidylinositol kinase activity in psoriatic epidermis. *J Invest Dermatol* **92**, 791–797 (1989).

27   Kim, H. R. *et al.* Up-regulation of IL-23p19 expression in rheumatoid arthritis synovial fibroblasts by IL-17 through PI3-kinase-, NF-kappaB- and p38 MAPK-dependent signalling pathways. *Rheumatology (Oxford)* **46**, 57–64, doi:10.1093/rheumatology/kel159 (2007).

LIST OF PUBLICATIONS

MANUSCRIPTS

1   Feys, H. B., **B. Van Aelst**, K. Devreese, R. Devloo, J. Coene, P. Vandekerckhove and V. Compernolle (2014). "Oxygen removal during pathogen inactivation with riboflavin and UV light preserves protein function in plasma for transfusion." Vox Sang. 2014 May;106(4):307–15. doi:10.1111/vox.12106

2   **Van Aelst, B.**, H. B. Feys, R. Devloo, K. Vanhoorelbeke, P. Vandekerckhove and V. Compernolle (2014). "Riboflavin and amotosalen photochemical treatments of platelet concentrates reduce thrombus formation kinetics in vitro." Vox Sang. 2015 May;108(4):328–39. doi: 10.1111/vox.12231.

3   Feys, H. B., J. Coene, R. Devloo, **B. Van Aelst**, H. Pottel, P. Vandekerckhove and V. Compernolle (2015). "Persistent aggregates in apheresis platelet concentrates." Vox Sang. 2015 May;108(4):368–77. doi: 10.1111/vox.12243

4   **Van Aelst, B.**, R. Devloo, P. Vandekerckhove, V. Compernolle and H. B. Feys (2015). "Ultraviolet C light pathogen inactivation treatment of platelet concentrates preserves integrin activation but affects thrombus formation kinetics on collagen in vitro" Transfusion. 2015 Oct;55(10):2404–14. doi: 10.1111/trf.13137

5   Feys, H. B., **B. Van Aelst**, R. Devloo, P. Vandekerckhove and V. Compernolle (2015). "The contribution of von Willebrand factor–GPIb interactions to persistent aggregate formation in apheresis platelet concentrates." Vox Sang. 2015 Dec 8. doi: 10.1111/vox.12365

6   **Van Aelst, B.**, H. B. Feys, R. Devloo, P. Vandekerckhove and V. Compernolle. "Microfluidic flow chambers using reconstituted blood to model hemostasis and platelet transfusion in vitro." JoVE. *In press*

7   **Van Aelst, B.**, R. Devloo, P. Vandekerckhove, V. Compernolle and H. B. Feys. "Acyl chain (un)saturation indirectly controls the class IA PI3K signaling axis." *In preparation*

ABSTRACTS

1   Hendrik B. Feys, **Britt Van Aelst**, Rosalie Devloo, Philippe Vandekerckhove, Veerle Compernolle "Ultraviolet C light treatment preserves activatability and amplification potential of platelets but affects thrombus formation kinetics on collagen in vitro." Abstract of AABB Annual meeting 2014, Philadelphia, PA

2   **Britt Van Aelst**, Rosalie Devloo, Philippe Vandekerckhove, Veerle Compernolle, Hendrik B. Feys "Riboflavin and ultraviolet light treatment activates platelets causing decreased thrombus formation kinetics on collagen in vitro." Abstract of AABB Annual meeting 2014, Philadelphia, PA

3   Hendrik B. Feys, **Britt Van Aelst**, Rosalie Devloo, Philippe Vandekerckhove, Veerle Compernolle "Treatment of platelet concentrates with amotosalen and ultraviolet light decreases platelet adhesion and activatability causing reduced thrombus formation kinetics in vitro." Abstract of AABB Annual meeting 2014, Philadelphia, PA

4   Hendrik B. Feys, **Britt Van Aelst**, Rosalie Devloo, José Coene, Philippe Vandekerckhove, Veerle Compernolle "Apheresis platelet concentrates with persistent particles." Abstract of Second EUPLAN Conference 2014, Le Bischenberg, France

DANKWOORD

Op de voorpagina van dit proefschrift staat enkel mijn naam, maar die zou daar eigenlijk niet alleen mogen staan. Het is een cliché, maar dit is een boekje waar veel mensen aan bijgedragen hebben, rechtstreeks en onrechtstreeks.

Toen ik mijn job als procesingenieur vaarwel zei om in TReC te komen werken, wist ik niet goed wat me te wachten stond. De schoolbanken waren al een tijdje verdwenen en de kennis over het labowerk had zich reeds in mijn grijze hersenmassa verstopt. Maar met Hendrik als leermeester kon ik dit geleidelijk aan terug naar boven halen. Hendrik, ik kan je dan ook niet genoeg bedanken voor alles wat je gedurende mijn onderzoekscarrière gedaan hebt. Je vormde me tot een kritische wetenschapper. Niet enkel door je kennis en ervaring te delen, maar vooral door me te begeleiden langsheen de vele obstakels en uitdagingen die deel uitmaken van goed wetenschappelijk onderzoek. Je ondersteunde me bij de praktische, uitvoerende kant in het labo en de theoretische, schrijvende kant op het bureau. Je hebt me laten zien en voelen wat wetenschap is, besmet met het virus van onderzoek.

Graag had ik ook Prof. Dr. Philippe Vandekerckhove bedankt om translationeel biomedisch wetenschappelijk onderzoek in het Rode Kruis-Vlaanderen te introduceren. Daarnaast gaat ook een bijzondere dank uit naar Prof. Dr. Veerle Compernolle die me de kans gaf dit doctoraat te maken. Ondanks uw drukbezette agenda, maakte u steevast tijd vrij om in 'de kelder' binnen te springen en met een frisse blik een andere invalshoek te openen. Ook de leden van mijn examencommissie, Prof. Dr. Katrien Devreese en Prof. Dr. Lucien Noens wil ik bedanken voor het advies en de begeleiding gedurende dit traject. Jullie expertise was een belangrijke meerwaarde voor dit onderzoek.

Als ik spreek over de praktische, uitvoerende kant, denk ik natuurlijk ook direct aan Rosalie. Bedankt om me onder te dompelen in de wereld van de pipetten en de gellekes. Door jou leerde ik de kneepjes van het vak kennen. Je zorgde ervoor dat alles steeds beschikbaar was in het labo en je was dat extra paar handen als ik met mijn duo niet toekwam. Maar naast dit alles was je vooral ook een zeer goede collega!

Verder ben ik ook Ruben en Koen van het Research Institute for Chromatography (RIC) dankbaar voor de vlotte samenwerking en hun bijdrage tot dit onderzoek.
En dan wil ik de medewerkers van PROLOG zeker niet vergeten. Jullie vroegen zich waar-

schijnlijk vaak af wat we allemaal uitspookten in 'de kelder' met de bloedplaatjes die jullie voor ons bereidden en de bloedstaaltjes die jullie doneerden. Van één ding mag je alleszins zeker zijn, zonder jullie was dit nooit gelukt en daarom een oprechte en welgemeende 'dank u wel!'. Dit geldt ook voor de medewerkers van IMS en administratie in Esploro die steeds bereid waren om een staaltje te doneren. Maar bovenal zijn jullie allemaal collega's die ik enorm waardeer! Jullie maken van onze campus een plaats waar ik graag kom werken. Bedankt!

Je voelt de lijn van de bedankingen al wijzigen in de richting van de onrechtstreekse bijdragen, maar daarom zeker niet minder belangrijk. De voetbaltrainingen en matchen om de frustraties en zorgen eens van me af te shotten, de gezelschapspel-momenten om alles te relativeren of gewoon samen gezellig eentje drinken. Jullie zorgen ervoor dat ik elke dag met nieuwe energie kan opstaan. De uitdagingen op het werk met een frisse mind kan aangaan om net dat 'ietske' meer te geven. Daarvoor lieve vrienden en schoonfamilie, ben ik jullie zeer dankbaar!

Dan zijn er nog die mensen die me steunen in alles wat ik onderneem, mijn ouders. Papa en mama, bedankt om me vrij te laten in mijn keuzes, maar me toch door jullie raad de goede richting uit te sturen. Ook mijn grote broer die me met zijn kritische kijk, vaak aan het denken zet, wil ik bedanken. Je herinnert me samen met Corinne, vaak aan jullie levensleuze om te genieten van elk moment van het leven. En zeker niet te vergeten Corinne, bedankt dat ik je creatief brein even mocht gebruiken voor de lay-out van deze thesis.

Zoals men wel eens zegt, ik heb het beste tot het einde bewaard en daarmee kom ik tot bij Anneloes. Je maakt van ons huis een thuis! Je optimisme, spontaniteit en eindeloos vertrouwen maakt me zoveel sterker! Al ga ik drie maand naar Ghana, al beslis ik ineens te doctoreren, je bent er steeds om mij te steunen. Bedankt! Met jou ben ik met mijn gat in de beste boerenboter gevallen!

Een oprechte merci aan jullie allemaal. Want ieder op zijn eigen manier heeft bijgedragen om dit mogelijk te maken!

Britt